Journal of Analytical Methods in Chemistry

Quality Control of Natural Product Medicine and Nutrient Supplements 2014

Guest Editors: Ying-Yong Zhao, Shuang-Qing Zhang, Feng Wei, Yu-Ming Fan, Feng Sun, and Shuhua Bai

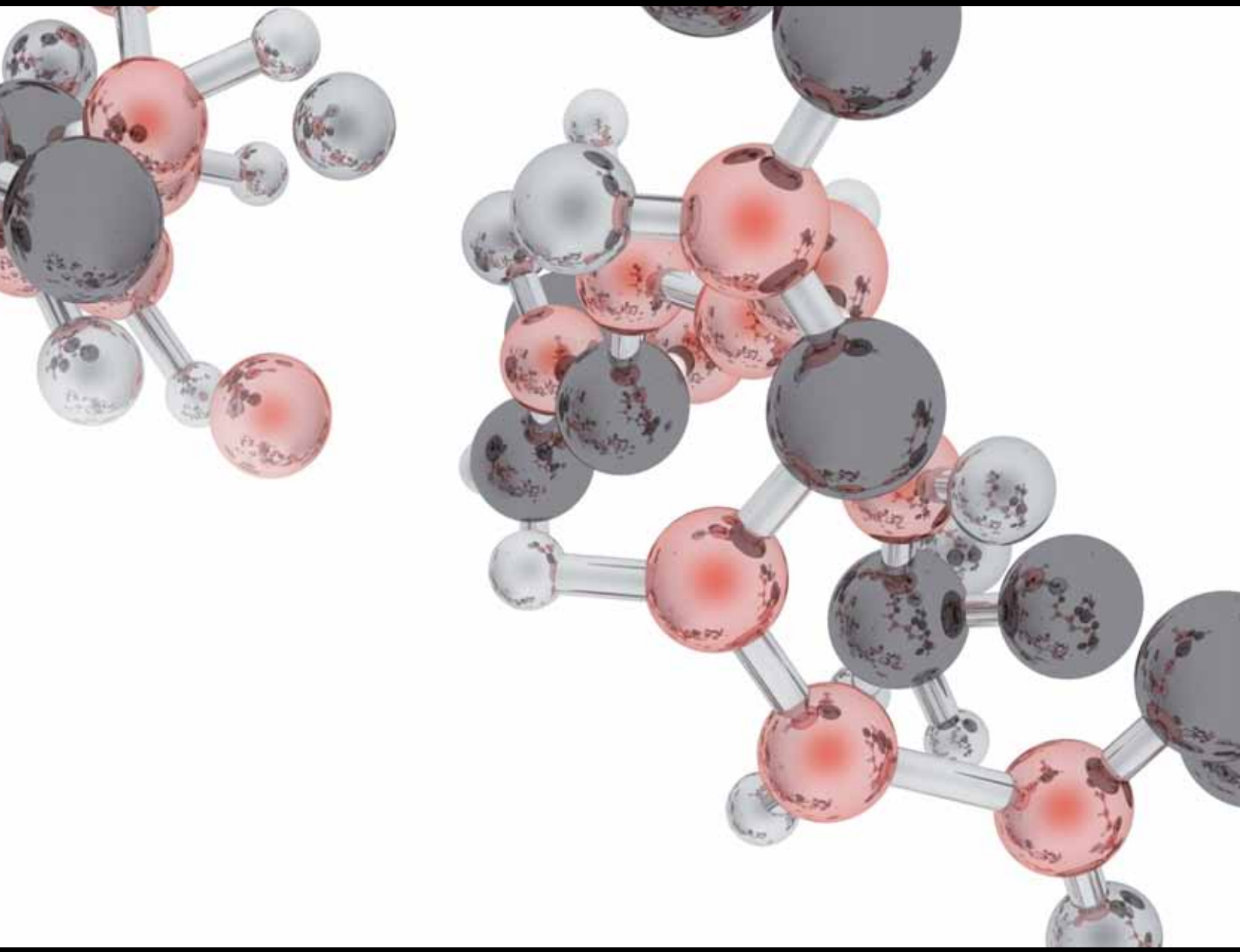

Quality Control of Natural Product Medicine and Nutrient Supplements 2014

Journal of Analytical Methods in Chemistry

Quality Control of Natural Product Medicine and Nutrient Supplements 2014

Guest Editors: Ying-Yong Zhao, Shuang-Qing Zhang, Feng Wei, Yu-Ming Fan, Feng Sun, and Shuhua Bai

Copyright © 2014 Hindawi Publishing Corporation. All rights reserved.

This is a special issue published in "Journal of Analytical Methods in Chemistry." All articles are open access articles distributed under the Creative Commons Attribution License, which permits unrestricted use, distribution, and reproduction in any medium, provided the original work is properly cited.

Editorial Board

Mohamed Abdel-Rehim, Sweden
Hassan Y. Aboul Enein, Egypt
Silvana Andreescu, USA
A. N. Anthemidis, Greece
Alberto N. Araújo, Portugal
Rolf W. Arndt, Switzerland
Ana C. B. Dias, Brazil
Pierangelo Bonini, Italy
Arthur C. Brown, USA
Antony C. Calokerinos, Greece
Ricardo J. Cassella, Brazil
Xin-Sheng Chai, China
Orawon Chailapakul, Thailand
Xingguo Chen, China
Christin Collombel, France
Warren T. Corns, UK
M. de la Guardia, Spain
I. Delgadillo, Portugal
Eduardo Dellacassa, Uruguay
Cevdet Demir, Turkey
M. Bonner Denton, USA
Gregory W. Diachenko, USA
M. Elena Diaz-Garcia, Spain
Dieter M. Drexler, USA
Jianxiu Du, China
Jenny Emnéus, Denmark
Gauthier Eppe, Belgium
J. Esteve-Romero, Spain
Juan F. Garcia-Reyes, Spain
C. Georgiou, Greece
K. Grudpan, Thailand
Arafa I. Hamed, Egypt
Karoly Heberger, Hungary
Bernd Hitzmann, Germany
Chih-Ching Huang, Taiwan
Ibrahim Isildak, Turkey
Jaroon Jakmunee, Thailand
Xiue Jiang, China
Selhan Karagöz, Turkey
Hiroyuki Kataoka, Japan
Skip Kingston, USA
C. Kontoyannis, Greece
Radosław Kowalski, Poland
Annamalai S. Kumar, India
Ilkeun Lee, USA
Joe Liscouski, USA
E. J. Llorent-Martinez, Spain
M. G. Lopez, Mexico
Miren Lopez de Alda, Spain
Larisa Lvova, Italy
Jose Carlos Marques, Portugal
Christophe A. Marquette, France
Jean Louis Marty, France
Somenath Mitra, USA
Serban C. Moldoveanu, USA
M. Branco Montenegro, Portugal
Gowda A. Nagana Gowda, USA
Mu. Naushad, Saudi Arabia
Milka Neshkova, Bulgaria
B. Nikolova-Damyanova, Bulgaria
Sune Nygaard, Denmark
Ciara K. O'Sullivan, Spain
Gangfeng Ouyang, China
Sibel A. Ozkan, Turkey
Ve. Pino, Spain
Krystyna Pyrzynska, Poland
J. B. Quintana, Spain
M. A. Rashid, Bangladesh
D. P S Rathore, India
Pablo Richter, Chile
F. R. Piovezan Rocha, Brazil
Erwin Rosenberg, Austria
Giuseppe Ruberto, Italy
Antonio Ruiz Medina, Spain
Bradley B. Schneider, Canada
Guoyue Shi, China
Jesus Simal-Gandara, Spain
H. Sklenarova, Czech Republic
Nicholas H. Snow, USA
Peter B. Stockwell, UK
FakhrEldin O. Suliman, Oman
It-Koon Tan, Singapore
D. G. Themelis, Greece
Nilgun Tokman, Turkey
Nelson Torto, South Africa
Marek Trojanowicz, Poland
Paris Tzanavaras, Greece
Bengi Uslu, Turkey
Krishna K. Verma, India
Adam Voelkel, Poland
Hai-Long Wu, China
Hui-Fen Wu, Taiwan
Qingli Wu, USA
Mengxia Xie, China
Rongda Xu, USA
Xiu-Ping Yan, China
Chunsheng Yin, China

Contents

Quality Control of Natural Product Medicine and Nutrient Supplements 2014, Ying-Yong Zhao, Shuang-Qing Zhang, Feng Wei, Yu-Ming Fan, Feng Sun, and Shuhua Bai
Volume 2014, Article ID 109068, 2 pages

The Therapeutic Effect of Zuogui Wan in Gestational Diabetes Mellitus Rats, Yuwei Wang, Qianjin Feng, Xin Niu, Xinshe Liu, Kaixia Xu, Xiangzhu Yang, Huifeng Wang, and Qiuju Li
Volume 2014, Article ID 737961, 6 pages

Quantitative Analysis of *Panax ginseng* by FT-NIR Spectroscopy, Xin-fang Xu, Li-xing Nie, Li-li Pan, Bian Hao, Shao-xiong Yuan, Rui-chao Lin, Hai-bo Bu, Dan Wang, Ling Dong, and Xiang-ri Li
Volume 2014, Article ID 741571, 6 pages

Studies on the Anti-Inflammatory Effect and Its Mechanisms of Sophoridine, Xiumei Huang, Bo Li, and Lianzhong Shen
Volume 2014, Article ID 502626, 6 pages

Urinary Metabolomics on the Biochemical Profiles in Diet-Induced Hyperlipidemia Rat Using Ultraperformance Liquid Chromatography Coupled with Quadrupole Time-of-Flight SYNAPT High-Definition Mass Spectrometry, Hua Miao, Hua Chen, Xu Zhang, Lu Yin, Dan-Qian Chen, Xian-Long Cheng, Xu Bai, and Feng Wei
Volume 2014, Article ID 184162, 9 pages

Simultaneous Quantitative and Qualitative Analysis of Flavonoids from Ultraviolet-B Radiation in Leaves and Roots of *Scutellaria baicalensis* Georgi Using LC-UV-ESI-Q/TOF/MS, Wen-Ting Tang, Min-Feng Fang, Xiao Liu, and Ming Yue
Volume 2014, Article ID 643879, 9 pages

Using the Doubly Charged Selected Ion Coupled with MS/MS Fragments Monitoring (DCSI-MS/MS) Mode for the Identification of Gelatin Species, Xian-Long Cheng, Feng Wei, Jia Chen, Ming-hua Li, Lei Zhang, Ying-Yong Zhao, Xin-Yue Xiao, Shuang-cheng Ma, and Rui-Chao Lin
Volume 2014, Article ID 764397, 7 pages

One Single Amino Acid for Estimation the Content of Total Free Amino Acids in *Qingkailing Injection* Using High-Performance Liquid Chromatography-Diode Array Detection, Li Zhang, Xue Wang, Jiankun Su, Haiyu Liu, Zhixin Zhang, Lingling Qin, Cheng He, Long Peng, Mingxing Guo, and Xiaoyan Gao
Volume 2014, Article ID 951075, 9 pages

A New Method for the Analysis of Bacterial Endotoxins in Ultrapure Paraffin Oil, Dandan Chen
Volume 2014, Article ID 575246, 4 pages

A Metabolomic Strategy to Screen the Prototype Components and Metabolites of *Shuang-Huang-Lian Injection* in Human Serum by Ultra Performance Liquid Chromatography Coupled with Quadrupole Time-of-Flight Mass Spectrometry, Mingxing Guo, Baosheng Zhao, Haiyu Liu, Li Zhang, Long Peng, Lingling Qin, Zhixin Zhang, Jian Li, Chengke Cai, and Xiaoyan Gao
Volume 2014, Article ID 241505, 12 pages

Analysis of Photosynthetic Characteristics and UV-B Absorbing Compounds in Mung Bean Using UV-B and Red LED Radiation, Fang-Min Li, Zhi-Guo Lu, and Ming Yue
Volume 2014, Article ID 378242, 5 pages

Hindawi Publishing Corporation
Journal of Analytical Methods in Chemistry
Volume 2014, Article ID 109068, 2 pages
http://dx.doi.org/10.1155/2014/109068

Editorial

Quality Control of Natural Product Medicine and Nutrient Supplements 2014

Ying-Yong Zhao,[1] Shuang-Qing Zhang,[2] Feng Wei,[3] Yu-Ming Fan,[4] Feng Sun,[5] and Shuhua Bai[6]

[1] *Key Laboratory of Resource Biology and Biotechnology in Western China, Ministry of Education, Department of Traditional Chinese Medicine, College of Life Sciences, Northwest University, No. 229 Taibai North Road, Xi'an, Shaanxi 710069, China*
[2] *Department of Nutrition and Metabolism, National Institute for Nutrition and Food Safety, China Center for Disease Control and Prevention, 27 Nanwei Road, Xicheng District, Beijing 100050, China*
[3] *Department of Traditional Chinese Medicine and Ethnic Medicine, National Institutes for Food and Drug Control, State Food and Drug Administration, 2 Tiantan Xili, Beijing 100050, China*
[4] *National Institutes for Food and Drug Control, State Food and Drug Administration, 2 Tiantan Xili, Beijing 100050, China*
[5] *Department of Obstetrics & Gynaecology, Yong Loo Lin School of Medicine, National University of Singapore, 10 Medical Drive, Singapore 117597*
[6] *Department of Basic Pharmaceutical Sciences, School of Pharmacy, Husson University, 1 College Circle, Bangor, ME 04401, USA*

Correspondence should be addressed to Shuhua Bai; bais@husson.edu

Received 13 August 2014; Accepted 13 August 2014; Published 21 August 2014

Copyright © 2014 Ying-Yong Zhao et al. This is an open access article distributed under the Creative Commons Attribution License, which permits unrestricted use, distribution, and reproduction in any medium, provided the original work is properly cited.

As one of the oldest remedies, the natural medicine products and nutrient supplements have been broadly used to prevent and treat various human diseases for thousands of years. Ginkgo (*Ginkgo biloba*) could treat circulatory disorders and enhance memory, kava-kava (*Piper methysticum*) could elevate mood and produce a feeling of relaxation, valerian (*Valeriana officinalis*) could help in sleep, and the list could go on [1]. Possibly recommended by medical practitioners, consumers consider natural products as an alternative to decrease health cost, alleviate self-diagnosed diseases, or supplement prescribed therapeutic regimens. The natural products have become a large sale on a global basis and they represent an increasing share in healthcare market reaching estimated $6 billion annually only in the USA [2, 3].

Labeled as "natural," the natural medications and nutrition supplements often puzzle consumers turning them to "completely safe" products based on the perception. In fact, many natural products affect the body in unwanted ways that can potentially lead to serious side effects, even life-threatening results, because many products contain unknown and unquantified active ingredients [4, 5]. It is very important to promote a full and open discussion on quality control of nature medicine products and nutrient supplements for consumers and professionals. Actually, studies on natural products are challenging by several reasons [6–9]. As nature products are plant-driven, product variation can occur at multiple stages of production, from season variation and identification of plant source to the manufacturing process. More importantly, unlike most modern medications, natural products are typical mixtures that vary greatly. The identity and quantity of the compounds contained within a given natural product is a frequent complication of studies [6]. Even when composition is relatively well understood, the lack of simple and effective analytical methods hampers the ability to extrapolate results beyond quality studied [8]. Furthermore, pharmacological effects of many components in the natural products are still not clear due, in large part, to deficiency of a number of fully developed systems of investigation and predication [9].

This special issue has been driven from the editors' hope that the readers will be able to obtain different kinds of knowledge on natural products from many contributors. Ten publications from original research are encompassing methods and techniques relevant to the detection, separation, purification, identification, and quantification of compounds in biochemistry, cellular and molecular biology,

and biotechnology fields. The authors of this thematic issue are researchers from a wide variety of areas and provide a comprehensive summary of the most recent knowledge and references on quality control of natural products.

From an analytical perspective, this focus issue provides a forum for discussion among researchers engaged in basic scientific work in natural product chemistry. As extraction procedures and ingredients of natural products are a permanently demanding challenge for the analytical chemist, highly efficient techniques to handle the problems associated with sample preparation, separation, and identification have been applied to reduce the complexity of plant materials in this issue. With the development of stationary phases allowing endless possibilities in terms of selectivity, analytical platforms including long-term enhanced ultraviolet-B (UV-B) spectroscopy, FI-NIR based imaging, doubly charged selected ion coupled with mass spectrometry, and liquid chromatography-ultraviolet detection coupled with electrospray ionization quadrupole time-of-flight mass spectrometry (LC-UV-ESI-Q/TOF/MS) have been established to profile and characterize plant materials and/or their extractives. Vibrational spectroscopies offer the advantages of fast, non-invasive, and simultaneous determination of chemical and physical properties being suitable for high-throughput analytical quality control.

From a drug development perspective, this issue provides a forum for scientific research expanding to preclinical studies. Novel approaches have been developed for screening the prototype components and *in vivo* metabolites based on rapid and sensitive techniques. The identification and structural elucidation of the chemical compounds provide essential data for further pharmacological and pharmacokinetic studies. Moreover, two articles are devoted to studying pharmacological effects of natural products. The complexity of single medication or compound preparations has had effect on biological signal transductions in animal models and those studies could provide key information for further exploration. With new technologies for diagnosis, studies on the therapeutic efficacy of natural products are always needed. Therefore, these areas are also included in the issue.

In this special issue, the publications have been included as described above, discussing various aspects of quality control of natural products in detail. More than hundreds of references totally found at the end of each publication will make this thematic issue useful not only for natural product researchers, but also for many scientists working in numerous fields. Much effort has been invested by all the contributing authors, reviewers, editors, and staff to have current information. Without their efforts and input, this issue could not exist. The editors sincerely appreciate the time spent and the knowledge shared in bringing this issue to fruition.

Ying-Yong Zhao
Shuang-Qing Zhang
Feng Wei
Yu-Ming Fan
Feng Sun
Shuhua Bai

References

[1] P. Goldman, "Herbal medicines today and the roots of modern pharmacology," *Annals of Internal Medicine*, vol. 135, no. 8, pp. 594–600, 2001.

[2] R. J. Ko, "A U.S. perspective on the adverse reactions from traditional Chinese medicines," *Journal of the Chinese Medical Association*, vol. 67, no. 3, pp. 109–116, 2004.

[3] W. I. Lu and D. P. Lu, "Impact of chinese herbal medicine on american society and health care system: perspective and concern," *Evidence-Based Complementary and Alternative Medicine*, vol. 2014, Article ID 251891, 6 pages, 2014.

[4] E. Ernst, "Prescribing herbal medications appropriately," *The Journal of Family Practice*, vol. 53, no. 12, pp. 985–988, 2004.

[5] D. H. Phua, A. Zosel, and K. Heard, "Dietary supplements and herbal medicine toxicities-when to anticipate them and how to manage them," *International Journal of Emergency Medicine*, vol. 2, no. 2, pp. 69–76, 2009.

[6] E. Guantai and K. Chibale, "How can natural products serve as a viable source of lead compounds for the development of new/novel anti-malarials?" *Malaria Journal*, vol. 10, supplement 1, article S2, 2011.

[7] J. White, "The challenge of rational development of complex natural products as cancer therapeutics," *Journal of the National Cancer Institute*, vol. 102, no. 12, pp. 834–835, 2010.

[8] M. Hur, A. A. Campbell, M. Almeida-De-Macedo et al., "A global approach to analysis and interpretation of metabolic data for plant natural product discovery," *Natural Product Reports*, vol. 30, no. 4, pp. 565–583, 2013.

[9] K. Kumar and H. Waldmann, "Synthesis of natural product inspired compound collections," *Angewandte Chemie*, vol. 48, no. 18, pp. 3224–3242, 2009.

Hindawi Publishing Corporation
Journal of Analytical Methods in Chemistry
Volume 2014, Article ID 737961, 6 pages
http://dx.doi.org/10.1155/2014/737961

Research Article

The Therapeutic Effect of Zuogui Wan in Gestational Diabetes Mellitus Rats

Yuwei Wang,[1] Qianjin Feng,[2] Xin Niu,[1] Xinshe Liu,[1] Kaixia Xu,[2] Xiangzhu Yang,[1] Huifeng Wang,[1] and Qiuju Li[3]

[1] *Beijing University of Chinese Medicine, No. 11 North Third Ring Road, Chaoyang District, Beijing 100029, China*
[2] *Shanxi University of Traditional Chinese Medicine, No. 89 Jinci road, Taiyuan, Shanxi 030024, China*
[3] *Zhejiang University, Hangzhou, Zhejiang 310058, China*

Correspondence should be addressed to Qianjin Feng; fengqianjin2015@163.com

Received 7 February 2014; Revised 28 June 2014; Accepted 2 July 2014; Published 22 July 2014

Academic Editor: Shuhua Bai

Copyright © 2014 Yuwei Wang et al. This is an open access article distributed under the Creative Commons Attribution License, which permits unrestricted use, distribution, and reproduction in any medium, provided the original work is properly cited.

In this experiment, we established an animal model of gestational diabetes mellitus rats using streptozotocin. Using the rat model of GDM, the pregnant rats in 1-19d were divided into three groups: (1) Zuogui Wan gestational diabetes mellitus group (group I, $n = 12$), (2) gestational diabetes mellitus rats as the control group (group II, $n = 11$), and (3) rats of normal pregnancy group (group III, $n = 11$). Compared with gestational diabetes mellitus rats as the control group, Zuogui Wan can change the indexes of fasting blood glucose, body weight, total cholesterol, insulin, and metabolism cage index significantly in Zuogui Wan gestational diabetes mellitus group. We can conclude that Zuogui Wan has the therapeutic effect on gestational diabetes mellitus.

1. Introduction

Gestational diabetes mellitus (GDM) is a heterogeneous entity, including carbohydrate intolerance of variable severity with onset or first recognition during pregnancy [1]. With rapid development of the society, living standard has been greatly increased, which made a big change to people's diet, lifestyle, and work patterns. The prevalence of gestational diabetes mellitus increased rapidly, which puts a large burden on families and the society. A large scale blood screening survey of pregnant in American showed that the incidence of Asian women with gestational diabetes mellitus was 6.3% [2]. In China, a large scale blood screening survey of pregnant women showed that the incidence of Chinese women with gestational diabetes mellitus was 5.1%, with 7.1% incidence in the South of China and 3.9% incidence in the North of China [3]. Gestational diabetes mellitus seriously affect health of mothers and infants and glucose metabolism of offspring [4–6].

2. Materials

2.1. Experimental Animals. Experimental Wistar rats (female = 100, male = 100) are all adult rats with a body weight between 200 g and 250 g. The experimental animals were provided by Beijing Vital River Laboratory Animal Technology Co., Ltd (License number: SCXK (BJ) 2012-0001). The conduct of the experiments was in accordance with international zoology ethical standards.

2.2. Medicines and Reagent. Materials of Zuogui Wan (*Rehmannia* : yam : *Cornus* : wolfberry : dodder : antler : turtle shell : *Cyathula* 8 : 4 : 4 : 4 : 4 : 4 : 4 : 3) were purchased from Beijing Tong Ren Tang and then verified by Medicine department of Beijing University of Chinese Medicine as genuine. We used ceramics to decoct and extract Chinese herbal medicines. The mass concentration is 1 g·mL^{-1} of dried herbs. Streptozotocin (STZ) was produced by American Sigma Corporation (Batch: B64927). We adjusted STZ dissolving solution to acidity (pH = 4.2) by 0.1 mol/L citric acid buffer solution, which was purchased from Beijing fraternity Port Company. Uric sugar test paper was purchased from Uritest Guilin Medical Electronic Sales Co., Ltd (Batch: 56130184). Chloral hydrate was purchased from Tianjin Fucheng Chemical Reagent Factory. Triglyceride detection kit was purchased from Beijing Wan Tai Derui Diagnostic Technology Co., Ltd (Batch: ZL2103AA02T). Cholesterol detection kit was

purchased from Beijing Wan Tai Derui Diagnostic Technology Co., Ltd (Batch: ZL2105AA31).

2.3. Feed. A basic diet (ID = 1022) and high fat and sugar diet (protein 20%, carbohydrate 20%, and fat 60%) were all purchased from Beijing, China Fukang Biological Technology Co., Ltd (License number: SCXK (BJ) 2009-0008).

2.4. Instruments. Instruments used in this study included blood sugar detector (Johnson stable fold easily type LF033/V02), glucose test strips (Johnson Lot3354358), automatic biochemical analyzer (Toshiba TBA-40PR), rotary microtome, automatic dyeing machine, BX51 microscope, and biological automatic photographic image analysis system.

3. Methods

3.1. Model Preparation

Model Preparation for Pregnant Rats. 100 female rats were fed for one week under the condition of a temperature of 20–22°C, 30%~65% for relative humidity, 150~300Lx for illumination, and 12 : 12 day and night ratio. During the adaptive feeding period, saline ($20\,\text{mL}\cdot\text{kg}^{-1}$) was administered to rats by gavage once a day. One week later, 100 sets of squirrels were fixed in shelves of hanging type. Meanwhile, a tray was placed under each squirrel. 100 female and 100 male rats were put together in cages in which the female/male ratios were 1 : 1. At the same time, two methods were used to examine the pregnant situation of female rats. Firstly, after 12 hours, the method of pessary in tray was used to observe whether there were pessaries (ivory and solid jelly). Then, rats with pessary in tray were taken to do vaginal smears. If sperm had been found by microscopic examination [4], then they were labeled as pregnant rats (0 d). A total of 34 pregnant rats were detected in this experiment. Then the pregnant rats were taken out, 23 were fed with high fat and sugar diet, 11 were fed with basic diet.

Grouping and Treatment. The 34 pregnant rats were divided into three groups: Zuogui Wan gestational diabetes mellitus group ($n = 12$), gestational diabetes mellitus as the control group ($n = 11$), normal pregnancy rats ($n = 11$). Both rats in Zuogui Wan gestational diabetes mellitus group and gestational diabetes mellitus as the control group were feed with high fat and sugar diet. Rats in normal pregnancy group were feed with basic diet. Zuogui Wan decoction (i.e., $1\,\text{g}\cdot\text{mL}^{-1}$, $20\,\text{mL}\cdot\text{kg}^{-1}$) was administered once a day to rats in Zuogui Wan gestational diabetes mellitus group by gavage for 19 days. Saline ($20\,\text{mL}\cdot\text{kg}^{-1}$) was administered once a day to rats in gestational diabetes mellitus group and normal pregnancy group by gavage for 19 days.

Establishment of Model of Rats of Gestational Diabetes Mellitus. The 34 pregnant rats taken from the preparation stage (the first day of pregnancy) were fasted for 12 h. After that, 23 of them were injected peritoneally with dissolved STZ (40 mg/kg) and labelled as Zuogui Wan gestational diabetes mellitus group ($n = 12$) and gestational diabetes mellitus as the control group ($n = 11$) and the remaining 11 rats were labelled as normal pregnant group and received injection of sodium citrate buffer solution. 23 rats were given normal water and high fat and sugar diet after 4 h.The film forming standard of gestational diabetes was fasting blood glucose after 72 h of the injection of STZ $\geq$ 11.1 mmol/L or random blood glucose $\geq$ 16.7 mmol/L and urine glucose > ++. Rats of 4 days pregnancy in Zuogui Wan gestational diabetes mellitus group and gestational diabetes mellitus as the control group were all in accord with film forming standard of gestational diabetes mellitus.

3.2. Detection Index

Observation of General Condition. Fasting blood glucose and weight were observed and recorded in pregnancy, 0, 7, and 14 d. Meanwhile water intake, urinary output, feed intake, and fecal output were observed in pregnancy, 15 d. The rest of the indexes were detected after lactation.

The Detection of Blood Lipid. The serum TC and TG were detected by using enzyme-conjugated colorimetric analysis method by automatic biochemistry analyzer according to the procedures of kits.

Insulin Determination. Blood was drawn from abdominal artery from all rats. All the blood samples were centrifuged to get serum. The insulin level was detected by using enzyme-immunoassay method according to the procedures of kits.

Pathomorphological Observation. We took materials from pancreas. The pancreas was embedded by paraffin, and then we got the slice 4 μm thick by routine paraffin section. Pathomorphological observation of pancreas collected for HE staining was examined by optical microscope.

3.3. Data Processing. Statistics work was completed with SPSS18.0 statistical software. Differences of measurement data were compared with one-way analysis of variance. $P < 0.05$ represented statistical significance. The comparison results were shown by notations as follows: $^{*/\#}P < 0.05$; $^{**/\#\#}P < 0.01$; $^{***/\#\#\#}P < 0.001$.

4. Results

4.1. Observation of General Condition. Rats in normal pregnancy group during pregnancy had good mental status, they were flexible and very active, and they had shiny white hair and had normal feed intake, normal urine, and normal rat tail temperature. Rats in gestational diabetes mellitus as the control group were dizzy and unresponsive, had rough brown hair, and lost hair easily and had an increase in feed intake and water intake and a significant increase in urine output and lower tail temperature. Rats in Zuogui Wan gestational diabetes mellitus group were dysphoric and had shiny brown hair, cool tail, and less hair loss. The food intake, water intake, and urinary output have increased.

Table 1: Impact of Zuogui Wan on fasting blood glucose and body weight in rats of gestational diabetes mellitus.

Group	Fasting blood glucose (mmol·L^{-1})			Body weight (g)		
	GD0	GD7	GD14	GD0	GD7	GD14
Normal pregnancy group (11)	5.32 ± 0.63	5.5 ± 0.55	5.29 ± 0.63	236.32 ± 18.58	263.16 ± 23.54	293.37 ± 30.73
Gestational diabetes mellitus as the control group (11)	5.11 ± 0.70	15.92 ± 4.39***	16.92 ± 8.65***	232.47 ± 12.61	228.32 ± 23.25***	248.67 ± 42.68**
Zuogui Wan gestational diabetes mellitus group (12)	5.23 ± 0.68	13.62 ± 3.55***	11.71 ± 5.55$^{*\#}$	234.99 ± 16.50	237.55 ± 16.05**	264.82 ± 33.15

Note: all results are presented as mean ± S.D. *indicates a significant difference compared with the normal pregnancy group. $^{\#}$indicates a significant difference compared with the gestational diabetes mellitus as the control group. $^{*/\#}P < 0.05$; $^{**/\#\#}P < 0.01$; $^{***/\#\#\#}P < 0.001$.

Table 2: Impact of Zuogui Wan on metabolism cage index in rats of gestational diabetes mellitus.

Group	Water intake (mL/kg/day)	Urinary output (mL/kg/day)	Feed intake (g/kg/day)	Fecal output (g/kg/day)
Normal pregnancy group (11)	139.18 ± 9.47	66.54 ± 9.98	73.09 ± 13.46	17.55 ± 4.70
Gestational diabetes mellitus as the control group (11)	761.18 ± 93.64***	638.82 ± 77.90***	159.82 ± 32.55***	85.18 ± 20.64***
Zuogui Wan gestational diabetes mellitus group (12)	290.50 ± 90.50$^{***\#\#\#}$	202.83 ± 79.57$^{***\#\#\#}$	106.33 ± 29.08$^{**\#\#\#}$	49.42 ± 14.61$^{***\#\#\#}$

Note: all results are presented as mean ± S.D. *indicates a significant difference compared with the normal pregnancy group. $^{\#}$indicates a significant difference compared with the gestational diabetes mellitus as the control group. $^{*/\#}P < 0.05$; $^{**/\#\#}P < 0.01$; $^{***/\#\#\#}P < 0.001$.

4.2. Impact of Zuogui Wan on Physiological Characteristics in Rats of Gestational Diabetes Mellitus

Fasting Plasma Glucose and Body Weight. As can be seen from Table 1, in the first 7 days of pregnancy, fasting plasma glucose was significantly higher ($P < 0.001$) in gestational diabetes mellitus as the control group and Zuogui Wan gestational diabetes mellitus group compared with normal pregnancy group. The means of fasting blood glucose in Zuogui Wan gestational diabetes group were lower than gestational diabetes mellitus as the control group, but the difference was not significant. In the 14th day of pregnancy, compared with gestational diabetes mellitus as the control group, fasting plasma glucose was significantly lower ($P < 0.05$) in Zuogui Wan gestational diabetes mellitus group. In terms of weight, in the 7th day of pregnancy, weight was significantly lower ($P < 0.001$, $P < 0.01$) in gestational diabetes mellitus as the control group and Zuogui Wan gestational diabetes mellitus group. Weight for gestational diabetes mellitus as the control group was lower in the first 7 days of pregnancy than in 0 days of pregnancy. In the first 14 days of pregnancy, compared with the normal pregnancy group, the weight of gestational diabetes mellitus as the control group reduced significantly ($P < 0.01$), but body weight in Zuogui Wan gestational diabetes mellitus group had no significant difference.

Metabolism Cage Index. As can be seen from Table 2, in the 15th day of pregnancy, compared with normal pregnancy group, water intake, urinary output, feed intake, and fecal output were all significantly higher ($P < 0.001$) in the control group and Zuogui Wan gestational diabetes group. Compared with gestational diabetes mellitus as the control group, water intake, urinary output, feed intake, and fecal output were all significantly lower ($P < 0.001$) in Zuogui Wan gestational diabetes mellitus group.

Biochemical Index. It is apparent in Table 3 that, compared with normal pregnancy group, triglyceride and insulin were all significantly higher ($P < 0.001$) in gestational diabetes mellitus as the control group and Zuogui Wan gestational diabetes mellitus group. Total cholesterol was significantly higher in gestational diabetes mellitus as the control group. Compared with gestational diabetes mellitus as the control group, total cholesterol and insulin were all significantly lower ($P < 0.001$) in Zuogui Wan gestational diabetes mellitus group.

Pathomorphological Observation. It is clear from HE staining sections (Figure 1) that morphology and structure of pancreas were normal in normal pregnancy group. Rats in gestational diabetes mellitus as the control group had mild atrophy of islet; B cells swelled and vacuolar degeneration occurred; a little infiltration of inflammatory cells was found in some islets; pancreatic ductal revealed medium dilatation; appeared pancreatic acinar cells of some rats occurred vacuolar degeneration with mild-moderate interstitial inflammatory cells infiltration. Rats in Zuogui Wan gestational diabetes mellitus were mild atrophy of islet; B cells had reduced and a few of pancreatic ducts revealed A medium dilatation which lead to some inflammatory cell infiltrations around.

Graduation statistics method had been given to pancreas in each group according to pancreatic endoscopic diagnostic criteria in Table 4. Compared with gestational diabetes mellitus as the control group, pancreatic lesions in Zuogui Wan gestational diabetes mellitus group reduced significantly ($P < 0.05$) (Table 5).

Table 3: Impact of Zuogui Wan on biochemical index in rats of gestational diabetes mellitus.

Group	Triglyceride ($mmol \cdot L^{-1}$)	Total cholesterol ($mmol \cdot L^{-1}$)	Insulin ($mIU \cdot L^{-1}$)
Normal pregnancy group (11)	0.49 ± 0.11	1.27 ± 0.37	7.68 ± 0.32
Gestational diabetes mellitus as the control group (11)	$0.94 \pm 0.16^{***}$	$2.02 \pm 0.38^{***}$	$9.35 \pm 0.42^{***}$
Zuogui Wan gestational diabetes mellitus group (12)	$0.89 \pm 0.18^{***}$	$1.32 \pm 0.26^{\#\#\#}$	$8.44 \pm 0.55^{***\#\#\#}$

Note: all results are presented as mean ± S.D. *indicates a significant difference compared with the normal pregnancy group. $^{\#}$indicates a significant difference compared with the gestational diabetes mellitus as the control group. $^{*/\#}P < 0.05$; $^{**/\#\#}P < 0.01$; $^{***/\#\#\#}P < 0.001$.

Table 4: Pancreatic endoscopic diagnostic criteria.

Grade	Lesions condition of pancreas
−	Normal morphology and structure of pancreas
+	Inflammatory cell infiltration, B cells swelled and occurred vacuolar degeneration; pancreatic acinar cells of some rates occurred vacuolar degeneration, mild interstitial inflammatory cells infiltration; pancreatic ductal revealed mild dilatation
++	Pancreatic B cells particles depigmentation, swelling and occurred vacuolar degeneration, mild atrophy of islet; the number of pancreatic B reduced slightly

Table 5: Comparison of pancreatic lesions of rats in each group.

Group	N	Pancreatic lesions			Rank sum test Rank values
		−	+	++	
Normal pregnancy group	11	11	0	0	7.50
Gestational diabetes mellitus as the control group	11	1	2	8	24.77
Zuogui Wan gestational diabetes mellitus group	12	2	6	4	20.00

5. Discussion

There are two kinds of model establishment methods of rats in gestational diabetes mellitus. One method is to prepare animal diabetes model in pregnant rats by intravenous injection of alloxan, which was proposed by Yang et al. [7]. As alloxan is poisonous to B cell and unstable, therefore in this study, we made a reference of another GDM proposed by Liu et al. [8], which is established by using streptozotocin. Compared with the alloxan's model, the symptoms by streptozotocin's model of diabetic ketoacidosis and serum free fatty acid are ease, and this model helped us achieve the required results of the experiment. The experiments of Wang et al., [9] confirmed that *Rehmannia glutinosa* oligosaccharides can reduce the blood glucose of gestational diabetes mellitus rats and improve the insulin release. The experiments of Qiu and Li [10] confirmed that *Ophiopogon japonicus* polysaccharide can reduce the blood glucose of gestational diabetes mellitus rats.

Zuogui Wan was first introduced in volume Fifty-one of Jing Yue Quan Shu. It is composed of Big Huai *Rehmannia* 240 g, yam 120 g (frying), medlar (120 g), *Cornus* 120 g, Chuanniuxi 120 g (wine washing and steam mature), dodder 120 g, deer adhesive 120 g (chopping and frying), and glue of tortoise plastron 120 g (chopping and frying). The efficacy of Zuogui Wan is nourishing Yin, tonifying the kidney, replenishing essence, and nourishing marrow. Modern pharmacological studies suggest that catalpol, *Rehmannia glutinosa* oligosaccharides and stachyose in *Rehmannia* has hypoglycemic effect [11–13]; doctors often use yam to treat XiaoKeBing; diosgenin and mannan in yam has hypoglycemic effect [14, 15]; wolfberry polysaccharide in medlar has hypoglycemic effect [16]; ursolic acid in *Cornus* has hypoglycemic effect [17]; Chuanniuxi, dodder, deer adhesive, and glue of tortoise plastron have hypoglycemic effect. Zuogui Wan is composed of the eight kinds of Chinese herbal medicines. So it has a strong hypoglycemic effect and can improve the body immunity efficiently. Experimental study of Yu et al. [18] shows that Zuogui Wan has hypoglycemic effect on the experimental diabetes mellitus rats.

The mechanism of Zuogui Wan reducing blood glucose in diabetic pregnant rats may have a relationship with the fact that the effect of Zuogui Wan can adjust hypothalamic-pituitary-adrenal axis. The balance of hypothalamic-pituitary-adrenal axis in gestational diabetes mellitus rats was destroyed. Zuogui Wan can recover the balance of adrenal axis of gestational diabetes mellitus rats. The experiments of Liu et al. [19] confirmed that Zuogui Wan can significantly

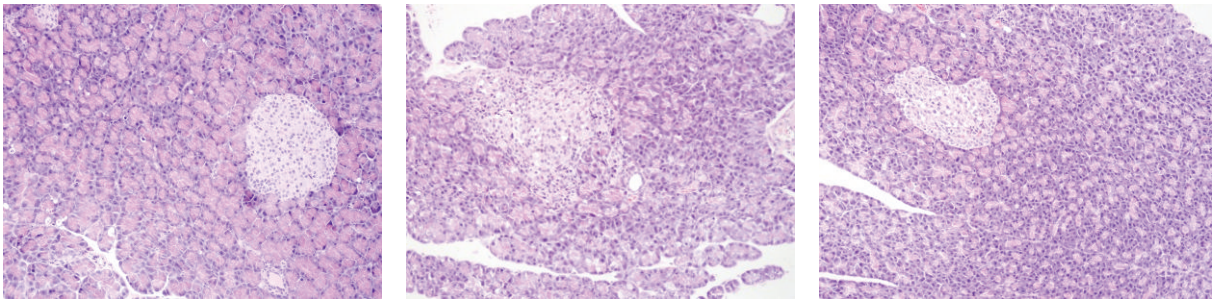

(a) (b) (c)

Figure 1: Comparison of pancreatic morphology of rats in three groups (HE, ×200). (a) Normal pregnancy group: normal pancreas. (b) Gestational diabetes mellitus as the control group: mild atrophy of islet, B cells moderate swelling, and interstitial inflammatory cells infiltration. (c) Zuogui Wan gestational diabetes mellitus group: pancreatic B cells swelled moderately and vacuolar degeneration occurred. The number of pancreatic B cells reduced slightly.

improve retardation caused by hypothalamic arcuate nucleus damaged by monosodium l-glutamate and abnormal proliferation reaction of thymocytes and lymphocytes cells. Gao [20] used Zuogui Wan to treat type 2 diabetic nephropathy. High blood pressure patients took conventional hypoglycemic drugs and at the same time took Zuogui Wan 6 g, 2 times a day. The total effective rate was 78.15%. Feng et al. [21] demonstrated that "Zuogui Wan drugs serum" has a significant role in promoting and improving zygote division of rats using technology of mouse fertilized in vitro. Xu et al. [22] confirmed that using Zuogui Wan in embryonic development of rats can promote intrauterine fetal development and the treatment of intrauterine growth retardation and can make the immune function of adult male offspring better.

What can be seen from the results of this experiment is that Zuogui Wan can reduce fasting blood glucose and maintain a stable growth speed of body weight in rats of gestational diabetes mellitus when Zuogui Wan was given to pregnant rats. Compared with gestational diabetes mellitus as the control group, the means of blood glucose of rats in Zuogui Wan gestational diabetes mellitus group in the first 14 days of pregnancy decreased, but a gap still existed compared with normal blood glucose of rats in normal pregnancy group. Compared with gestational diabetes mellitus as the control group, water intake, urinary output, feed intake, and fecal output were all significantly lower ($P < 0.001$) in Zuogui Wan gestational diabetes mellitus group. The results proved that Zuogui Wan can significantly relieve symptoms of diabetes when given in embryonic rats of gestational diabetes mellitus.

There was no significant difference in total cholesterol between Zuogui Wan gestational diabetes mellitus group and normal pregnancy group. Compared with gestational diabetes mellitus as the control group, total cholesterol and insulin were significantly lower ($P < 0.001$) in gestational diabetes mellitus group. Therefore, it is clear that Zuogui Wan can reduce the level of total cholesterol and insulin when given in embryonic rats of gestational diabetes mellitus. But a gap still existed compared with normal pregnancy group.

Chinese medicine believes that patients with diabetes often have some characteristics like "Yang is usually excessive while Yin is frequently deficient." Maternal gestation period needs blood filling. Gestational diabetes rats must have characteristics of Yin which is often inadequate. The efficacy of Zuogui Wan is nourishing Yin and tonifying the kidney, replenishing essence, and nourishing marrow. Thus, it has a therapeutic effect on the rats of gestational diabetic, but a gap still exists compared with normal pregnancy group. There are two possible reasons to explain this phenomenon. On the one hand, sample size of this study is small. On the other hand, high fat and sugar diet might have some uncontrollable effects. Body weight of rats in gestational diabetes mellitus group grew slowly in this study, which might be attributed to the loss of large quantity of sugar, protein, and some of the nutrients through urine during pregnancy. What is more, Zuogui Wan can maintain a stable growth speed of body weight in rats of gestational diabetes mellitus group when Zuogui Wan was given to pregnant rats. This study provides experimental evidence for the fact that "kidney is responsible for growth, development, and reproduction" and acts as an important basis for later studies of gestational diabetes mellitus.

Conflict of Interests

The authors declare that there is no conflict of interests regarding the publication of this paper.

Acknowledgment

This work was supported by the National Science and Technology Cooperation Projects (no. 0102012DFA31330).

References

[1] S. B. Harris, L. E. Caulfield, M. E. Sugamori, E. A. Whalen, and B. Henning, "The epidemiology of diabetes in pregnant Native Canadians: a risk profile," *Diabetes Care*, vol. 20, no. 9, pp. 1422–1425, 1997.

[2] S. Y. Chu, K. Abe, L. R. Hall, S. Y. Kim, T. Njoroge, and C. Qin, "Gestational diabetes mellitus: all Asians are not alike," *Preventive Medicine*, vol. 49, no. 2-3, pp. 265–268, 2009.

[3] Y. Wei, H. Yang, and X. Gao, "Analysis of the factors of diabetes and its influencing national survey of pregnancy," *Chinese Medical Association of Obstetrics and Gynecology*, vol. 2, 2007, Chinese Medical Association of the first session of the global Chinese Department of gynaecology and obstetrics and the third National Congress of Obstetrics and gynecology in young physician academic conference proceedings.

[4] B. Reusens, S. E. Ozanne, and C. Remacle, "Fetal determinants of type 2 diabetes," *Current Drug Targets*, vol. 8, no. 8, pp. 935–941, 2007.

[5] D. Dabelea and T. Crume, "Maternal environment and the transgenerational cycle of obesity and diabetes," *Diabetes*, vol. 60, no. 7, pp. 1849–1855, 2011.

[6] L. Poston, "Developmental programming and diabetes—the human experience and insight from animal models," *Best Practice and Research: Clinical Endocrinology and Metabolism*, vol. 24, no. 4, pp. 541–552, 2010.

[7] S. Yang, M. Wen, J. Liang, and W. Su, "Intravenous injection of alloxan diabetic pregnancy four preparation of rat animal model," *Journal of Hainan Medical University*, vol. 2, pp. 118–120, 2006.

[8] G. Liu, L. Zhao, H. Liu, and J. Kang, "Experimental study on streptozotocin induced diabetes in pregnancy affect fetal development," *China Journal of Pediatrics*, vol. 1, pp. 26–30, 65, 2008.

[9] X. Wang, Y. Li, Z. Su, and J. Zhao, "The effect of Rehmannia glutinosa oligosaccharides on gestational diabetes mellitus rats blood glucose and insulin levels," *The British Medical Journal*, vol. 3, pp. 204–206, 2007.

[10] B. Qiu and R. Li, "Effect of Ophiopogon japonicus polysaccharide on blood glucose in diabetic pregnant rats," *Journal of Jinan University (Medical Science Edition)*, vol. 4, pp. 367–369, 2008.

[11] J. Liu, *Study on the Mechanism of Reducing Blood Glucose of Rehmannia glutinosa Oligosaccharides*, Lanzhou University, Gansu, China, 2009.

[12] D. Pu, *Rehmannia Catalpol in Enrichment and Purification Process and Evaluation of Hypoglycemic*, Southwestern University, 2011.

[13] R. Zhang, G. Gu, Y. Zhang, and J. Zhou, "Modulatory effects of Rehmannia glutinosa oligosaccharides on glucose metabolism in experimental diabetic and hyperglycemic rats," *Clinical Pharmacology of Traditional Chinese Medicine*, vol. 1, pp. 14–17, 1996.

[14] Z. Hao, B. Hang, and Y. Wang, "Hypoglycemic effect of yam decoction on experimental mice," *Journal of China Medicine University*, vol. 3, pp. 158–160, 1991.

[15] Y. Hang, "Chinese yam drugs on animal hypoglycemic and hypolipidemic effects," vol. 4, pp. 59–60, 1994.

[16] Y. Xinbo, H. Zhengming, C. Wenbin, and C. Hongyan, "Effect of Lycium barbarum polysaccharides on normal mice and alloxan induced hyperglycemia four hyperglycemia mice," *People's Military Medical Pharmacy*, vol. 1, pp. 11–13, 1998.

[17] W. Pi, *Pharmaceutical Research Fruit of Cornus officinalis and Its Treatment of Diabetic Microvascular Complications of Effective Parts*, Nanjing University of Chinese Medicine, 2003.

[18] R. Yu, Y. Wu, J. Ge, and S. Lin, "Experimental study of Zuogui Wan and subtraction experimental diabetic hypoglycemic effect," *China Medicine Science and Technology*, vol. 3, pp. 157–158, 2000.

[19] Y. Liu, D. Cai, X. Chen, and Z. Shen, "Effect of Zuogui Wan on the thymus and lymphocyte proliferative response in MSG-rats," *Journal of Clinical Laboratory Science China*, vol. 4, pp. 3–5, 1998.

[20] S. Gao, "Type 2 diabetic nephropathy therapy of Zuogui Wan," *Traditional Chinese Medicine*, vol. 1, article 98, 2004.

[21] Q. J. Feng, M. Feng, Y. L. Wang, Y. H. Yang, and Y. P. Wu, "Kidney tonifying prescription Zuogui Wan (soup) influence on early embryonic development in mice," *Journal of Integrated Traditional Chinese and Western Medicine Chinese*, vol. 11, pp. 673–675, 1996.

[22] K. Xu, Y. Wang, X. Yang, X. Niu, Y. Liu, and Q. Feng, "Effect of tonifying kidney recipes on the generation of mice nonspecific immune function," *Journal of Clinical Laboratory Science China*, vol. 9, pp. 161–164, 2012.

Hindawi Publishing Corporation
Journal of Analytical Methods in Chemistry
Volume 2014, Article ID 741571, 6 pages
http://dx.doi.org/10.1155/2014/741571

Research Article

Quantitative Analysis of *Panax ginseng* by FT-NIR Spectroscopy

Xin-fang Xu,[1] Li-xing Nie,[2] Li-li Pan,[1] Bian Hao,[1] Shao-xiong Yuan,[1] Rui-chao Lin,[1] Hai-bo Bu,[1] Dan Wang,[1] Ling Dong,[1] and Xiang-ri Li[1]

[1] *School of Chinese Materia Medica, Beijing University of Chinese Medicine, No. 6 Wangjing Zhonghuannan Road, Beijing 100102, China*
[2] *National Institutes for Food and Drug Control, State Food and Drug Administration, No. 2 Tiantan Xili, Beijing 100050, China*

Correspondence should be addressed to Ling Dong; dongling@bucm.edu.cn and Xiang-ri Li; lixiangri@sina.com

Received 20 January 2014; Revised 21 March 2014; Accepted 14 April 2014; Published 5 May 2014

Academic Editor: Feng Sun

Copyright © 2014 Xin-fang Xu et al. This is an open access article distributed under the Creative Commons Attribution License, which permits unrestricted use, distribution, and reproduction in any medium, provided the original work is properly cited.

Near-infrared spectroscopy (NIRS), a rapid and efficient tool, was used to determine the total amount of nine ginsenosides in *Panax ginseng*. In the study, the regression models were established using multivariate regression methods with the results from conventional chemical analytical methods as reference values. The multivariate regression methods, partial least squares regression (PLSR) and principal component regression (PCR), were discussed and the PLSR was more suitable. Multiplicative scatter correction (MSC), second derivative, and Savitzky-Golay smoothing were utilized together for the spectral preprocessing. When evaluating the final model, factors such as correlation coefficient (R^2) and the root mean square error of prediction (RMSEP) were considered. The final optimal results of PLSR model showed that root mean square error of prediction (RMSEP) and correlation coefficients (R^2) in the calibration set were 0.159 and 0.963, respectively. The results demonstrated that the NIRS as a new method can be applied to the quality control of *Ginseng Radix et Rhizoma*.

1. Introduction

Ginseng, the dried root and rhizome of *Panax ginseng* C.A. Meyer, [1] is one of the most famous and valuable traditional Chinese herbs in Asia. In recent years, it has been widely used for making functional foods in many other countries like in Europe and in the USA. Ginsenosides are confirmed to be the principal active compounds of ginseng and its products. Ginsenosides are named as "Rx," where the "R" stands for the root and the "x" describes the chromatographic polarity in an alphabetical order [2]. According to different aglycones, ginsenosides can be classified into three types: the 20(S)-protopanaxadiol type such as ginsenoside Rb_1, Rc, Rb_2, and Rd, the 20(S)-protopanaxatriol type such as ginsenoside Rg_1 and Re, and the oleanolic acid type including ginsenoside Ro and polyacetyleneginsenoside Ro, respectively. There are compositional differences between the types of ginseng with respect to the 7 fingerprint ginsenosides (Rb_1, Rb_2, Rc, Rd, Re, Rg_1, and Rf) that are often measured to standardize ginseng extracts. With the exception of Rf, the 6 ginsenosides are the most abundant ginsenosides in the *Panax ginseng* [3]. Even the rare ginsenosides such as ginsenoside Rb_3, Rf, and Rg_2 also have significant pharmacological activities [4]. Ginsenosides have many pharmaceutical effects, for example, an anticarcinogenic effect, an immune-modulatory effect, anti-inflammatory, antiallergic effects, and so on [5]. In general, ginseng and even a single compound of ginsenoside produce their effects on multiple sites of action, which makes it an ideal candidate to develop multitarget drugs. Recently, ginsenosides have been found to play an important role in the central nervous system. These diseases are prevalent all over the world, which include Alzheimer's disease, Parkinson's disease, cerebral ischemia, depression, and many other neurological disorders including neurodevelopmental disorders [6].

The analysis of ginsenosides has been performed with various analytical methods such as thin layer chromatography (TLC) [7], GC [8], high performance liquid chromatography (HPLC) [9], capillary electrophoresis [10], tandem instrumentation of high performance liquid chromatography with mass spectroscopy (HPLC-MS) [11], and enzyme

immunoassay [12], while the high performance liquid chromatography has been routinely used. But all these methods need complex preliminary treatments of the samples; meanwhile they also spend a lot of time and energy. Additionally, many methods of quantitative analysis must have the standards of ginsenosides as reference.

By contrast, the near-infrared spectrometry (NIRS) technology is an appropriate alternative method. NIRS has been widely applied in various areas, such as foods, pharmaceuticals, and petroleum [13, 14]. The advantages of this technique are mainly attributed to its speed, economy, accuracy, and precision in comparison with other analytical techniques. Recently, NIRS has been widely employed in the study of traditional Chinese herbs for qualitative analysis [15] and quantitative analysis [16]. Liu et al. [17] have developed a method for the determination of ginsenoside Rb_1, Re, and Rb_1, as well as the total ginsenosides in folium ginseng by near-infrared spectroscopy.

In the study, the total amount of nine different ginsenosides (ginsenoside Rb_1, Rb_2, Rb_3, Rc, Rd, Re, Rf, Rg_1, and Rg_2) in *Panax ginseng* was determined. A new analytical method was developed using FT-NIR with multivariate regression methods. This is the first report for the quantitative analysis of the total amount of nine ginsenosides in ginseng by NIRS.

2. Experiment Methods

2.1. Sample Preparation. 56 ginseng samples, in which 29 samples were from Fusong County of Jilin province of China, 20 samples from Ji'an City of Jilin province, and 7 samples from Tonghua County of Jilin province, were collected for the content determination. These 56 samples were pulverized into powder and sieved on a sieve of 65 meshes. To ensure the moisture did not interfere as far as possible, these 56 samples were heated for 6 h at 50°C in a dryer.

All of these samples were identified by Professor Xiangri Li (School of Chinese Materia Medica, Beijing University of Chinese Medicine) and deposited in the specimen cabinet of traditional Chinese medicine of Beijing University of Chinese Medicine.

2.2. NIR Spectra Collection. Near-infrared diffuse reflectance spectra of ginseng samples were acquired using an NIR system (Thermo Electron Corp., USA) with an Integrating Sphere Module over the wavenumber range of 10000–4000 cm^{-1} and recorded in absorbance with air as the reference standard. The spectra were collected at the resolution of 8 cm^{-1} and the interval of 2 cm^{-1} per spectrum by averaging 64 scans. The InGaAs detector and the software of RESULT 3.0 were used to collect the NIR spectra.

2.3. Determination of Nine Kinds of Ginsenosides. The chemical structures of the nine ginsenosides are shown in Figure 1. We developed a method for simultaneous determination of nine kinds of ginsenosides [18]. Table 1 lists the linear regression equations of these nine kinds of ginsenosides.

For each sample, 0.4 g of powder, precisely weighed, was extracted by refluxing twice with 50 mL of methanol for 60 min each time. After cooling, both extracts were evaporated to dryness and then dissolved in and diluted to the volume scale by methanol in a 10 mL volumetric flask. This solution was filtered through a 0.45 μm membrane filter and injected into the HPLC system.

A Waters 1525 HPLC system consisting of four pumps, on line degasser, a thermostat maintained at 30°C, and a Waters 2487 UV detector was used in this study. The chromatographic separation was accomplished on an Agilent Zorbax column SB-C18 (250 × 4.6 mm, 5 μm). The mobile phase consisted of (A) H_2O and (B) acetonitrile (v/v). The linear gradient program was shown in Table 2. The flow rate was set at 1.0 mL/min and the sample injection volume was 10 μL. The absorbance was measured at a wavelength of 203 nm.

2.4. Spectral Data Preprocessing. While the spectral data was acquired by the NIR instrument, the noise, baseline drift, and scatter effects have simultaneously appeared in the spectra. It is indispensable to preprocess the spectra before modeling. Multiplicative scatter correction (MSC) [19] was developed to eliminate the scatter effects caused by different particle size distribution. The processing by spectral derivatives [20] can protect against the influence of baseline drift. It was effective to discriminate overlapping peaks and increase the resolution and sensitivity. To avoid enhancing the noise induced by the derivatives, the spectra need to be smoothed. The frequently used smoothing methods are the Savitzky-Golay (SG) filter [21] and the Norris derivative (ND) filter.

2.5. Multiple Multivariate Regression Methods and Software. Partial least square regression (PLSR) and principal component regression (PCR) were used to establish the quantitative models in the study [22]. The performance of the final model was evaluated in terms of RMSEC, RMSEP, and R^2. The models in this study were all conducted with the chemometric software TQ analyst 7.2 (Thermo Electron Corp., USA).

3. Results and Discussion

3.1. Results and Analysis of Content Determination. The results which determined by HPLC were regarded as actual values (or called reference values) to establish the calibration models. Before the modeling of NIR, the Chauvenet test [23] was applied to find the spectral outliers at the 90% confidence level using the TQ software. The spectra that failed the Chauvenet test were judged as spectral outliers and neglected firstly. After the test, 4 spectral outliers were removed from the ginsenosides model.

The remaining 52 samples were divided into the calibration set and the validation set with the ratio of 3 : 1. For each model, the calibration set was used to develop the calibration model and the validation set was used to predict the calibration model. This can make sure that the model was stable and precise. It must be guaranteed that the ranges of the actual values in the validation set cover the values in validation set (see Table 3). The best calibration equation for each analysis was selected in terms of the lowest

Table 1: The linear regression equations of nine ginsenosides.

Ginsenoside	Regression equation	Linear ranges/μg	R^2
Rg_1	$Y = 383524X - 65359$	0.456–2.280	0.9997
Rb_1	$Y = 3080694X - 2960$	0.516–2.580	0.9999
Re	$Y = 375112X - 76321$	0.382–1.910	0.9994
Rf	$Y = 407560X - 43377$	0.174–0.870	0.9999
Rc	$Y = 290956X - 62647$	0.342–1.710	0.9999
Rb_2	$Y = 288739X - 46577$	0.253–1.270	0.9998
Rg_2	$Y = 469440X - 23253$	0.034–0.170	0.9998
Rb_3	$Y = 419332X - 14938$	0.029–0.150	0.9998
Rd	$Y = 650313X - 24730$	0.068–0.340	0.9993

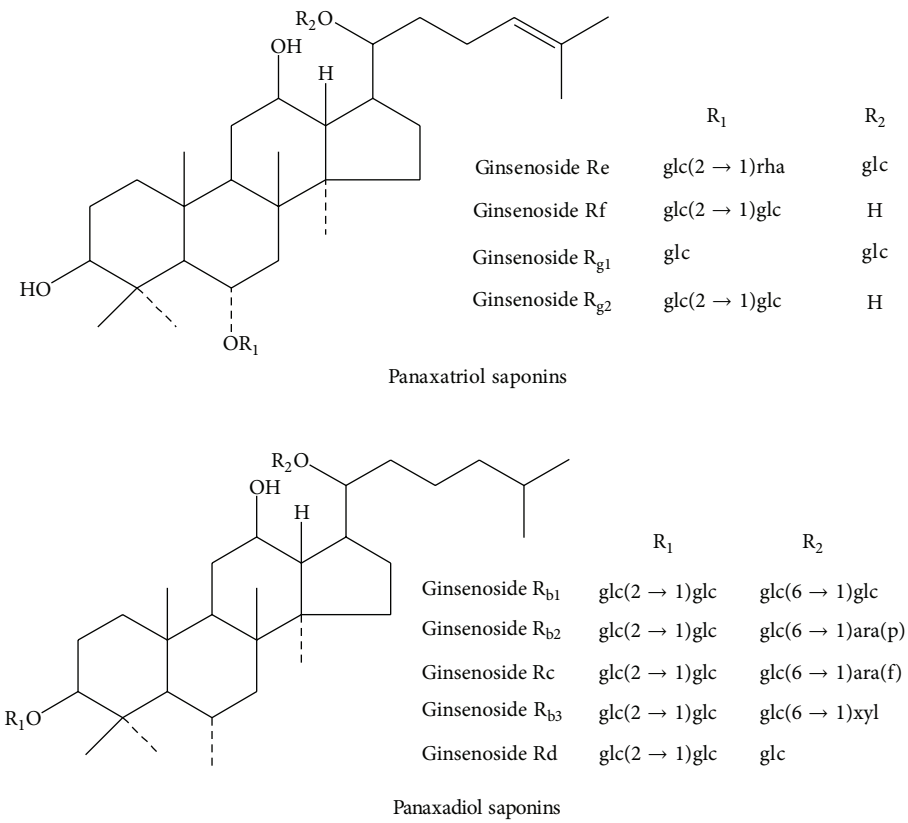

Figure 1: Chemical structures of the nine ginsenosides.

Table 2: The linear gradient program of nine kinds of ginsenosides.

	Time (min)								
	0	30	45	60	90	100	105	110	120
H_2O-A (%)	81	81	72	72	65	60	5	81	81
Acetonitrile-B (%)	19	19	28	28	35	40	95	19	19

Table 3: The content ranges of ginsenosides from calibration and validation set.

	Sets	Number of samples	Rang (%)	Mean (%)
Ginsenosides	Calibration set	39	0.63–1.70	0.83
	Validation set	13	1.42–1.70	1.49

root mean square error of cross-validation (RMSECV), root mean square error of calibration (RMSEC), root mean square error of prediction (RMSEP), and the highest correlation coefficient (R^2).

3.2. NIR Calibration Model

3.2.1. Spectral Regions Choosing. NIR spectra of samples are shown in Figure 2(a). It can be easily found that the spectral regions, 10000–9000 cm^{-1} and 4100–4000 cm^{-1}, present

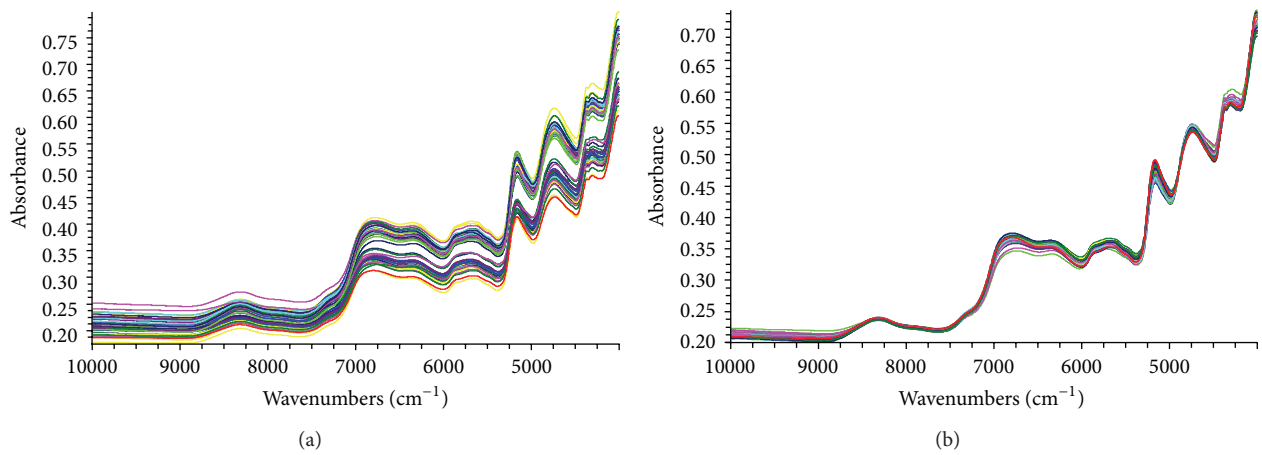

Figure 2: NIR spectra of ginseng samples obtained from original data (a) and MSC processing (b).

Table 4: Optimization of spectra processing in carlibration models.

Preprocessing	RMSEP	RMSEC	R^2
MSC + SG	0.254	0.302	0.656
MSC + SG + 1st derivative	0.266	0.186	0.886
MSC + SG + 2nd derivative	0.159	0.083	0.963
MSC + ND + 1st derivative	0.252	0.269	0.739
MSC + ND + 2nd derivative	0.403	0.124	0.852

Table 5: RMSEC, RMSEP, and R^2 for the calibration models.

Algorithm	RMSEP (%)	RMSEC (%)	R^2
PLSR	0.159	0.083	0.963
PCR	0.360	0.233	0.673

a high noise level. When choosing the modeling regions, the above spectral absorption information must not be neglected. After many trials, 8367.18–4242.6 cm^{-1} for ginsenosides was chosen to establish the calibration models.

3.2.2. Spectral Preprocessing. Figure 2 shows the spectra acquired from original data and MSC processing. The great change is that the differences of all the NIR spectra get much smaller after MSC processing. The spectra preprocessing was chosen (Table 4) by the lowest RMSEP and RMSEC and the highest R^2. The optimum spectra processing was MSC + SG + 2nd derivative and was used for the total amount of nine ginsenosides. It also can be observed that the main absorption peaks are distributed in the selected region from Figure 3.

3.2.3. Effect of Statistical Model. Table 5 shows the model results with the different statistical algorithms. PLSR was superior to PCR for developing the calibration model for the total amount of nine ginsenosides between the two statistical models.

3.2.4. Optimization of Factors of Models. Each calibration model has an optimum number of factors. The appropriate number of factors can be used for preventing the occurrence of underfitting and overfitting. The optimum numbers of factors were chosen according to which corresponded to the lowest RMSECV obtained by leave-one-out cross-validation (LOOCV) [24]. The optimum numbers of factors were 4 in the model of ginsenosides.

3.2.5. Best Calibration Models. Usually, RMSEC, RMSEP, and corresponding R^2 values are used for evaluating the NIR calibration models. Table 5 lists the RMSEC, RMSEP, and R^2 data for the optimum calibration equations of the total amount of nine ginsenosides using the above optimum parameters. Correlation diagram between the NIR model calculated values and the actual values is shown in Figure 4. It can be observed that the correlation coefficient of calibration model is 0.963, which shows a good correlation between the actual values and the NIR model calculated values. Additionally it is also suggested that the stable and precise model established can be used for quantitative analysis of the chemical compositions in *Ginseng Radix et Rhizoma*.

4. Conclusions

A method for determining the total amount of nine ginsenosides in *Panax ginseng* was developed using FT-NIR with multivariate regression methods for the first time. The results indicate that the model is precise and stable and has the good properties of prediction. Compared with traditional methods such as HPLC and TLC, NIRS has great merits for nondestruction, convenience, and environmental protection. Ginsenosides in *Panax ginseng* can be analyzed quickly and easily from the study. Additionally, it provides a new idea for the quality control of *Panax ginseng* in many commodities.

Disclosure

Xin-fang Xu and Li-Xing Nie are the first coauthors.

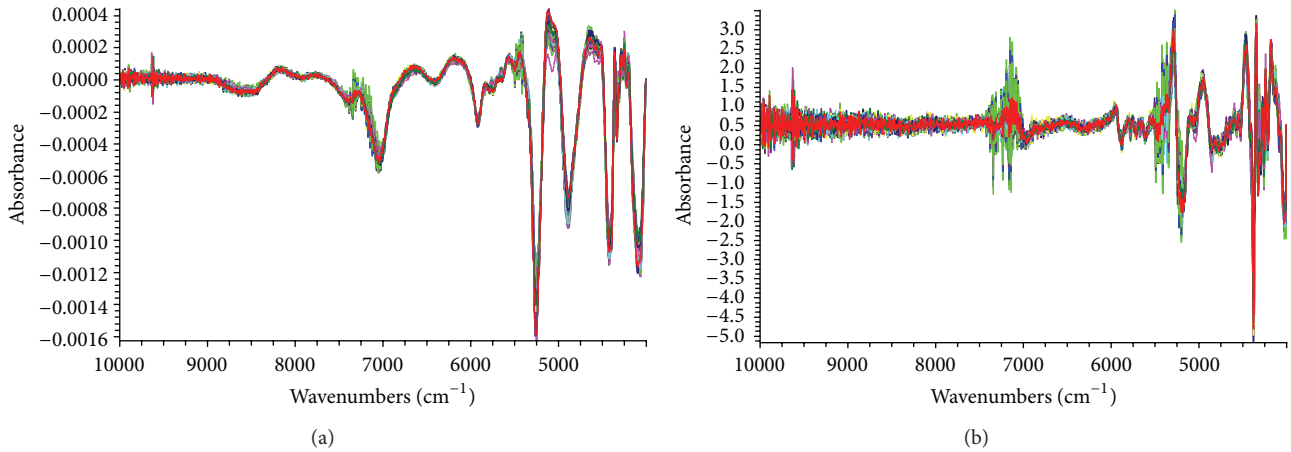

Figure 3: NIR spectra for ginseng samples processed by 1st derivative + SG + MSC (a) and MSC + SG + 2nd derivative (b).

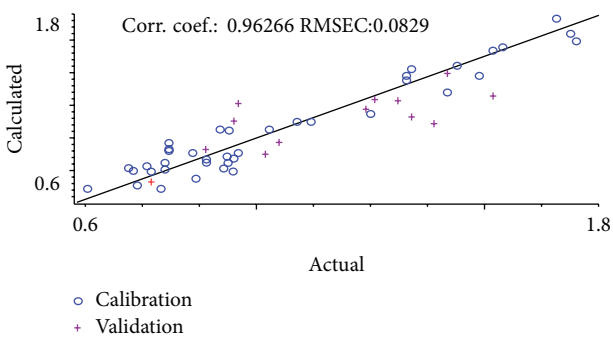

Figure 4: Correlation diagram between the NIR model calculated values and the actual values of the total amount of nine ginsenosides.

Conflict of Interests

The authors declare that there is no conflict of interests regarding the publication of this paper.

Authors' Contribution

Ling Dong and Xiang-ri Li have contributed equally to this project.

Acknowledgments

This study was supported by Grants from the National Natural Science Foundation of China (no. 81073041 and no. 81274081) and Specialized Research Fund for the Doctoral Program of Higher Education of China (no. 20100013120010).

References

[1] Chinese Pharmacopeia Committee, *Pharmacopeia of People's Republic of China*, Chinese Medicine Science and Technology, Beijing, China, 2010.

[2] S. Shibata, M. Fujita, H. Itokawa, O. Tanako, and T. Ishii, "Studies on the constituents of Japanese and Chinese crude drugs. XI. Panaxadiol, a sapogenin of ginseng roots," *Chemical & Pharmaceutical Bulletin*, vol. 11, no. 6, pp. 759–761, 1963.

[3] D. G. Popovich, C.-R. Yeo, and W. Zhang, "Ginsenosides derived from Asian (*Panax ginseng*), American ginseng (*Panax quinquefolius*) and potential cytoactivityl," *International Journal of Biomedical and Pharmaceutical Sciences*, vol. 6, no. 1, pp. 56–62, 2012.

[4] Y. Wei, W. Zhao, Q. Zhang, Y. Zhao, and Y. Zhang, "Purification and characterization of a novel and unique ginsenoside Rg_1-hydrolyzing β-D-Glucosidase from *Penicillium sclerotiorum*," *Acta Biochimica et Biophysica Sinica*, vol. 43, no. 3, pp. 226–231, 2011.

[5] L. P. Christensen, "Chapter 1 Ginsenosides: chemistry, biosynthesis, analysis, and potential health effects," *Advances in Food and Nutrition Research*, vol. 55, pp. 1–99, 2008.

[6] J. K. Hee, K. Pitna, and Y. S. Chan, "A comprehensive review of the therapeutic and pharmacological effects of ginseng and ginsenosides in central nervous system," *Journal of Ginseng Research*, vol. 37, no. 1, pp. 8–29, 2013.

[7] J. Corthout, T. Naessens, S. Apers, and A. J. Vlietinck, "Quantitative determination of ginsenosides from *Panax ginseng* roots and ginseng preparations by thin layer chromatography-densitometry," *Journal of Pharmaceutical and Biomedical Analysis*, vol. 21, no. 1, pp. 187–192, 1999.

[8] E. W. Chung, W. H. Kwok, D. K. K. Leung et al., "Detection and confirmation of ginsenosides in horse urine by GC-MS and LC-MS," *Chromatographia*, vol. 69, no. 9-10, pp. 923–932, 2009.

[9] F.-Q. Chen, J.-G. Luo, and L.-Y. Kong, "Determination of 10 ginsenosides in *Panax ginseng* of different harvest times based on HPLC fingerprints and principal component analysis," *Natural Product Research*, vol. 27, no. 9, pp. 851–854, 2013.

[10] S. Ye, S.-F. Wang, H.-B. Qu, and Y.-Y. Cheng, "Separation and determination of five saponins in Fufang Danshen Pian by reversed migration micellar electrokinetic chromatography," *Chinese Journal of Analytical Chemistry*, vol. 35, no. 1, pp. 115–118, 2007.

[11] Y. Liang, T.-Y. Guan, Y. Zhou et al., "Effect of mobile phase additives on qualitative and quantitative analysis of ginsenosides by liquid chromatography hybrid quadrupole-time of flight mass spectrometry," *Journal of Chromatography A*, vol. 1297, pp. 29–36, 2013.

[12] B. Sritularak, O. Morinaga, C.-S. Yuan, Y. Shoyama, and H. Tanaka, "Quantitative analysis of ginsenosides Rb1, Rg1, and Re in American ginseng berry and flower samples by ELISA using monoclonal antibodies," *Journal of Natural Medicines*, vol. 63, no. 3, pp. 360–363, 2009.

[13] S. A. Haughey, S. F. Graham, E. Cancouët, and C. T. Elliott, "The application of Near-Infrared Reflectance Spectroscopy (NIRS) to detect melamine adulteration of soya bean meal," *Food Chemistry*, vol. 136, no. 3-4, pp. 1557–1561, 2013.

[14] G. P. Sabin, V. A. Lozano, W. F. C. Rocha, W. Romão, R. S. Ortiz, and R. J. Poppi, "Characterization of sildenafil citrate tablets of different sources by near infrared chemical imaging and chemometric tools," *Journal of Pharmaceutical and Biomedical Analysis*, vol. 85, pp. 207–212, 2013.

[15] H.-B. Bu, L.-X. Nie, D. Wang, H. Du, G.-L. Wang, and X.-R. Li, "Nondestructive identification of the root of mountain cultivation ginseng and growth years by near infrared spectroscopy," *Spectroscopy and Spectral Analysis*, vol. 32, no. 7, pp. 1801–1805, 2012.

[16] Y. Chen, M.-Y. Xie, H. Zhang, Y. Wang, S. Nie, and C. Li, "Quantification of total polysaccharides and triterpenoids in *Ganoderma lucidum* and *Ganoderma atrum* by near infrared spectroscopy and chemometrics," *Food Chemistry*, vol. 135, no. 1, pp. 268–275, 2012.

[17] H. Liu, X. Zhao, T. Qi, Y. P. Qi, and G. R. Fan, "Establishment of the model for online monitoring of the column separation and purification process by near-infrared spectroscopy and determination of total ginsenosides in Folium Ginseng," *Spectroscopy and Spectral Analysis*, vol. 33, no. 12, pp. 3226–3230, 2013.

[18] S. Li, D. Wang, J. Lv, and X. Li, "Study of quantitative determination of nine ginsenosides in *Panax ginseng*," Paper Symposium in Chinese Crude Drugs Preparations Branch of China Association of Chinese Medicine in 2011, 2011.

[19] M. R. Maleki, A. M. Mouazen, H. Ramon, and J. de Baerdemaeker, "Multiplicative scatter correction during on-line measurement with near infrared spectroscopy," *Biosystems Engineering*, vol. 96, no. 3, pp. 427–433, 2007.

[20] Å. Rinnan, F. V. D. Berg, and S. B. Engelsen, "Review of the most common pre-processing techniques for near-infrared spectra," *TrAC Trends in Analytical Chemistry*, vol. 28, no. 10, pp. 1201–1222, 2009.

[21] B. Zimmermann and A. Kohler, "Optimizing Savitzky-Golay parameters for improving spectral resolution and quantification in infrared spectroscopy," *Applied Spectroscopy*, vol. 67, no. 8, pp. 892–902, 2013.

[22] Y.-F. Xie, Y. Song, Y. Zhang, and B. Zhao, "Near-infrared spectroscopy quantitative determination of Pefloxacin mesylate concentration in pharmaceuticals by using partial least squares and principal component regression multivariate calibration," *Spectrochimica Acta A: Molecular and Biomolecular Spectroscopy*, vol. 75, no. 5, pp. 1535–1539, 2010.

[23] Q. Zhang and S. L. Wu, *Measurement Error and Data Processing*, Tsinghua University Press, Beijing, China, 2010.

[24] R. Brereton, *Chemometrics for Pattern Recognition*, John Wiley & Sons, New York, NY, USA, 2009.

Hindawi Publishing Corporation
Journal of Analytical Methods in Chemistry
Volume 2014, Article ID 502626, 6 pages
http://dx.doi.org/10.1155/2014/502626

Research Article

Studies on the Anti-Inflammatory Effect and Its Mechanisms of Sophoridine

Xiumei Huang,[1,2] Bo Li,[1] and Lianzhong Shen[1]

[1] *National Institutes for Food and Drug Control, Beijing 100050, China*
[2] *Qinghai Province Institute for Food and Drug Control, Xining 810003, China*

Correspondence should be addressed to Xiumei Huang; 912174631@qq.com

Received 21 February 2014; Accepted 20 March 2014; Published 9 April 2014

Academic Editor: Yu-Ming Fan

Copyright © 2014 Xiumei Huang et al. This is an open access article distributed under the Creative Commons Attribution License, which permits unrestricted use, distribution, and reproduction in any medium, provided the original work is properly cited.

This work is to study the anti-inflammatory effect and its mechanisms of sophoridine in vitro and in vivo. For this aim, the influences of sophoridine on several inflammatory mediators were investigated. Excessive inflammatory response in vitro model was developed by using lipopolysaccharide (LPS) to stimulate the mouse peritoneal macrophages and HL-60 cells to produce IL-6 and IL-8. Carrageenin-induced mouse paw edema model was used as inflammatory response in vivo model. MTT method, ultraviolet spectrophotometric method, and radioimmunoassay were used to measure the changes of TNFα, IL-6, PGE_2, and IL-8 in in vitro cell culture supernatant or in the local inflammatory exudates. The results showed that sophoridine inhibited the production of IL-8 in in vitro cell culture supernatant and inhibited the production of TNFα, PGE_2, and IL-8 in the local inflammatory exudates but had no significant effects on the production of IL-6 in vitro and in vivo. It is demonstrated that sophoridine's anti-inflammatory effect was due to its ability to inhibit the production of cytokine and inflammatory mediators.

1. Introduction

Inflammation is a complex physiological and pathological process accompanied by the activation of the immune system, local vascular system, and various cells within the damaged tissue. During an inflammatory process cells become activated and several mediators, such as inflammatory cytokines (TNFα, IL-6, and IL-8) and inflammation media (PGE_2, histamine), are released.

The inflammation model of carrageenin-induced edema is usually used to assess the activity of natural products in inhibiting the pathological changes associated with acute inflammation. Carrageenin can induce acute inflammation by increasing infiltration of phagocytes and oxidative stress as well as release of inflammatory mediators.

Sophoridine (SRI, $C_{15}H_{24}N_2O$, relative molecular weight 248.36) is a quinolizidine alkaloid. SRI is also called matridine-15-one (allomatrine). It exists in overground part of Leguminous plant *Sophora alopecuroides* L., overground part of *Euchresta japonica* Benth., and root of *Sophora alopecuroides* Ait. It has been reported that SRI has marked pharmacological activity on anti-inflammatory [1–4], antitumor [5–7], and antivirus [8, 9]. In our preliminary studies [10–13], we had reported some of the anti-inflammatory effects and the mechanism of SRI, including the inhibitory effects on TNFα production by murine peritoneal macrophages, the effect on COX in supernatant of cultured macrophages, the effect on leukotrienes (LTC_4 and LTB_4) biosynthesis in cells, and the effect on histamine in isolated tracheal smooth muscle and the isolated ileum of guinea pig. This work is to study the anti-inflammatory action and its mechanisms of sophoridine on cells and in vivo models continuously. For this aim, the influences of sophoridine on several inflammatory mediators IL-6 and IL-8 in LPS-stimulated mouse peritoneal macrophages and HL-60 cells and the influences of sophoridine on TNFα, IL-6, IL-8, and PGE_2 in the inflammatory exudates of carrageenin-induced mouse paw edema model were investigated.

2. Materials

Sophoridine (SRI, white crystal, freely soluble in water) was provided by Pharmacology Department of National

Institutes for Food and Drug Control. Ibuprofen (Batch no. 2000704) was purchased from Anhui Huaen Pharm Co. Ltd. Actinomycin D, lipopolysaccharide (LPS) (Batch no. L2880), thiazolyl blue (MTT), and arachidonic acid (AA) (A3555-10MG) were purchased from Sigma. Brewer thioglycollate medium (BTM) was the product of Difco. RPMI-1640 culture medium was purchased from Gibco. Fetal bovine serum (FBS) was purchased from Hyclone. Carrageenin (Batch no. 021M0038V) was purchased from Sigma. rhlL-6 was provided by Bioassay Department of National Institutes for Food and Drug Control. L929 cell strain (Mouse fibroblast cell strain) and HL-60 cell strain (Human promyelocytic leukemia cells) were provided by Pharmacology Department of National Institutes for Food and Drug Control. 7TD1 cell strain (IL-6 dependent cell strain) was kindly provided as a gift by Academician Beifen Shen (Worked in the third institute of Academy of Military Science). ^{125}I-lL-8 radioimmunoassay kit was purchased from East Asia Immune Technology Institute (Beijing).

3. Instruments

RS-232C Microplate Reader (Labsystems, Finland), IMT-2 phase-contrast microscope (Olympus, Japan), Radioimmunoassay counter (LKB-Wallac CliniGamma 1272-002, Finland), Low temperature normal speed centrifuge (Hettich, Germeny), MP230 pH meter (METTLER, Switchland).

4. Animals

Male C57BL/6 mice (6~8 weeks) and male and female Kunming mice, body weight 18~23 g, were obtained from Experimental Animal breeding Center of National Institutes for Food and Drug Control.

5. Methods

5.1. The Influences of SRI on the Production of IL-6 in LPS-Stimulated Mouse Peritoneal Macrophages: Preparation of the Mouse Peritoneal Macrophages and Calculation of the SRI Concentration Range Which Does Not Influence the Normal Growth of Peritoneal Macrophages. The methods were the same as previously described [14]. Briefly, each male C57BL/6 mice was given an intraperitoneal injection of 1 mL 3% sodium thioglycollate solution. The animals were sacrificed after 4 days. The peritoneal macrophages were washed out with phosphate buffer solution (PBS) under a sterile environment and were washed twice with RPMI-1640 (contained 5% FBS). The cells were counted and adjusted to 2×10^6 cells per mL.

The 96-cell culture plate, which contained 100 μL macrophage suspension (2×10^6 cells/mL) each well, was incubated at 37 ± 0.5°C under 5% CO_2 humidified air for 2 hours. 100 μL SRI solutions (concentration range 1×10^{-8}~1×10^{-6} mol/L) were added and the plate was incubated continually for 20 hours under the same condition. 50 μL MTT (2.5 mg/mL) was added each well and the plate was incubated for 4 hours. The supernatant solutions were discarded; 100 μL dimethyl sulfoxide (DMSO) was added each well and mixed thoroughly. The OD values were determined at 570 nm on Microplate Reader after 5 minutes.

5.2. The Culture of Mouse Peritoneal Macrophages and Drug Treatment. 200 μL macrophage suspension (2×10^6 cells/mL) was added to 48-cell culture plate and incubated for 2 hours at 37 ± 0.5°C in 5% CO_2 humidified air. The nonadherent cells were washed away with PBS. 200 μL RPMI-1640 culture medium (contained 10% FBS) was added to each well, and 200 μL SRI solutions at different concentrations were added. After 0.5 hours of incubation, 50 μL irritant agent lipopolysaccharide (LPS, 25 μg/mL) was added to each well. Incubate the plate again for 24 hours before the supernatants were collected for the measurement of IL-6.

5.3. Determination of IL-6 [15]. 50 μL supernatant was added to 96-cell culture plate, and then 50 μL 7TD1 cell suspension (1.2×10^5 cells/mL) was added. After 48 hours incubation, MTT (5 mg/mL) 20 μL was added to each well, and incubated for 4 hours. After Centrifuged under low temperature, the supernatant discarded, then DMSO 100 μL was added to each well, mixed and detected the OD values at 570 nm on Microplate Reader. The decrease of the OD value in drug group indicated that the production of IL-6 in mouse peritoneal macrophages is inhibited by the drug, which was expressed in inhibition percentage. Inhibition percentage (%) = $(OD_{LPS} - OD_{Drug})/OD_{LPS} \times 100\%$. Samples were assayed in triplicate and results are reported at means (±SD).

5.4. The Influence of SRI on the Production of IL-8 in LPS-Stimulated HL-60 Cells: Calculation of the SRI Concentration Range Which does not Influence the Normal Growth of HL-60 Cells. The methods were as previously described [14]. Briefly, 100 μL HL-60 cell suspension (10^5 cells/mL) was added to the 96-cell culture plate and incubated at 37 ± 0.5°C under 5% CO_2 humidified air for 2 hours. 100 μL SRI solutions (concentration range 1×10^{-8}~1×10^{-6} mol/L) were added; the plate was incubated continually for 20 hours under the same condition. 50 μL MTT (2.5 mg/mL) was added each well; the plate was incubated for 24 hours. The supernatant solutions were discarded after centrifuging under low temperature. 100 μL dimethyl sulfoxide (DMSO) was added each well and mixed thoroughly; the OD values were determined at 570 nm on Microplate Reader after 5 minutes.

5.5. The Culture of HL-60 Cells and Drug Administration. HL-60 cells were cultured in RPMI-1640 culture medium (containing 10% FBS) and were subcultured after one or two days. The HL-60 cells in logarithm stage were washed with D-Hunks solution and counted. The concentration of HL-60 cells was adjusted to 1×10^9 cell/L before use. 200 μL HL-60 cell suspension was added to 48-cell culture plate. 200 μL different concentrations of SRI were added and incubated for 20 minutes at 37 ± 0.5°C under 5% CO_2 humidified air. 50 μL irritant agent lipopolysaccharide (LPS, 90 μg/mL) was added, and the reference was added with the same amount

Table 1: The results of SRI inhibited the production of IL-6 and IL-8 in LPS-stimulated mouse peritoneal macrophages and HL-60 cells ($n = 9$).

Group	IL-6		IL-8	
	OD value (mean ± SD)	Inhibition (%)	Content (ng/mL) (mean ± SD)	Inhibition (%)
Blank	$1.408 \pm 0.050^{(2)}$		$20.2700 \pm 1.3110^{(2)}$	
LPS (5 μg/mL)	1.627 ± 0.013		39.9700 ± 2.6230	
LPS + SRI (1×10^{-8})	1.508 ± 0.079	7.3	$13.910 \pm 2.474^{(2)}$	65.2
LPS + SRI (1×10^{-7})	1.436 ± 0.099	11.7	$13.230 \pm 1.167^{(2)}$	66.9
LPS + SRI (1×10^{-6})	$1.431 \pm 0.081^{(1)}$	12.0	$7.787 \pm 1.910^{(2)}$	80.5

Compared with LPS, $^{(1)}P < 0.05$, $^{(2)}P < 0.01$.

Table 2: The influences of SRI on carrageenin-induced mouse paw edema model ($n = 20$).

Group	Dosage (mg/kg)	Difference between left and right paw (mg) (mean ± SD)	Inhibition (%)
Model		0.083 ± 0.211	
Ibuprofen	176.5	$0.039 \pm 0.009^{(1)}$	53.01
SRI ($LD_{50}/5$)	48.60	$0.057 \pm 0.010^{(1)}$	31.32
SRI ($LD_{50}/20$)	12.15	$0.058 \pm 0.019^{(1)}$	30.12

Compared with model group, $^{(1)}P < 0.01$.

of solvent instead of LPS and incubated again for 24 hours before the supernatant was collected under low temperature. The supernatant was stored at −20°C for the measurement of IL-8.

5.6. Determination of IL-8. The IL-8 was measured by radio immunity with a ^{125}I-lIL-8 radioimmunoassay kit. The decrease of the IL-8 amount in drug group indicated that the production of IL-8 in HL-60 cells is inhibited by the drug which was expressed in inhibition percentage, inhibition percentage (%) = $(\text{IL-8}_{\text{LPS}} - \text{IL-8}_{\text{Drug}})/\text{IL-8}_{\text{LPS}} \times 100\%$. Samples were assayed in triplicate and results are reported at means (±SD).

5.7. The Influences of SRI on Carrageenin-Induced Mouse Paw Edema and the Contents of TNFα, IL-6, IL-8, and PGE_2 in the Local Inflammatory Exudates: Effect in Carrageenin-Induced Mouse Paw Edema Model. Male and female Kunming mice (half and half, body weight 18~23 g) were used and divided into four groups (twenty per group). Two dosages of SRI ($LD_{50}/5$ and $LD_{50}/20$) were given orally for 5 days (one time for each day). LD_{50} of SRI is 243 mg/kg (intragastric administration). Ibuprofen was used as a positive control. 30 minutes after the last intragastric administration, 30 μL of 1% carrageenan solution (solvent: 0.9% saline solution) was injected intradermally into the plantar of right hind paw. Mice were killed after 5 hours; the paws were cut at joint and weighted. The degree of swelling was expressed in the difference between the left paw weight and right paw weight. Inhibition percentage (%) = (swelling $\text{degree}_{\text{Model}}$ − swelling $\text{degree}_{\text{Drug}}$)/swelling $\text{degree}_{\text{Model}} \times 100\%$.

5.8. Sample Preparation for TNFα, IL-6, IL-8, and PGE_2 Determination. Swollen paws of the mice were weighted, skinned, and soaked into 5 mL physiological saline at 4°C for 1 hour after cut into pieces. The swollen paw pieces were discarded and the soak solution was centrifuged. The supernatant was filtered with 0.22 μm filter to remove bacteria before analysis.

5.9. Determination of TNFα. The methods were as previously described [10]. Briefly, 100 μL RPMI-1640 culture solution (contained actinomycin D 2 μg/mL) was added to 96-cell culture plate which is covered with a monolayer L929 cell. Then 100 μL RPMI-1640 culture solution or 100 μL supernatant obtained under "*Samples for TNFα, IL-6, IL-8, and PGE_2 determination*" was added and incubated for 20 hours at 37 ± 0.5°C under 5% CO_2 humidified air. 50 μL MTT (2.5 mg/mL) was added, incubated for 4 hours. After the supernatant discarded, 100 μL DMSO was added to each well and mixed thoroughly. Then the OD values were read at 570 nm on Microplate Reader in 5 minutes.

The RPMI-1640 culture solution wells were used as the reference. The activity of TNFα in samples was expressed in cytotoxic percent. Cytotoxic percent (%) = $(1 - \text{OD}_{\text{sample}}/\text{OD}_{\text{reference}}) \times 100$. The inhibition percentage indicated the degree of depression on the production of TNFα. Inhibition percentage (%) = $(1 - \text{cytotoxic percent}_{\text{sample}}/\text{cytotoxic percent}_{\text{reference}}) \times 100\%$.

5.10. Determination of IL-6 and IL-8. The detection methods were the same as described under IL-6 and IL-8 determination in mouse peritoneal macrophages and HL-60 cells.

5.11. Determination of PGE_2. The methods were as described in [16]. Briefly, added 2 mL 0.1 mol/L KOH methanol solution to 0.1 mL supernatant obtained under "*Samples for TNFα, IL-6, IL-8 and PGE_2 determination*". Then stored at 50°C for 20 minutes until isomerization reaction finished. Added

Table 3: The influences of SRI on the production of TNFα, IL-6, IL-8, and PGE_2 in the local inflammatory exudates of carrageenin-induced mouse paw edema model ($n = 12$).

Group	Dosage (mg/kg)	TNF (OD value) (mean ± SD)	IL-6 (OD value) (mean ± SD)	PGE_2 (OD value) (mean ± SD)	IL-8 (ng/mL) (mean ± SD)	Inhibition (%)			
						TNFα	IL-6	PGE_2	IL-8
Control		0.680 ± 0.011	1.341 ± 1.156						
Model		0.532 ± 0.023	3.379 ± 0.261	0.303 ± 0.008	0.267 ± 0.081				
Ibuprofen	176.5	0.437 ± 0.025$^{(2)}$	2.413 ± 0.210	0.170 ± 0.029$^{(2)}$	0.146 ± 0.042$^{(2)}$	−64.5	28.6	43.7	45.3
SRI	48.60	0.564 ± 0.030	3.167 ± 0.090$^{(2)}$	0.193 ± 0.011$^{(2)}$	0.210 ± 0.044$^{(1)}$	21.6	6.3	36.4	21.3
SRI	12.15	0.547 ± 0.022	3.132 ± 0.157$^{(1)}$	0.218 ± 0.040$^{(1)}$	0.256 ± 0.073	10.1	7.3	27.9	4.1

Compared with model group, $^{(1)}P < 0.05$, $^{(2)}P < 0.01$.

methanol up to the volume of 25 mL. Absorbency value of the mixture, which represented the content of PGE_2, was determined at 278 nm on Microplate Reader.

6. Results

6.1. Finding of the SRI Concentration Range Which Does Not Influence the Normal Growth of Peritoneal Macrophages and HL-60 Cells by MTT Method. The result showed that, in the SRI concentration range of 1×10^{-8} ~1×10^{-6} mol/L, there was no significant difference between the absorbance of the experimental groups and reference well which contained RPMI-1640 culture solution. The result indicated that SRI had no discernible effects on the growth of macrophage and HL-60 cells within the experimental concentration range.

6.2. The Influences of SRI on the Production of IL-6 and IL-8 in LPS-Stimulated Mouse Peritoneal Macrophages and HL-60 Cells. The results indicated that in the range of 1×10^{-8} ~1×10^{-6} mol/L, SRI could inhibit the production of IL-6 and IL-8 in LPS-stimulated mouse peritoneal macrophages and HL-60 cells in a dose-dependent manner. The IL-6 content of each SRI group had no significant difference compared with that of LPS group. But the IL-8 content of each SRI group was significantly lower than that of LPS group ($P < 0.01$). The results were listed in Table 1.

6.3. The Influences of SRI on Carrageenin-Induced Mouse Paw Edema Model and the Contents of TNFα, IL-6, IL-8, and PGE_2 in the Local Inflammatory Exudates. Pretreatment with SRI at doses of 48.60 and 12.15 mg/kg body weight markedly attenuated paw edema after carrageenin stimulation. When the dosage is one fifth of LD_{50}, SRI could inhibit the production of IL-6 and IL-8 in the local inflammatory exudates ($P < 0.05$), and SRI could significantly inhibit the production of PGE_2 in the local inflammatory exudates ($P < 0.01$). When the dosage is one twentieth of LD_{50}, SRI could inhibit the production of PGE_2 ($P < 0.05$) but could not inhibit the production of IL-6 and IL-8. The results are listed in Tables 2 and 3.

7. Discussion

It has been reported [1] that SRI had some immunoregulation effect on mouse immunologic function. It could enhance the mouse macrophage phagocytic function and antagonize the immunosuppression induced by cyclophosphamide. Our previous work [10–13] had proved that SRI could significantly inhibit the production of TNFα and PGE_2 in LPS-stimulated mouse peritoneal macrophages in a concentration dependent manner. And SRI had little effect on the biosynthesis of LTC_4 but inhibited the biosynthesis of LTB_4 obviously. In a certain range of concentration, SRI could significantly inhibit the contract of isolated guinea pigs bronchial smooth and ileum caused by histamine.

Based on these preliminary results, the current work is to study the anti-inflammatory effect and its mechanism of sophoridine on cells, isolated organ, and in vivo models and to discuss the relationship between anti-inflammatory effect in vivo and inflammation media in cells.

The results showed that in a certain concentration range, SRI could significantly inhibit the production of TNFα, PGE_2, and IL-8 in LPS-stimulated mouse peritoneal macrophages and HL-60 cells, and the inhibition effect was dose dependent. But the inhibition effect on the production of IL-6 was not significant. SRI markedly attenuated paw edema after carrageenin stimulation. Similarly, SRI could significantly inhibit the production of TNFα, PGE_2, and IL-8 in the local inflammatory exudates in dose-dependent manner but could not inhibit the production of IL-6 in the local inflammatory exudates.

In summary, SRI showed inhibitory effects on inflammatory cytokines (TNFα, IL-6, and IL-8) and inflammation media prostaglandin E_2 (PGE_2) both in cell culture supernatant (in vitro) and in the local inflammatory exudates (in vivo). Based on the experimental results obtained from both in vitro and in vivo models, the anti-inflammatory effect of SRI might be attributed to its ability to inhibit the production of cytokines (TNFα, IL-8, and LTB_4) and inflammation media (PGE_2 and histamine) in the initial phase of inflammation.

Conflict of Interests

The authors declare that there is no conflict of interests regarding to the publication of this paper.

References

[1] Y. Zhou, N. Wang, J. Zhao et al., "Effects of sophoridine on the function of peritoneal macrophages in mice," *Liaoning Journal of Traditional Chinese Medicine*, vol. 27, no. 2, p. 84, 2000.

[2] T. Liu, D. Liu, J. Wang et al., "Effects of matrine, oxymatrine and sophordine on activity and TNF-α secretion of macrophage RAW264.7," *Chinese Journal of Information on Traditional Chinese Medicine*, vol. 17, no. 3, p. 31, 2010.

[3] T.-H. Liu, D.-F. Liu, J. Wang, X.-J. Wang, and C. Luo, "Matrine, oxymatrine and sophordine inhibit secretion of TNF-α and expression of CD91 and CD13 in macrophage RAW264.7," *Academic Journal of Second Military Medical University*, vol. 31, no. 4, pp. 399–403, 2010.

[4] W. Zhang, Y. Zhang, T. Zhang et al., "Studies on antibacterial and anti-inflammafory effect of alkaloid of Sophora alopecuraids L.," *Progress in Veterinary Medicine*, vol. 26, no. 10, pp. 82–85, 2005.

[5] B. Zhou, G. Su, D. Ma et al., "Apoptosis of gastric carcinoma MGC-803 cells induced by sophoridine," *Tumor*, vol. 23, no. 3, p. 197, 2003.

[6] L. Liang, X.-H. Zhang, X.-Y. Wang, Y. Chen, and H.-Z. Deng, "Effect of sophoridine on proliferation and apoptosis of human colon adenocarcinoma cells (SW620)," *Chinese Pharmacological Bulletin*, vol. 24, no. 6, pp. 782–787, 2008.

[7] X. Li, Y. Wu, D. Pan et al., "Sophoridine is a new antitumor medicine with new molecular structure," *Chinese Journal of New Drugs*, vol. 15, no. 8, p. 654, 2006.

[8] Z. Yang, Y. Zhou, and X. Cao, "The effects of alkaloids of Sophora alopecuroides against Coxsackie B3 viruses (CVB3),"

Sichuan Journal of Traditional Chinese Medicine, vol. 21, no. 3, p. 14, 2003.

[9] H. Nie, J. Chen, Y. Gao et al., "Inhibitory effects of sophoridine on HBSAg and HBeAg in vitro," *Beijing Journal of Traditional Chinese Medicine*, vol. 26, no. 10, p. 678, 2007.

[10] X. Huang, B. Li, L. Shen et al., "Inhibitory effects of four alkaloids of Sophora alopecuroides on TNFα production by murine peritoneal macrophages," *Pharmacology and Clinics of Chinese Materia Medica*, vol. 17, no. 3, p. 12, 2001.

[11] X. Huang and B. Li, "Effect of four alkaloids of Sophora Alopecuroides on COX in supernatant of culture macrophages," *Chinese Traditional Patent Medicine*, vol. 27, no. 3, p. 297, 2005.

[12] X. Huang and B. Li, "Effects of six alkaloids of Sophora Alopecuroides on LTC_4 and LTB_4," *Chinese Traditional Patent Medicine*, vol. 25, no. 10, p. 824, 2003.

[13] X. Huang, B. Li, and L. Shen, "Effects of 6 kinds of Sophora Alopecuroides alkaloids on histamine of inflammatory mediators," *Chinese Journal of Clinical Medicine*, vol. 5, no. 2, p. 61, 2004.

[14] X. Huang and B. Li, "Effect of oxymatrine on TNFα, IL-6 and IL-8 in mice," *Chinese Traditional Patent Medicine*, vol. 25, no. 11, p. 903, 2003.

[15] S. Peng, X. Kang, S. Ling, X. Song, J. Wang, and X. Ma, "MTT colorimetric method for determinatiion of IL-6 activity and its applications," *Bulletin of the Academy of Military Medical Sciences*, vol. 18, no. 1, pp. 72–74, 1994.

[16] Q. Chen, *Traditional Chinese Medicine Pharmacology Research Methodology*, People's Medical Publishing House, Beijing, China, 1995.

Hindawi Publishing Corporation
Journal of Analytical Methods in Chemistry
Volume 2014, Article ID 184162, 9 pages
http://dx.doi.org/10.1155/2014/184162

Research Article

Urinary Metabolomics on the Biochemical Profiles in Diet-Induced Hyperlipidemia Rat Using Ultraperformance Liquid Chromatography Coupled with Quadrupole Time-of-Flight SYNAPT High-Definition Mass Spectrometry

Hua Miao,[1] Hua Chen,[2] Xu Zhang,[1] Lu Yin,[2] Dan-Qian Chen,[2] Xian-Long Cheng,[3] Xu Bai,[4] and Feng Wei[3]

[1] *Department of Physical Education, Northwest University, No. 229 Taibai North Road, Xi'an, Shaanxi 710069, China*
[2] *Department of Traditional Chinese Medicine, The College of Life Sciences, Northwest University, No. 229 Taibai North Road, Xi'an, Shaanxi 710069, China*
[3] *National Institutes for Food and Drug Control, State Food and Drug Administration, 2 Tiantan Xili, Beijing 100050, China*
[4] *Solution Centre, Waters Technologies (Shanghai) Ltd., No. 1000 Jinhai Road, Shanghai 201203, China*

Correspondence should be addressed to Feng Wei; weifengs@gmail.com

Received 8 January 2014; Accepted 23 January 2014; Published 18 March 2014

Academic Editor: Ying-Yong Zhao

Copyright © 2014 Hua Miao et al. This is an open access article distributed under the Creative Commons Attribution License, which permits unrestricted use, distribution, and reproduction in any medium, provided the original work is properly cited.

Ultraperformance liquid chromatography coupled with quadrupole time-of-flight synapt high-definition mass spectrometry metabolomics was used to characterize the urinary metabolic profiling of diet-induced hyperlipidaemia in a rat model. Analysis was done by orthogonal partial least squares discriminant analysis, correlation analysis, heat map analysis, and KEGG pathways analysis. Potential biomarkers were chosen by S-plot and were identified by accurate mass, isotopic pattern, and MS/MS fragments information. Significant differences in fatty acid, amino acid, nucleoside, and bile acid were observed, indicating the perturbations of fatty acid, amino acid, nucleoside, and bile acid metabolisms in diet-induced hyperlipidaemia rats. This study provides further insight into the metabolic profiling across a wide range of biochemical pathways in response to diet-induced hyperlipidaemia.

1. Introduction

Metabolomics is the quantitative measurement of the dynamic multiparametric metabolic responses of living systems to pathophysiological stimuli or genetic modifications [1]. Metabolomics is based on the determination of global metabolite profiles in biological fluids and tissues with subsequent data analysis via a range of multivariate statistical approaches [2]. As a powerful analytical platform, the application of metabolomics has dramatically increased in the fields of physiological evaluation, disease diagnosis, disease prognosis, therapy, biomarker discovery, drug therapy monitoring, and safety and toxicity evaluation [3].

Hyperlipidaemia, as a major risk factor of coronary heart disease, is one of the most important public health problems, with increasing rates of incidence and prevalence [4]. Hyperlipidaemia is defined as a disorder of lipid metabolism leading to abnormal increase of triglycerides (TG), total cholesterol (TC), low-density lipoprotein cholesterol (LDL-C), very low-density lipoprotein cholesterol (VLDL-C), and decrease of high-density lipoprotein cholesterol (HDL-C) [5]. As a progressive chronic and metabolic disease, cardiovascular disease begins in adult and progresses to morbidity and mortality throughout the lifespan. Hyperlipidaemia has an important effect on development and progression of various cardiovascular diseases and atherosclerosis. Both moderate

hyperlipidaemia and severe hyperlipidaemia are associated with cardiovascular disease [6]. Recent study indicates that a fundamental defect is an overproduction of large VLDL-C, which triggers a sequence of lipoprotein changes, leading to increased remnant particles, smaller LDL-C, and decreased HDL-C [7]. LDL-C is the primary target for the lipid-lowering therapy and cardiovascular diseases prevention.

Mass spectrometry (MS) and proton nuclear magnetic resonance (^{1}H NMR) spectroscopy are two analytical tools commonly used in metabolomics. Recently, an increasing number of ^{1}H NMR and gas chromatography-MS (GC-MS) based on metabolomics have been conducted to characterize hyperlipidaemia models and to assess drug treatment [8–12].

Proteomic profiling from insulin resistance and metabolic dyslipidemia rats demonstrated hepatic ER proteins ERp29, ERp46, and ER60; TAP1 and glutamate dehydrogenase were downregulated, whereas P-glycoprotein, α-glucosidase, protein disulfide isomerase, fibrinogen, GRP94, and apolipoprotein E were upregulated in the hepatic ER of the fructose-fed hamster [13]. ^{1}H NMR-based metabolomics indicated that major metabolic processes like Krebs cycle, cholesterol metabolism, and osmoregulation are perturbed in hypercholesterolaemic rats [9]. GC-MS based on metabolomics showed amino acids (alanine, valine, aspartic acid, phenylalanine, etc.), fatty acids (octadecadienoic acid, arachidonic acid, etc.), and propanoic acid, and glucose and cholesterol were identified as biomarkers in diet-induced hyperlipidaemia rats [12]. Among the analytical techniques in metabolomics research, liquid chromatography is recognized as one of the best analytical techniques in selectivity, sensitivity, and reproducibility [14]. Furthermore, among the various liquid chromatography platforms, ultraperformance liquid chromatography (UPLC) is considered to be suitable for metabolite profiling and metabolomics study, especially for large-scale untargeted metabolic profiling due to its enhanced reproducibility of retention time. UPLC operates with sub-2 μm chromatographic particles and a fluid system capable of operating at pressures up to 15000 psi, providing an increased chromatographic resolution compared to conventional high performance liquid chromatography (HPLC) using larger particles.

In 2005, Wrona et al. introduced the mass spectrometry^{ElevatedEnergy} (MS^E) data collection technique [15], in which two scanning functions are simultaneously used for data collection. In other words, MS^E can provide parallel alternating scans for acquisition at either low collision energy to obtain precursor ion information or high collision energy to obtain full-scan accurate mass fragment, precursor ion, and neutral loss information [14]. MS^E involves a simultaneous acquisition through alternating between high and low collision energies during a single chromatographic run. This ability is of major importance, as it offers the structural information required for the identification of unknown biomarkers in the context of untargeted analyses. Recently, the novel quadrupole time-of-flight mass spectrometry with MS^E technique has been proven to be a powerful and reliable analytical approach for metabolite identification [16–20]. UPLC Q-TOF/HDMS with MS^E technique is becoming increasingly popular in the analysis of biological fluids in the field of metabolomics because it provides high resolution, accurate mass measurement, and structural information [14, 16–20]. A method using UPLC Q-TOF/HDMS/MS^E-based metabolomics combined with multivariate statistical analysis was applied to rapidly identify urinary metabolite profiling of diet-induced hyperlipidaemia in a rat model. Orthogonal partial least squares discriminant analysis (OPLS-DA), correlation analysis, heat map analysis, and KEGG pathways analysis were performed for investigating the metabolic changes of diet-induced hyperlipidaemia and control rats, and the potential biomarkers were identified accordingly.

2. Materials and Methods

2.1. Animals and Sample Collection. The study was conducted in accordance with the Regulations of Experimental Animal Administration issued by the State Committee of Science and Technology of People's Republic of China. All procedures and the care of the rats were in accordance with institutional guidelines for animal use in research. Male Sprague-Dawley rats were obtained from the Central Animal Breeding House of Fourth Military Medical University (Xi'an, China). They were maintained at a constant humidity (ca. 60%) and temperature (ca. 23°C) with a light/dark cycle of 12 h. Male rats underwent an adaptation period of several days, during which they were fed a commercial feed. After that they were separated randomly into two groups (n = 8/group). Rats were randomly assigned into a diet-induced hyperlipidaemia group and control group. The control group was fed with the common diet during the whole experimental period, and the diet-induced hyperlipidaemia group was fed with high fat diets including 81% basic diet, 10% yolk powder, 7.5% lards, 0.3% sodium cholate, 0.2% methylthiouracil, and 1% cholesterol for continuous 6 weeks. After 6 weeks, individual rats were placed in metabolic cages (1 per cage) to obtain 24-hour urine collections. When urine samples were collected, rats were only freely accessible to water. All the samples were stored at −80°C before analysis.

2.2. Sample Preparation. Prior to analysis, urine samples were thawed at room temperature and then centrifuged at 13000 rpm for 10 min to remove solid materials. The supernatant was diluted at a ratio of 3 : 1 with distilled water, mixed, and centrifuged for UPLC analysis.

2.3. Chromatographic Separation. The UPLC analysis was performed on a Waters ACQUITY Ultra Performance LC system (Waters, USA) equipped with a Waters Xevo G2 QTof MS. Chromatographic separation was carried out at 45°C on an ACQUITY UPLC HSS T3 column (2.1 mm × 100 mm, 1.8 μm). The mobile phase consisted of water (A) and acetonitrile (B), each containing 0.1% formic acid. The optimized UPLC elution conditions were 0–0.5 min, 1% B; 0.5–12.0 min, 1–30% B; 12.0–15.0 min, 30–99% B; 15.0–16.0 min, 99% B; 16.0–20.0 min, 99.0–1.0% B. The flow rate

was 0.45 mL/min. The autosampler was maintained at 4°C. Every 2 μL sample solution was injected for each run.

2.4. Mass Spectrometry. Mass spectrometry was performed on a quadrupole and orthogonal acceleration time-of-flight tandem mass spectrometer. The scan range was from 50 to 1200 m/z. For both positive and negative electrospray modes, the capillary and cone voltage were set at 2.5 kV and 45 V, respectively. The desolvation gas was set at 900 L/h at a temperature of 550°C; the cone gas was set at 50 L/h; the source temperature was set at 120°C. The mass spectrometry was operated in W optics mode with 12,000 resolution using dynamic range extension. The data acquisition rate was set to 0.1 s, with a 0.1 s interscan delay. All analyses were acquired using the LockSpray to ensure accuracy and reproducibility. Leucine-enkephalin was used as the lockmass at a concentration of 300 ng/mL and flow rate of 5 μL/min. Data were collected in centroid mode, the LockSpray frequency was set at 10 s, and data were averaged over 10 scans. All the acquisition and analysis of data were operated by Waters MassLynx v4.1 software.

2.5. Analytical Method Assessment. The precision and repeatability of this experiment were tested for assessment of the developed UPLC-MS method according to different chemical polarities and m/z values; 8 ions including m/z 284.2934, 340.1060, 282.2779, 256.2620, 367.1490, 296.2360, 372.2366, and 330.0618 were extracted for the assessment according to the variation of their peak areas and retention times. The six parallel random samples were injected to evaluate the sample preparation repeatability. Sample of quality control (QC) was injected. There were six control rats and six diet-induced hyperlipidemia rats; six batches of data from one QC sample could be obtained to evaluate the stability of the UPLC-MS system for the large-scale sample analysis.

2.6. Data Analysis. The raw data were analyzed using the MarkerLynx XS software. This software allowed deconvolution, alignment, and data reduction to give a list of mass and retention time pairs with corresponding intensities for all the detected peaks from each data file in the data set. The main parameters were set as follows: retention time range 1–18 min, mass range 50–1000 amu, minimum intensity 1%, mass tolerance 0.01, retention time window 0.20, mass window 0.05, marker intensity threshold 500, and noise elimination level 6. All of the data were normalized to the summed total ion intensity per chromatogram, and the resultant data matrices were introduced to the EZinfo 2.0 software for OPLS-DA. Metabolite peaks were assigned by MS^E analysis or interpreted with available biochemical databases, such as HMD, ChemSpider, and KEGG. Potential markers were extracted from S-plots. Correlation analysis and heat maps were analyzed by MetaboAnalyst software. The other statistical analysis was performed by SPSS 11.0. The significant differences between control group and diet-induced hyperlipidemia group were assessed by analysis of variance (ANOVA) followed by t-test for multiple comparisons. When comparing with the control group, P values less than 0.05 were considered significant.

3. Results and Discussion

3.1. Sample Preparation and UPLC-MS Analysis. Urine is a complex sample containing various endogenous and exogenous acidic, basic, and neutral compounds with high polarity. Sample preparation by conventional methods including solid-phase extraction or liquid-liquid extraction may lead to loss of high polarity and high hydrophilicity metabolites. While metabolomics is an untargeted analysis of the global changes in endogenous metabolites, conventional methods may cause loss of potential biomarker. Therefore, minimal sample preparation steps were performed on urinary samples in order to avoid the loss of the endogenous metabolites. Urinary samples were centrifuged and diluted prior to the direct injection into UPLC-MS.

The complexity of the urinary sample makes the separation very difficult and consequently results in severe ion suppression. UPLC employs sub-2 μm particle size column, which generates high efficiency to the compound separation and concurrently increases sensitivity and resolution. Thus, UPLC was applied to urinary metabolomics of diet-induced hyperlipidaemia rats in the positive and negative ESI modes. Representative base peak intensity (BPI) chromatogram of the urine of diet-induced hyperlipidaemia rats in the positive ESI mode is shown in Figure 1. Reproducibility was determined from six replicated analyses of the same urinary sample. The variations of m/z values and retention times of selected peaks in positive ESI mode were less than 8 mDa and 0.05 min, respectively, and the relative standard deviations of peak area and retention time are below 2.9% and 0.78%, respectively. These results indicated the excellent reproducibility and stability during the whole sequence.

3.2. Multivariate Data Analysis. Metabolomics aims at the comparison of samples from a control group and from a case group. The OPLS-DA is an extension of the partial least squares discriminant analysis which integrates an orthogonal signal correction filter to distinguish variations that are useful for prediction of a quantitative response from variations that are orthogonal to prediction. OPLS-DA was demonstrated as a powerful tool for the analysis of qualitative data structures. OPLS-DA score plot was performed on the urinary metabolites from diet-induced hyperlipidemia rats and control rats. According to UPLC-MS data, 8642 peaks of positive ions were detected and processed by MarkerLynx using the same acquiring method. Figure 2(a) shows the OPLS-DA score plot of the diet-induced hyperlipidemia rats and control rats. The OPLS-DA score plot revealed good fitness and high predictability of the OPLS-DA model with high statistical values of R^2 and Q^2. The R^2 and Q^2 values are 0.975 and 0.933, respectively. S-plot is a tool for visualization and interpretation of multivariate classification models. It images both the covariance and correlation between the metabolites and the modeled class designation for identification of statistically significant and biochemically interesting

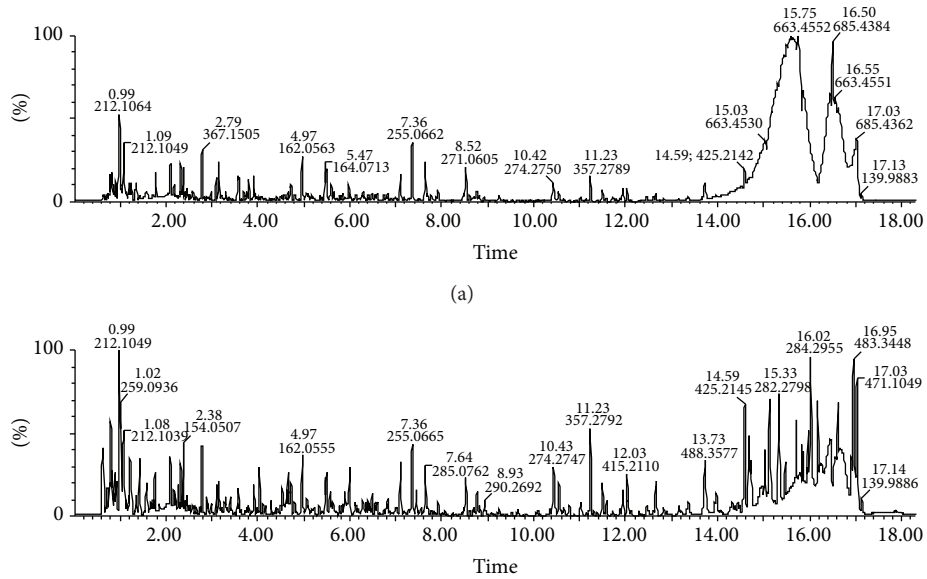

Figure 1: Base peak intensity (BPI) chromatograms obtained from the positive ion UPLC-MS analyses of control (a) and diet-induced hyperlipidemia (b) rats.

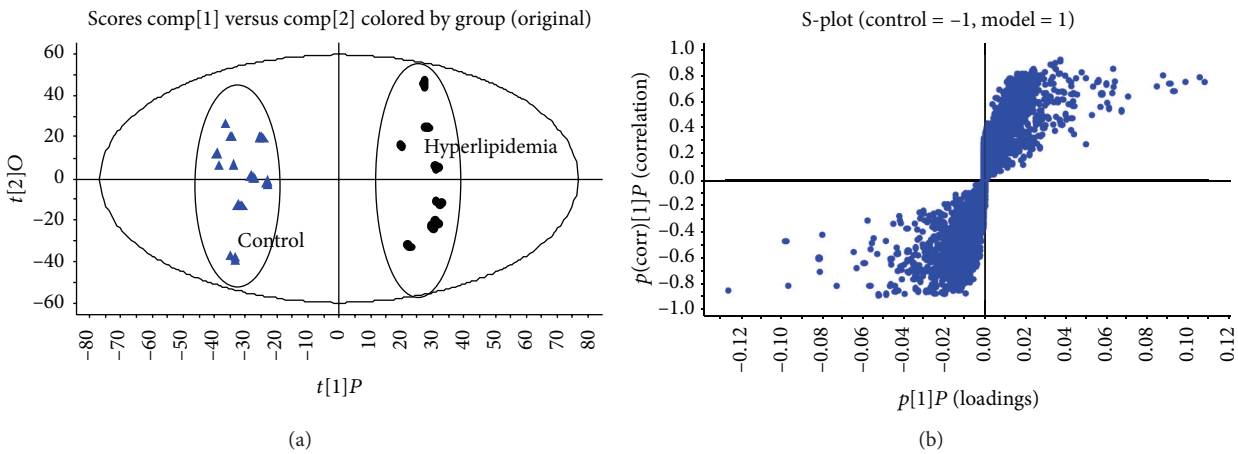

Figure 2: (a) OPLS-DA score plot based on the urinary metabolic profiling of the hyperlipidemia (●) and control (▲) rats; the results indicated that the urinary metabolic pattern was significantly changed in the diet-induced hyperlipidemia rats. (b) S-plot used in our biomarkers selection. The variables marked (□) are the metabolites selected as potential biomarkers. The significant metabolites were selected as potential biomarkers from S-plot and these urinary metabolites are associated with diet-induced hyperlipidemia.

metabolites which can avert the increase of false positives (type I error). The significant metabolites were selected as potential biomarkers from S-plot (Figure 2(b)). These urinary metabolites are associated with diet-induced hyperlipidemia.

3.3. Identification of Potential Biomarkers. For metabolomics research, the biggest challenge is the identification of potential biomarkers obtained from comparative samples, particularly when they are novel and published work on the compound class is unavailable or prior information is lacking otherwise. All the detected ions were arranged in descending order according to VIP (Variable Importance in the Projection) values, which reflect the influence of each metabolite in control rats and diet-induced hyperlipidemia rats. The more the variable deviates from the origin, the higher the VIP value will be obtained. According to the result of S-plot and reported methods, 16 variables were predicted by comparing the accurate MS and MS^E fragments with the metabolites searching in ChemSpider, HMDB, and KEGG, and according to the possible fragment mechanisms, compounds without the given mass fragment information were removed from the candidate list and only the most probable compounds were

Table 1: 13 biomarkers of hyperlipidemia detected by UPLC Q-TOF/MS in negative ion mode in the 4th week.

Number	Mass	Metabolite	i-FIT[a], elemental composition	Molecular weight	Formula	Trend[b]	Related pathway
1	284.2934	Octadecanamide	0.9, $C_{18}H_{38}NO$	283.4925	$C_{18}H_{37}NO$	↑**	Fatty acid metabolism
2	282.2779	Oleamide	1.2, $C_{18}H_{36}NO$	281.2718	$C_{18}H_{35}NO$	↑**	Fatty acid metabolism
3	188.0713	Tryptophan	0.9, $C_{11}H_{10}N_1O_2$	204.2252	$C_{11}H_{12}N_2O_2$	↑**	Amino acid metabolism
4	193.1235	Citric acid	0.7, $C_6H_9O_7$	192.1243	$C_6H_8O_7$	↓**	TCA cycle
5	330.0618	Adenosine 2′,3′-cyclic phosphate	1.0, $C_{10}H_{13}N_5O_6P$	329.2059	$C_{10}H_{12}N_5O_6P$	↓**	Purine metabolism
6	393.3002	Ursodeoxycholic acid	0.8, $C_{24}H_{41}O_4$	392.5720	$C_{24}H_{40}O_4$	↑**	Bile acid metabolism
7	114.0641	Creatinine	1.2, $C_4H_8N_3O$	113.1179	$C_4H_7N_3O$	↑**	Energy metabolism
8	281.0979	Ascorbalamic acid	0.9, $C_9H_{17}N_2O_8$	263.2014	$C_9H_{13}NO_8$	↑**	Carbohydrate metabolism
9	259.0913	3-Methyluridine	1.2, $C_{10}H_{15}N_2O_6$	258.228	$C_{10}H_{14}N_2O_6$	↑**	Nucleoside metabolism
10	212.1025	3-O-Methyldopa	1.7, $C_{10}H_{14}NO_4$	211.2145	$C_{10}H_{13}NO_4$	↓**	Amino acid metabolism
11	162.1108	Proline	0.7, $C_7H_{13}O_3$	115.1305	$C_7H_{12}O_3$	↓**	Amino acid metabolism
12	282.1216	1-Methyladenosine	1.2, $C_{11}H_{16}N_5O_4$	281.2679	$C_{11}H_{15}N_5O_4$	↓**	Nucleoside metabolism
13	162.0538	Indole-3-carboxylic acid	0.8, $C_9H_8NO_2$	161.1574	$C_9H_7NO_2$	↑**	Amino acid metabolism
14	368.1594	Tryptophyl-tyrosine	1.2, $C_{20}H_{22}N_3O_4$	367.3984	$C_{20}H_{21}N_3O_4$	↑**	Amino acid metabolism
15	166.0708	Phenylalanine	0.9, $C_9H_{12}NO_2$	165.1891	$C_9H_{11}NO_2$	↓**	Amino acid metabolism
16	126.0643	5-Methylcytosine	1.3, $C_5H_8N_3O$	125.1286	$C_5H_7N_3O$	↓**	Nucleoside metabolism

[a]i-FIT; the i-FIT is the correctness of isotope patterns of elemental composition. The lower i-FIT normalized values mean high precision of the elemental composition; [b]change trend of hyperlipidemia rats versus control rats. The potential biomarkers were labeled with (↓) downregulated and (↑) upregulated. $^{*}P < 0.05$ and $^{**}P < 0.01$.

reserved [21, 22]. MassLynx i-FIT algorithm is used to screen suggested elemental compositions by the likelihood that the isotopic pattern of the elemental composition matches a cluster of peaks in the spectrum, increasing confidence in identified compounds and simplifying results. The lower the i-FIT value, the better the fit [23]. By comparing the retention times and mass spectra to the authentic chemicals, 16 compounds were tentatively identified and shown in Table 1.

3.4. Study of Metabolic Changes and Biochemical Interpretation in Diet-Induced Hyperlipidemia Rats. Differences in the levels of metabolites between diet-induced hyperlipidemia rats and control rats were compared using OPLS-DA. The metabolic profiling and multivariate pattern recognition may observe a wider range of metabolites. Since metabolites can be regulated through a number of metabolic pathways, an investigation of the overall features rather than of several selected metabolites enabled us to understand the underlying pathophysiological status more comprehensively.

To investigate the change of identified metabolites in diet-induced hyperlipidemia rats, relative intensity of identified metabolites compared diet-induced hyperlipidemia rats with control rats. Increased urinary octadecanamide, oleamide, tryptophan, ursodeoxycholic acid, creatinine, ascorbalamic acid, 3-methyluridine, indole-3-carboxylic acid, and tryptophyl-tyrosine and decreased urinary citric acid, adenosine 2′,3′-cyclic phosphate, 3-O-methyldopa, proline, 1-methyladenosine, phenylalanine, and 5-methylcytosine were observed in diet-induced hyperlipidemia rats (Figure 3(a)). Above-mentioned metabolites might play important roles in the metabolic changes of diet-induced hyperlipidemia rats. OPLS-DA loading plot was also generated in diet-induced hyperlipidemia rats and control rats. The loading plot indicated that identified metabolites were quantitatively higher or lower in diet-induced hyperlipidemia rats compared with control rats. Concentrations of identified metabolites including octadecanamide, oleamide, tryptophan, ursodeoxycholic acid, creatinine, ascorbalamic acid, 3-methyluridine, indole-3-carboxylic acid, and tryptophyl-tyrosine were significantly increased in diet-induced hyperlipidemia rats, whereas the concentrations of citric acid, adenosine 2′,3′-cyclic phosphate, 3-O-methyldopa, proline, 1-methyladenosine, phenylalanine, and 5-methylcytosine were decreased in diet-induced hyperlipidemia rats (Figure 3(a)), which are in agreement with the changes of relative intensity (Figure 3(b)). The

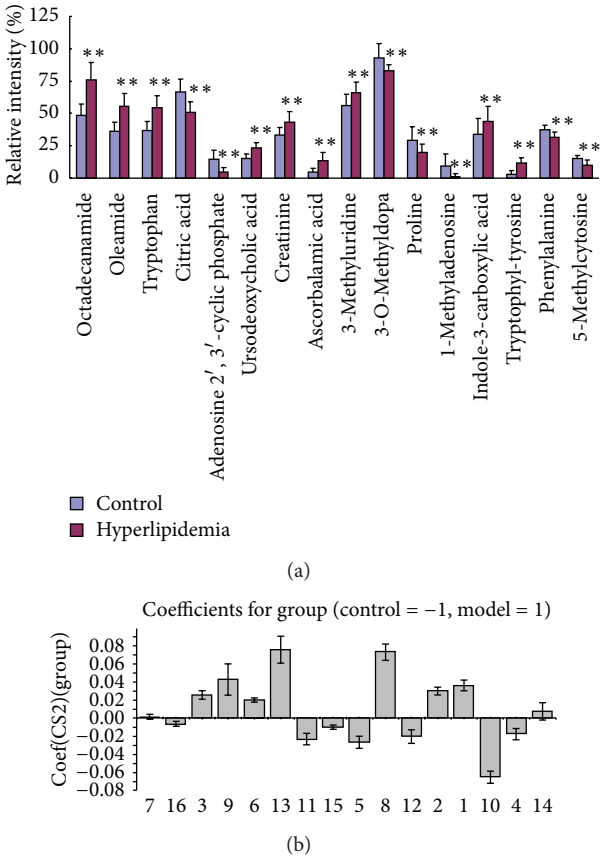

Figure 3: (a) Comparison of the relative intensity and (b) OPLS-DA loading plot of putative potential biomarkers in control and diet-induced hyperlipidaemia rats. The loading plots represent which metabolites are quantitatively higher or lower in diet-induced hyperlipidaemia rats compared with control rats. Numbers consist with Table 1.

results demonstrated that these upregulated or downregulated metabolites are associated with diet-induced hyperlipidemia.

To further understand the metabolic differences between diet-induced hyperlipidemia rats and control rats, identified metabolites were analyzed using correlation analysis and clustering heat maps. Correlation analysis showed the relation of differential metabolites. From the above plots, identified metabolites could be considered as being responsible for the separation between diet-induced hyperlipidemia rats and control rats and were therefore regarded as potential biomarkers. Heat map showed directly the variation of each metabolite, and the identified metabolites were visualized in a clustering heat map. Identified metabolites are showed in heat map, which shows the relative increase (red) or decrease (green) compared with control rats (Figure 4(a)). The hyperlipidemia model was capable of distinguishing diet-induced hyperlipidemia rats from control rats. The metabolites octadecanamide, oleamide, tryptophan, ursodeoxycholic acid, creatinine, 3-methyluridine, indole-3-carboxylic acid, and tryptophyl-tyrosine showed an increasing tendency in diet-induced hyperlipidemia rats. Although these metabolites showed similar tendencies to increase, some of the metabolites showed different increasing levels in diet-induced hyperlipidemia rats. In contrast, the metabolites citric acid, adenosine 2′,3′-cyclic phosphate, 3-O-methyldopa, proline, 1-methyladenosine, phenylalanine, and 5-methylcytosine showed a decreasing tendency in diet-induced hyperlipidemia rats. These results are consistent with the relative intensity and OPLS-DA loading plots.

Amino acids serve as substrates for protein synthesis, metabolic energy (oxidation through TCA cycle), or gluconeogenesis and ketogenesis [24]. Increased urinary tryptophan and tryptophyl-tyrosine and decreased urinary phenylalanine were observed in diet-induced hyperlipidemia rats. Tryptophan is essential amino acid which cannot be synthesized by the body. Tryptophan either participates in proteins or is broken down for energy and metabolic intermediates. Dopamine is an important neurotransmitter as 5-hydroxytryptamine, which is derived from tryptophan metabolism. 3-O-Methyldopa is one of the main biochemical markers for aromatic amino acid decarboxylase deficiency, which affects dopamine biosynthesis. An obvious decrease of 3-O-methyldopa was observed in diet-induced hyperlipidemia rats compared with control rats. Indole-3-carboxylic acid is the metabolite of tryptophan, the precursor of neurotransmitter 5-hydroxytryptamine. Level of indole-3-carboxylic acid was significantly increased in diet-induced hyperlipidemia rats compared with control rats. Phenylalanine is an essential amino acid and its hydroxylation by phenylalanine hydroxylase to tyrosine is the major metabolic pathway for phenylalanine. Significant fate of tyrosine is a conversion to the catecholamines, for example, dopamine, norepinephrine, and epinephrine [25]. Diet-induced hyperlipidemia associated with dysfunction of tryptophan and phenylalanine, which were identified as potential biomarkers for hyperlipidemia or atherosclerosis, has been demonstrated [9, 26]. Proline is the catabolite of peptide degradation by proline iminopeptidase and is a precursor of pyruvate. Pyruvate can be converted into acetyl-CoA, which is the main input for a series of reactions known as the TCA cycle. Decreases in levels of proline and citric acid were observed in diet-induced hyperlipidemia rats. Decrease in proline was related to the glutamate/P5C synthase pathway via inactivating P5C synthase or other enzymes involved [27]. The previous study demonstrated that urinary citric acid was significantly decreased in diet-induced hyperlipidemia [9]. These results indicated that amino acids metabolism and TCA cycle were disturbed in diet-induced hyperlipidemia rats.

Increased 3-methyluridine and decreased 1-methyladenosine and 5-methylcytosine were observed in diet-induced hyperlipidemia rats. It has been demonstrated that 3-methyluridine and 1-methyladenosine were significantly increased in the pathogenesis of Alzheimer's disease [28]. 1-Methyladenosine is one of the modified nucleosides; the level is elevated in urine of patients with malignant tumors. Examination of expression of 1-methyladenosine is expected to be useful for the histological diagnosis of intraocular tumors. However, the previous study did not report that 3-methyluridine, 1-methyladenosine, and 5-methylcytosine

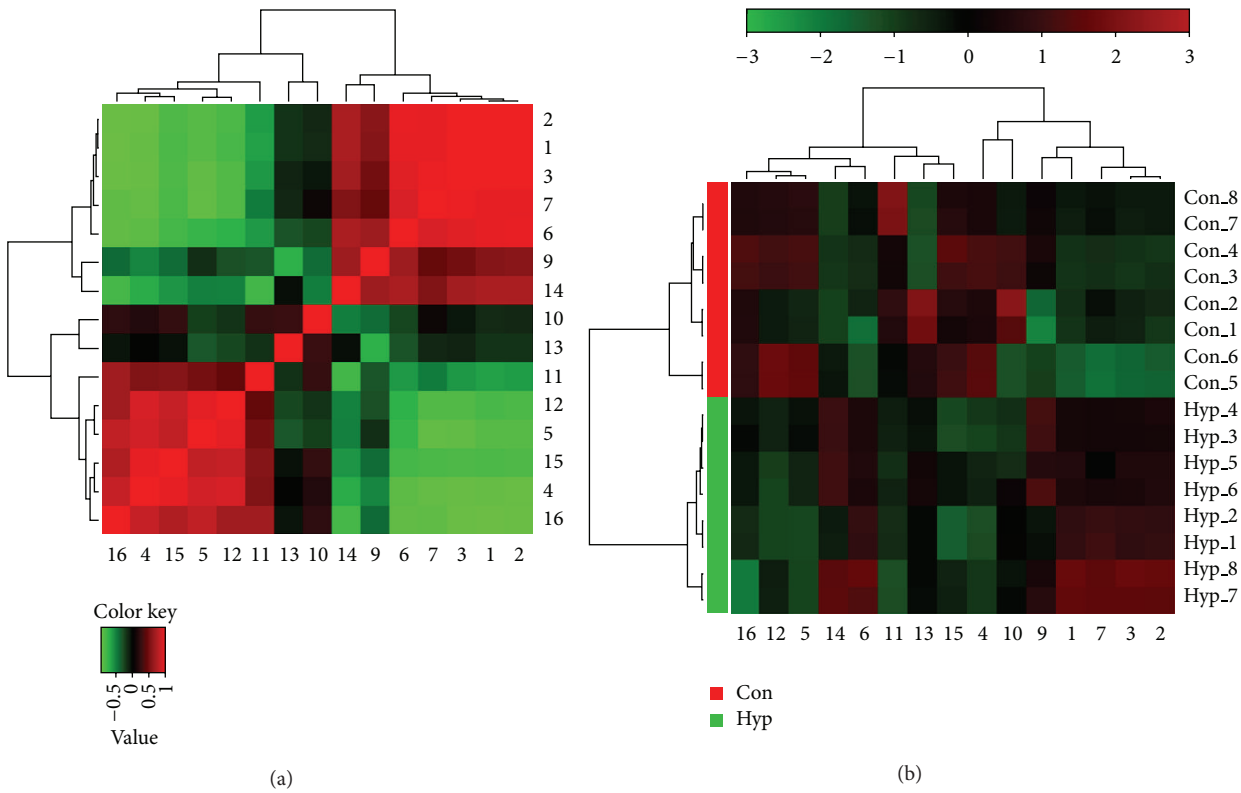

Figure 4: Correlation analysis (a) of the differential metabolites in control rats and diet-induced hyperlipidaemia rats. Heat map (b) for identified metabolites in control rats and diet-induced hyperlipidaemia rats. The color of each section is proportional to the significance of change of metabolites (red, upregulated; green, downregulated). Rows: samples; columns: metabolites. Numbers consist with Table 1.

were identified as potential biomarkers in diet-induced hyperlipidemia rats.

The concentrations of octadecanamide and oleamide were higher in diet-induced hyperlipidemia rats than in control rats. Fatty acids are reported to be associated with atherosclerotic and inflammatory diseases because they are the major components of the cytoplasmic membrane and the precursor fatty acids for prostaglandins and leukotrienes [29]. Bile acids have many important physiological functions such as lipid absorption, cholesterol homeostasis, and generation of bile flow that help in the recirculation and excretion of exogenous and endogenous metabolites. Increased urinary ursodeoxycholic acid was observed in diet-induced hyperlipidemia rats compared with control rats. It has been demonstrated that increased ursodeoxycholic acid was associated with atherosclerosis and ursodeoxycholic acid was identified as a potential biomarker in atherosclerosis rats [26]. In addition, the previous study demonstrated that urinary cholesterol was significantly increased in diet-induced hyperlipidemia [12]. Creatinine is usually produced at a relatively constant rate by the human body. Although serum creatinine is a commonly used indicator of renal function, increased urinary creatinine is observed only when significant injury occurs in renal function. Therefore, an increased level of urinary creatinine observed in the diet-induced hyperlipidaemia rats might indicate renal injury caused by hyperlipidaemia.

4. Conclusions

Urinary metabolomics based on UPLC Q-TOF/HDMS, a novel MS^E data collection technique, and a multivariate statistical technique has been used to study diet-induced hyperlipidaemia in a rat model. The OPLS-DA score plot showed the complete distinction of diet-induced hyperlipidaemia rats and control rats. Furthermore, significant differences in the urinary levels of fatty acids, amino acids, nucleosides, and bile acids were observed in diet-induced hyperlipidaemia rats. These results demonstrated the perturbations of fatty acids metabolism, amino acid metabolism, and nucleosides metabolism of diet-induced hyperlipidaemia. This research also demonstrated that UPLC-MS-based metabolomics was a promising tool to find and identify potential biomarkers in diet-induced hyperlipidaemia rats.

Conflict of Interests

There is no conflict of interests to declare.

Authors' Contribution

Hua Miao and Hua Chen contributed to this paper as co-first authors.

Acknowledgments

This study was supported by the Program for the New Century Excellent Talents in University (NCET-13-0954) and the Changjiang Scholars and Innovative Research Team in University (IRT1174) from Ministry of Education of China, the National Natural Science Foundation of China (J1210063, 81001622, and 81073029), National Innovation Training Plan Program (201310697004), the Project "As a Major New Drug to Create a Major National Science and Technology Special" (2011ZX09401-308-034, 2014ZX09304-307-02), and the China Postdoctoral Science Foundation (2012M521831).

References

[1] J. K. Nicholson, J. C. Lindon, and E. Holmes, "'Metabonomics': understanding the metabolic responses of living systems to pathophysiological stimuli via multivariate statistical analysis of biological NMR spectroscopic data," *Xenobiotica*, vol. 29, no. 11, pp. 1181–1189, 1999.

[2] J. K. Nicholson, J. Connelly, J. C. Lindon, and E. Holmes, "Metabonomics: a platform for studying drug toxicity and gene function," *Nature Reviews Drug Discovery*, vol. 1, no. 2, pp. 153–161, 2002.

[3] J. C. Lindon, E. Holmes, M. E. Bollard, E. G. Stanley, and J. K. Nicholson, "Metabonomics technologies and their applications in physiological monitoring, drug safety assessment and disease diagnosis," *Biomarkers*, vol. 9, no. 1, pp. 1–31, 2004.

[4] J. H. O'Keefe and D. S. H. Bell, "Postprandial hyperglycemia/hyperlipidemia (postprandial dysmetabolism) is a cardiovascular risk factor," *The American Journal of Cardiology*, vol. 100, no. 5, pp. 899–904, 2007.

[5] E. Esteve, W. Ricart, and J. M. Fernández-Real, "Dyslipidemia and inflammation: an evolutionary conserved mechanism," *Clinical Nutrition*, vol. 24, no. 1, pp. 16–31, 2005.

[6] J. Genest, R. McPherson, J. Frohlich et al., "2009 Canadian Cardiovascular Society/Canadian guidelines for the diagnosis and treatment of dyslipidemia and prevention of cardiovascular disease in the adult—2009 recommendations," *The Canadian Journal of Cardiology*, vol. 25, no. 10, pp. 567–579, 2009.

[7] M. Adiels, S.-O. Olofsson, M.-R. Taskinen, and J. Borén, "Overproduction of very low-density lipoproteins is the hallmark of the dyslipidemia in the metabolic syndrome," *Arteriosclerosis, Thrombosis, and Vascular Biology*, vol. 28, no. 7, pp. 1225–1236, 2008.

[8] D. J. Wu, B. J. Zhu, and X. D. Wang, "Metabonomics-based omics study and atherosclerosis," *Journal of Clinical Bioinformatics*, vol. 1, no. 30, 2011.

[9] F. Liu, P. P. Gan, H. Wu, W. S. Woo, E. S. Ong, and S. F. Y. Li, "A combination of metabolomics and metallomics studies of urine and serum from hypercholesterolaemic rats after berberine injection," *Analytical and Bioanalytical Chemistry*, vol. 403, no. 3, pp. 847–856, 2012.

[10] X. Zhang, C. Wu, H. Wu et al., "Anti-hyperlipidemic effects and potential mechanisms of action of the caffeoylquinic acid-rich *Pandanus tectorius* fruit extract in hamsters fed a high fat-diet," *PLoS ONE*, vol. 8, no. 4, Article ID e61922, 2013.

[11] Q. Zhang, G.-J. Wang, J.-Y. A et al., "Application of GC/MS-based metabonomic profiling in studying the lipid-regulating effects of *Ginkgo biloba* extract on diet-induced hyperlipidemia in rats," *Acta Pharmacologica Sinica*, vol. 30, no. 12, pp. 1674–1687, 2009.

[12] Q. Zhang, G. Wang, J. A et al., "Metabonomic profiling of diet-induced hyperlipidaemia in a rat model," *Biomarkers*, vol. 15, no. 3, pp. 205–216, 2010.

[13] J.-P. F. Morand, J. Macri, and K. Adeli, "Proteomic profiling of hepatic endoplasmic reticulum-associated proteins in an animal model of insulin resistance and metabolic dyslipidemia," *The Journal of Biological Chemistry*, vol. 280, no. 18, pp. 17626–17633, 2005.

[14] Y. Y. Zhao, "Metabolomics in chronic kidney disease," *Clinical Chimica Acta*, vol. 422, pp. 59–69, 2013.

[15] M. Wrona, T. Mauriala, K. P. Bateman, R. J. Mortishire-Smith, and D. O'Connor, "'All-in-One' analysis for metabolite identification using liquid chromatography/hybrid quadrupole time-of-flight mass spectrometry with collision energy switching," *Rapid Communications in Mass Spectrometry*, vol. 19, no. 18, pp. 2597–2602, 2005.

[16] Y.-Y. Zhao, J. Liu, X.-L. Cheng, X. Bai, and R.-C. Lin, "Urinary metabonomics study on biochemical changes in an experimental model of chronic renal failure by adenine based on UPLC Q-TOF/MS," *Clinica Chimica Acta*, vol. 413, no. 5-6, pp. 642–649, 2012.

[17] Y. Y. Zhao, X. Shen, X. L. Cheng, F. Wei, X. Bai, and R. C. Lin, "Urinary metabonomics study on the protective effects of ergosta-4, 6, 8(14), 22-tetraen-3-one on chronic renal failure in rats using UPLC Q-TOF/MS and a novel MS^E data collection technique," *Process Biochemistry*, vol. 47, no. 12, pp. 1980–1987, 2012.

[18] Y. Y. Zhao, Y. L. Feng, X. Bai, X. J. Tan, R. C. Lin, and Q. Mei, "Ultra performance liquid chromatography-based metabonomic study of therapeutic effect of the surface layer of *Poria cocos* on adenine-induced chronic kidney disease provides new insight into anti-fibrosis mechanism," *PLoS ONE*, vol. 8, no. 3, Article ID e59617, 2013.

[19] Y. Y. Zhao, P. Lei, D. Q. Chen, Y. L. Feng, and X. Bai, "Renal metabolic profiling of early renal injury and renoprotective effects of *Poria cocos* epidermis using UPLC Q-TOF/HSMS/MS^E," *Journal of Pharmaceutical and Biomedical Analysis*, vol. 81-82, pp. 202–209, 2013.

[20] Y. Y. Zhao, H. T. Li, Y. L. Feng, X. Bai, and R. C. Lin, "Urinary metabonomic study of the surface layer of *Poria cocos* as an effective treatment for chronic renal injury in rats," *Journal of Ethnopharmacology*, vol. 148, no. 2, pp. 403–410, 2013.

[21] Y. Y. Zhao, L. Zhang, F. Y. Long et al., "UPLC-Q-TOF/HSMS/MS^E-based metabonomics for adenine-induced changes in metabolic profiles of rat faeces and intervention effects of ergosta-4, 6, 8(14), 22-tetraen-3-one," *Chemico-Biological Interactions*, vol. 201, no. 1–3, pp. 31–38, 2013.

[22] Y.-Y. Zhao, X.-L. Cheng, F. Wei et al., "Intrarenal metabolomic investigation of chronic kidney disease and its TGF-β1 mechanism in induced-adenine rats using UPLC Q-TOF/HSMS/MS^E," *Journal of Proteome Research*, vol. 12, no. 2, pp. 692–703, 2013.

[23] Y.-Y. Zhao, X.-L. Cheng, F. Wei, X. Bai, and R.-C. Lin, "Application of faecal metabonomics on an experimental model of tubulointerstitial fibrosis by ultra performance liquid chromatography/high-sensitivity mass spectrometry with MS^E data collection technique," *Biomarkers*, vol. 17, no. 8, pp. 721–729, 2012.

[24] B. K. Lopansri, N. M. Anstey, G. J. Stoddard et al., "Elevated plasma phenylalanine in severe malaria and implications for pathophysiology of neurological complications," *Infection and Immunity*, vol. 74, no. 6, pp. 3355–3359, 2006.

[25] J. D. Fernstrom and M. H. Fernstrom, "Tyrosine, phenylalanine, and catecholamine synthesis and function in the brain," *The Journal of Nutrition*, vol. 137, no. 6, pp. 1539S–1547S, 2007.

[26] F. Zhang, Z. Jia, P. Gao et al., "Metabonomics study of atherosclerosis rats by ultra fast liquid chromatography coupled with ion trap-time of flight mass spectrometry," *Talanta*, vol. 79, no. 3, pp. 836–844, 2009.

[27] M. Watford, "Glutamine metabolism and function in relation to proline synthesis and the safety of glutamine and proline supplementation," *The Journal of Nutrition*, vol. 138, no. 10, pp. 2003S–2007S, 2008.

[28] S. H. Lee, I. Kim, and B. C. Chung, "Increased urinary level of oxidized nucleosides in patients with mild-to-moderate Alzheimer's disease," *Clinical Biochemistry*, vol. 40, no. 13-14, pp. 936–938, 2007.

[29] J. Dyerberg, "Linolenate-derived polyunsaturated fatty acids and prevention of atherosclerosis," *Nutrition reviews*, vol. 44, no. 4, pp. 125–134, 1986.

Hindawi Publishing Corporation
Journal of Analytical Methods in Chemistry
Volume 2014, Article ID 643879, 9 pages
http://dx.doi.org/10.1155/2014/643879

Research Article

Simultaneous Quantitative and Qualitative Analysis of Flavonoids from Ultraviolet-B Radiation in Leaves and Roots of *Scutellaria baicalensis* Georgi Using LC-UV-ESI-Q/TOF/MS

Wen-Ting Tang, Min-Feng Fang, Xiao Liu, and Ming Yue

Key Laboratory of Resource Biology and Biotechnology in Western China, Ministry of Education, The College of Life Sciences, Northwest University, No. 229 Taibai North Road, Xi'an, Shaanxi 710069, China

Correspondence should be addressed to Ming Yue; yueming@nwu.edu.cn

Received 18 January 2014; Accepted 13 February 2014; Published 13 March 2014

Academic Editor: Feng Wei

Copyright © 2014 Wen-Ting Tang et al. This is an open access article distributed under the Creative Commons Attribution License, which permits unrestricted use, distribution, and reproduction in any medium, provided the original work is properly cited.

Scutellaria baicalensis Georgi is one of the most widely used traditional Chinese herbal medicines. It has been used for anti-inflammatory, anticancer, antibacterial activities, and so forth. Long-term enhanced ultraviolet-B (UV-B) radiation caused more effect on leaves than on roots of the plant. Liquid chromatography-ultraviolet detection coupled with electrospray ionization quadrupole time-of-flight mass spectrometry (LC-UV-ESI-Q/TOF/MS) method was applied for simultaneous quantitative and qualitative analysis of flavonoids in leaves and roots of *S. baicalensis* by enhanced UV-B radiation. Both low-intensity radiation and high-intensity radiation were not significantly increaseing the contents of baicalin, wogonoside, and wogonin in roots. However different intensity of radiation has different effects on several flavonoids in leaves. Both low-intensity radiation and high-intensity radiation had no significant effect on contents of baicalin and tectoridin in leaves; the content of scutellarin was significantly decreased by low-intensity radiation; chrysin was detected in low-intensity radiation and high-intensity radiation, and chrysin content is the highest in low-intensity radiation, but chrysin was not detected in control group. Different changes of different flavonoids under enhanced UV-B radiation indicate that induction on flavonoids is selective by enhanced UV-B radiation.

1. Introduction

Scutellaria baicalensis Georgi (Labiatae) is a kind of perennial herb. It is one of the most widely used traditional Chinese medicines and is officially listed in the Chinese Pharmacopoeia. Its roots have been used for anti-inflammation and anticancer, treating bacterial and viral infections of the respiratory and the gastrointestinal tract, cleaning away heat, moistening aridity, purging fire, detoxifying toxicosis, reducing the total cholesterol level, and decreasing blood pressures. This herb also possesses cholagogic, diuretic, and cathartic actions. Some concentrated composite herbal preparations that contain *S. baicalensis* as a major ingredient in their prescriptions are widely used in oriental countries [1, 2].

S. baicalensis contains a variety of flavonoids, phenylethanoids, amino acids sterols, and essential oils. Its dried roots contain over 30 kinds of flavonoids, such as baicalin, baicalein, wogonin, wogonin 7-O-glucuronide, oroxylin A, and oroxylin A 7-O-glucuronide [3]. Baicalin, baicalein, wogonin, and wogonoside are the main components and have significant pharmacological effects [4, 5]. Chemical composition of root of *S. baicalensis* has been comprehensive studies [3]. However chemical components of leaf were still inadequate.

Researchers have paid attention to ultraviolet-B (UV-B) radiation on the effects of plant secondary metabolism. It has significant effects on contents of secondary metabolites in many natural medicines. Several studies showed that contents of phenols, alkaloids, essential oil, and cannabinoids could be induced by enhanced UV-B radiation [6–9]. UV-B radiation has important effects on antioxidant systems and secondary metabolism of *S. baicalensis*. The determination of current LC-UV-ESI-Q/TOF/MS focuses on enhanced UV-B radiation effects on active ingredient contents in the leaves and roots of *S. baicalensis*. This study can understand effects

of long-term enhanced UV-B radiation on contents of the flavonoids from leaves and roots of *S. baicalensis*.

2. Experimental

2.1. Chemicals and Reagents. Baicalin (number 110715-201016), tectoridin (number 111632-200501), and chrysin (number 111701-200501) were purchased from National Institute for the Control of Pharmaceutical and Biological Products; wogonoside (number E-0664), scutellarin (number E-0554), and wogonin (number E-0103) were purchased from Shanghai Tongtian Biotech Company. LC-grade acetonitrile was purchased from the Fisher Company. Ultrahigh purity water was prepared using a Milli-Q water purification system. Other chemicals were of analytical grade and their purity was above 99.5%.

2.2. Plant Materials and UV-B Irradiation. Seeds were bought from planting base in Shangluo, Shaanxi, in April 2009. Seeds were sowed at the Northwest University Biological Park and then routine management were conducted. Plants were randomly divided into control group (CK), low-intensity UV-B group (TL), and high-intensity UV-B group (TH) in April 19, 2010. Enhanced UV-B treatment was conducted every day from 9:00 to 17:00 for the TL and TH groups, except rainy day. The treatment was conducted until September 3, 2010. UV-B radiation was provided by UV-B Lamps (40 W, wavelength 313 nm), and the lamps were placed below the treatment group. UV-B intensities were measured using a UV radiometer intensity of UV-B radiation for TL and TH groups at the top of plants that were 12.1 μW/cm and 34.5 μW/cm, respectively.

2.3. Sample Preparation and Determination. After harvesting, seven plants CK, TL, and TH groups were dried at 105°C for 30 min and then were dried 80°C for 72 h. Roots and leaves were crushed with a muller and filtered through 40 mesh sieve. After that, they were placed in cool, dry, and dark environment. Samples were prepared following reported methods and made appropriate modification [10]. 0.1 g leaf sample and 0.05 g root sample were extracted with 50 mL solvent including methanol : water : formic acid (70 : 29 : 1) by ultrasonic method for 120 min. Extracted solutions were centrifuged for 7 min at 13000 rpm; then, the supernatant was filtered through 0.22 μm filters.

2.4. LC-MS Condition and LC Condition. LC-UV-ESI-Q/TOF/MS analysis was carried out according to the reported method by Horvath et al. [10], with minor modifications. Analysis was performed with an UltiMate3000 liquid chromatographic system (Dionex, USA) equipped with a MacroTOF-QII (Bruker, German). The chromatographic separation was performed on a C18 analytical column (4.6 mm × 150 mm, 5 μm i.d.) with the column temperature set at 30°C. The mobile phase consisted of acetonitrile (A) and formic acid water (pH = 3) (B). The optimized HPLC elution conditions were as follows: 0–5.0 min, 17–30% A; 5.0–10.0 min, 30–50% A; 10.0–15.0 min, 50–100% A; 15.0–20.0 min, 100–17% A; and 20.0–25.0 min, 17% A. The flow rate was 0.3 mL/min with detector wavelength set at 278 nm, and the injection volume was 10 μL. Mass spectrometry was performed on electrospray ionization source in the negative mode.

LC-UV analysis was determined following reported methods [10], with minor modification. Analysis was performed with an UltiMate3000 liquid chromatographic system (Dionex, USA). The chromatographic separation was performed on a Hypersil ODS2 analytical column (4.6 mm × 150 mm, 5 μm i.d.) with the column temperature set at 30°C. The mobile phase consisted of acetonitrile (A) and formic acid water (pH = 3) (B). The optimized LC elution conditions were as follows: 0–5.0 min, 17%–30% A; 5.0–10.0 min, 30%–50% A; 10.0%–15.0 min, 50%–100% A; 15.0–20.0 min, 100%–17% A; and 20.0–25.0 min, 17% A. The flow rate was 1.0 mL/min with detector wavelength set at 278 nm, and the injection volume was 10 μL.

2.5. Preparation of Standard Solutions. Standard stock solutions of scutellarin (1000 μg/mL), tectoridin (120 μg/mL), baicalin (1120 μg/mL), chrysin (1140 μg/mL), wogonoside (120 μg/mL), and wogonin (1160 μg/mL) were prepared by dissolving suitable amounts of pure substance in methanol and were stored in darkness at 4°C. Working standard solutions containing scutellarin (100 μg/mL), tectoridin (50 μg/mL), baicalin (100 μg/mL), chrysin (114 μg/mL), wogonoside (50 μg/mL), and wogonin (116 μg/mL) were prepared by diluting the stock solutions with methanol to a series of proper concentrations. All the solutions were stored in the refrigerator at 4°C before analysis.

2.6. Calibration Curves, Correlation Coefficient, and Linear Range of Six Flavonoids. A calibration curve is used to determine the calculated concentration of the samples and triplicate injections. The curve is a plot of the standards' concentration against the area of tested compound by known concentration on the x-axis and the measured area on the y-axis. The calibration curve of each compound was performed with at least six appropriate concentrations. The linearity was evaluated by linear regression analysis calculated by the least square regression method.

2.7. Statistical Analysis. All experiments were performed in six times repeatedly. Statistical analyses were performed with STATISTICA 6.0. The results were expressed as the means ± standard error (S.E.) of triplicate. The data were subjected to one-way analysis of variance (ANOVA) and the significance of difference between samples means was calculated by Duncan's multiple range test and P values less than 0.05 were considered significant.

3. Results

3.1. Linearity, Limit of Detection, and Limit of Quantification. To improve quantification precision and repeatability, the

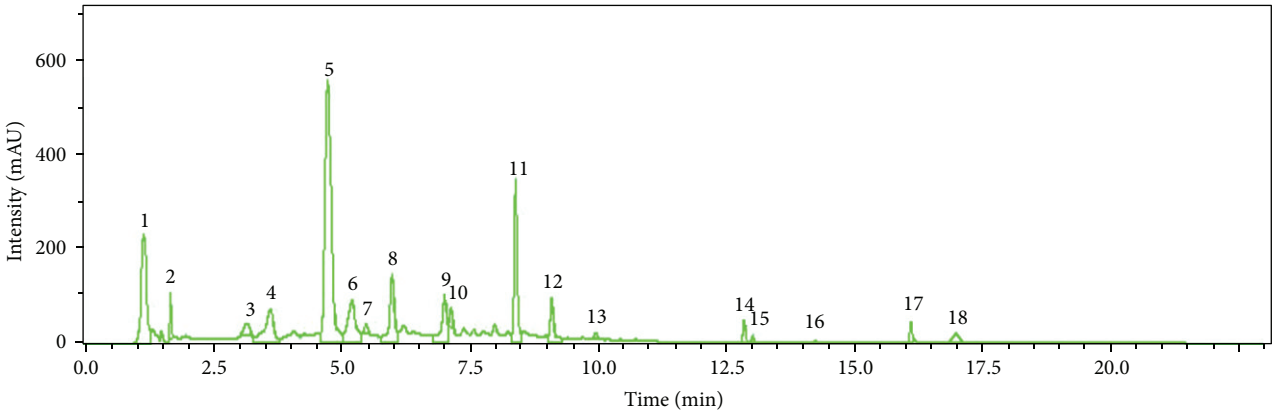

Figure 1: Typical chromatogram of LC-UV-MS from TL-leaves of *S. baicalensis*.

Table 1: Calibration curves, correlation coefficient, and linear range of six flavonoids.

Analyte	Calibration curve	r	Linear range (μg/mL)
Scutellarin	$y = 12671 \times -42837$	0.9979	3.13–100
Tectoridin	$y = 25559 \times -18475$	0.9957	0.75–24.0
Baicalin	$y = 26364 \times -1345$	0.9973	0.36–11.40
Chrysin	$y = 29604 \times -56360$	0.9982	1.75–112.0
Wogonoside	$y = 45361 \times -8145$	0.9987	0.38–24.0
Wogonin	$y = 39610 \times -3237$	0.9978	0.20–12.76

curves of six flavonoids are plots of the standards' concentration against the area of tested flavonoids. It then applies the area of the flavonoids in real samples to the curves and finds the concentration from the x-axis to determine the calculated concentration. Calibration curves, correlation coefficient, and linear range of six tested flavonoids were shown in Table 1. The calibration curves generated from detection of sample containing known amounts of the six flavonoids were linear over the quantities ranges from 0.2 μg/mL to 100 μg/mL. The correlation coefficient (r) for each of these calibration curves was over 0.99, indicating a good linear detector response dynamic range that was investigated.

3.2. Results of LC-UV-ESI-Q/TOF/MS Analysis. LC-UV-ESI-Q/TOF/MS chromatograms and corresponding mass spectra of the TL-leaves of *S. baicalensis* were shown in Figures 1 and 2. Peaks 5 and 6 were *m/z* 463.0. It has been confirmed that scutellarin existed in leaves of *S. baicalensis* (*m/z* is 462.3). *m/z* 462.4 was fragment ion of tectoridin, which was close to scutellarin and both of the two compounds were isoflavone, so we concluded that peaks 5 and 6 were scutellarin and tectoridin, respectively. Peaks 8 and 11 were *m/z* 445.0, which suggested that the possible compositions were apigenin-7-O-glucuronide (*m/z* 446.3) and baicalin (*m/z* 446.3). Peak 9 was consistent with several peaks, in which the greatest relative abundance was *m/z* 287.0 and it was baicalein's peak (*m/z* 286.6). Peaks 14 and 15 were *m/z* 253.0 and it was chrysin's peaks.

Table 2: Relative peak area of CK, TL, and TH from leaves of *S. baicalensis*.

Number	CK	TL	TH
1	0.14	0.17	0.15
2	0.14	0.13	0.12
3	0.19	0.20	0.24
4	0.17	0.14	0.17
5	1.00	1.00	1.00
6	0.90	0.96	1.30
7	0.33	0.40	0.38
8	0.31	0.39	0.33
9	0.10	0.11	0.09
10	0.16	0.31	0.22
11	0.11	0.09	0.17
12	0.09	0.18	0.11
13	#	#	0.04
14	0.06	0.61	0.21
15	0.04	0.06	0.03
16	#	0.16	0.03
17	#	0.08	0.04

(#): not detected.

3.3. Comparison of the Relative Peak Area of Flavonoids. Typical chromatograms of CK, TL, and TH from leaves of *S. baicalensis* were shown in Figure 3 and the relative peak area from leaves of *S. baicalensis* was shown Table 2. Relative peak areas of peaks 6, 7, 10, and 14 were significantly increased in low-intensity UV-B radiation group and high-intensity UV-B radiation group compared with control group. Relative peak areas of peaks 1, 8, 12, and 15 were significantly increased in low-intensity UV-B radiation group compared with control group. Relative peak areas of peaks 3 and 11 were significantly increased in high-intensity UV-B radiation group compared with control group. Other relative peak area of peaks had a slight change in low-intensity UV-B radiation group and high-intensity UV-B radiation group. The relative peak area of the peak 14 produced a maximum increase by 10 times in

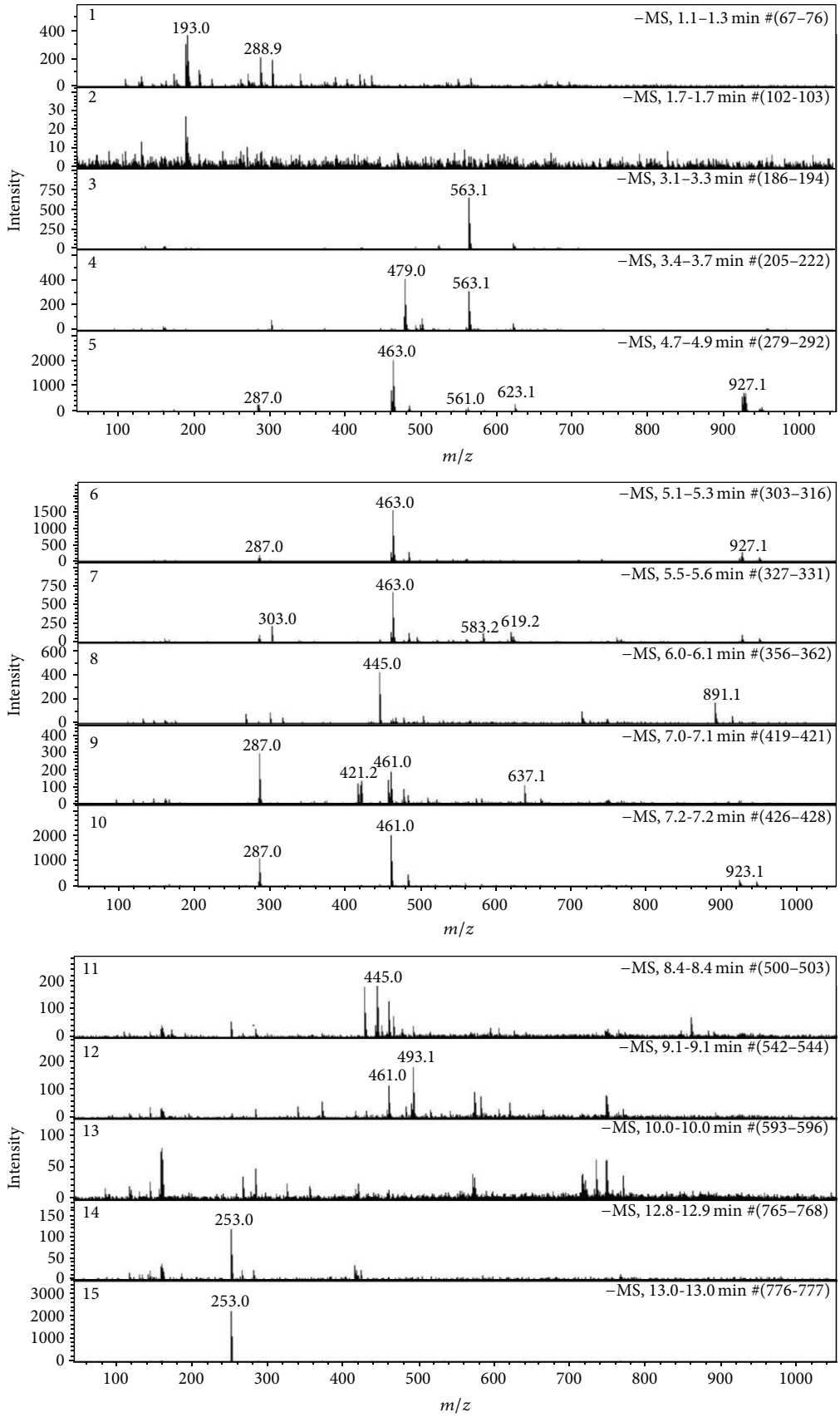

Figure 2: Corresponding mass spectra from HPLC-UV chromatogram in TL-leaves of *S. baicalensis*. Numbers consist with Figure 1.

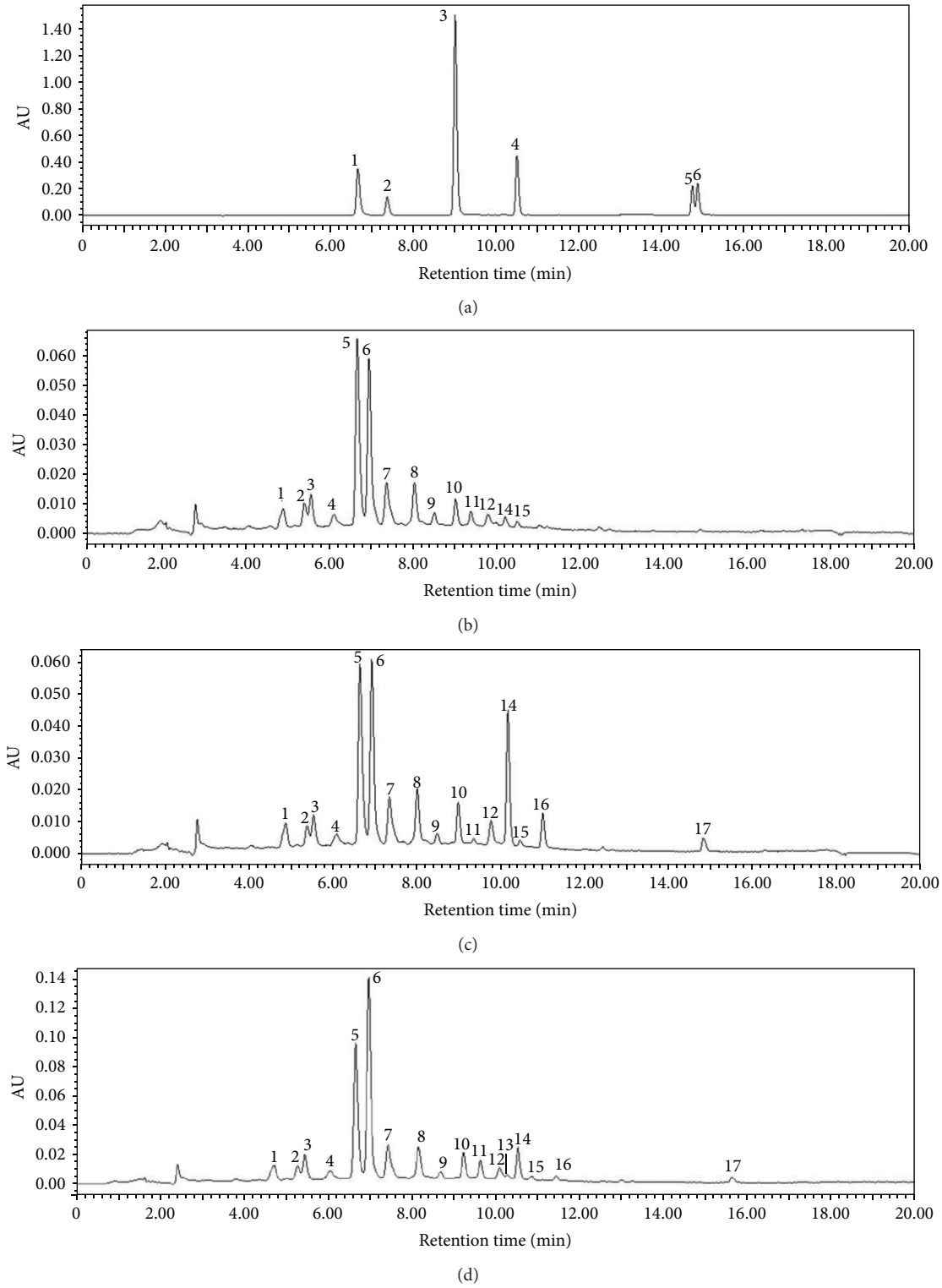

Figure 3: Typical chromatograms of flavonoids standards (a) and chromatograms of CK (b), TL (c), and TH (d) from leaves of *S. baicalensis*. Peaks 5, 7, 10, and 17 are the chromatogram peaks of scutellarin, tectoridin, baicalin, and chrysin, respectively. 1: scutellarin, t_r = 6.64 min; 2: tectoridin, t_r = 7.31 min; 3: baicalin, t_r = 9.02; 4: wogonoside, t_r = 10.55 min; 5: wogonin, t_r = 14.70 min; 6: chrysin, t_r = 14.81 min.

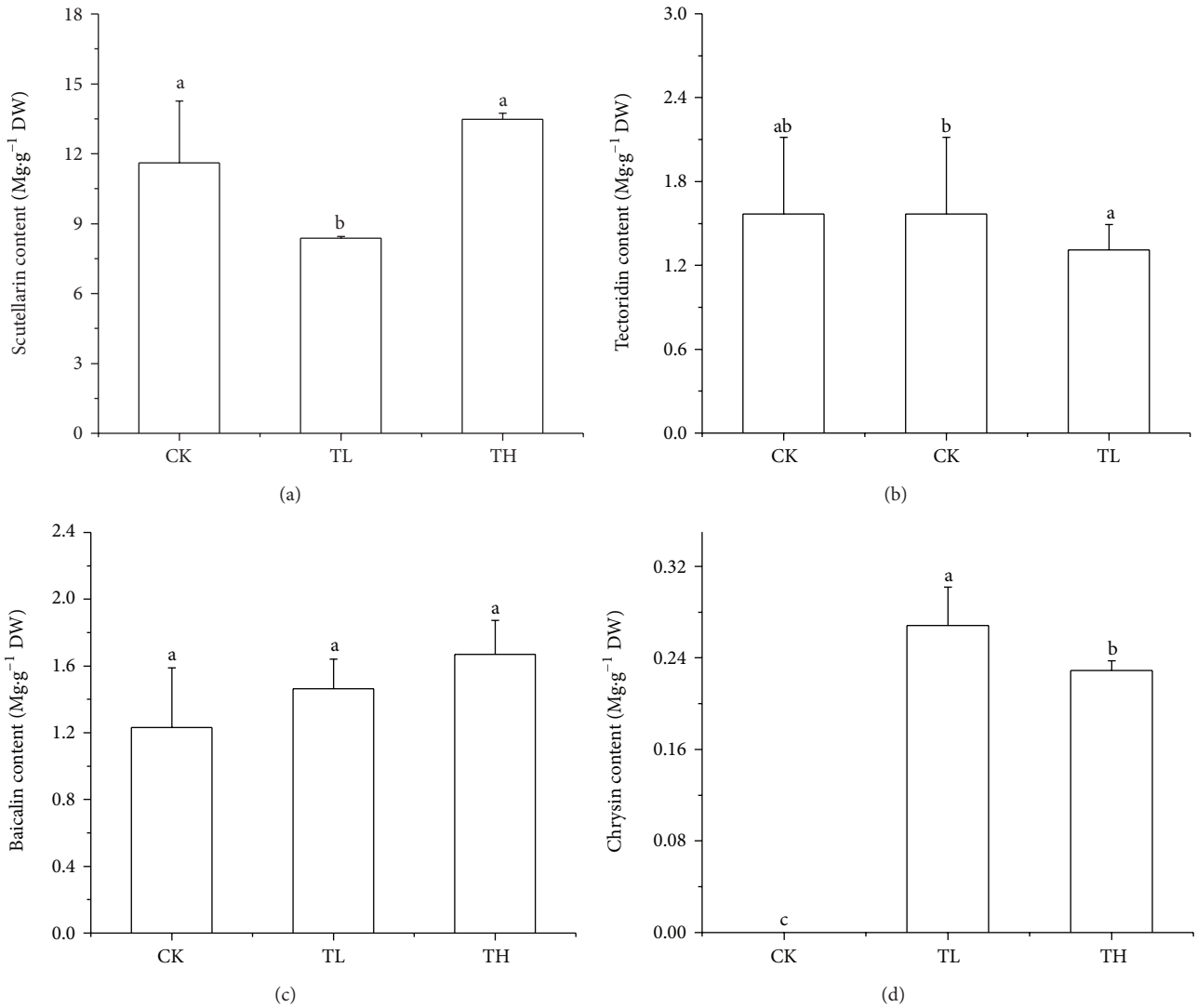

Figure 4: The contents of scutellarin, tectoridin, baicalin, and chrysin of CK, TL, and TH from leaves of *S. baicalensis*. Different alphabet followed the data of same index at the same treatment time that indicates significant difference among treatments.

low-intensity UV-B radiation. The relative peak area of the peak 6 produced a maximum increase by 1.4 times in high-intensity UV-B radiation. This may indicate that these types of flavonoids were induced by UV-B radiation and led to the contents increased significantly. However relative area of peak 2 was decreased in low-intensity UV-B radiation group and high-intensity UV-B radiation group. Relative peak area of the peak 4 was decreased in low-intensity UV-B radiation. Except 14 common peaks, some peaks only appeared under low- and/or high-intensity UV-B radiation. Peaks 16 and 17 were detected in two enhanced UV-B radiation groups and their relative peak areas were larger in low-intensity UV-B radiation, while peak 13 was only detected in high-intensity UV-B radiation. These results showed that enhanced UV-B radiation could increase contents of flavonoids in leaves of *S. baicalensis*. We inferred that enhanced UV-B radiation could increase content of some flavonoids in the leaves of *S. baicalensis*.

3.4. Quantitative Analysis of Several Flavonoids. Figure 3 showed LC of CK, TL, and TH from leaves of *S. baicalensis*. Peak 1, 2, 3, and 6 are scutellarin, tectoridin, baicalin, and chrysin, respectively. Figure 4 showed flavonoid contents in leaves of *S. baicalensis*. It can be seen that different intensities of UV-B radiation have different effects on several flavonoids in leaves of *S. baicalensis*. Low-intensity and high-intensity UV-B radiation had no significant effects on contents of baicalin and tectoridin in leaves of *S. baicalensis*; low-intensity UV-B radiation significantly decreased the content scutellarin; chrysin was not detected in the control group while chrysin was detected in low-intensity and high-intensity UV-B radiation groups, and chrysin content is the highest in the low-intensity UV-B radiation group.

Figure 5 showed LC of extracts from roots of *S. baicalensis*. Peaks 3, 4, and 5 are baicalin, wogonoside, and wogonin, respectively. Figure 6 showed flavonoid contents in roots of *S. baicalensis*. It can be seen that both the low-intensity

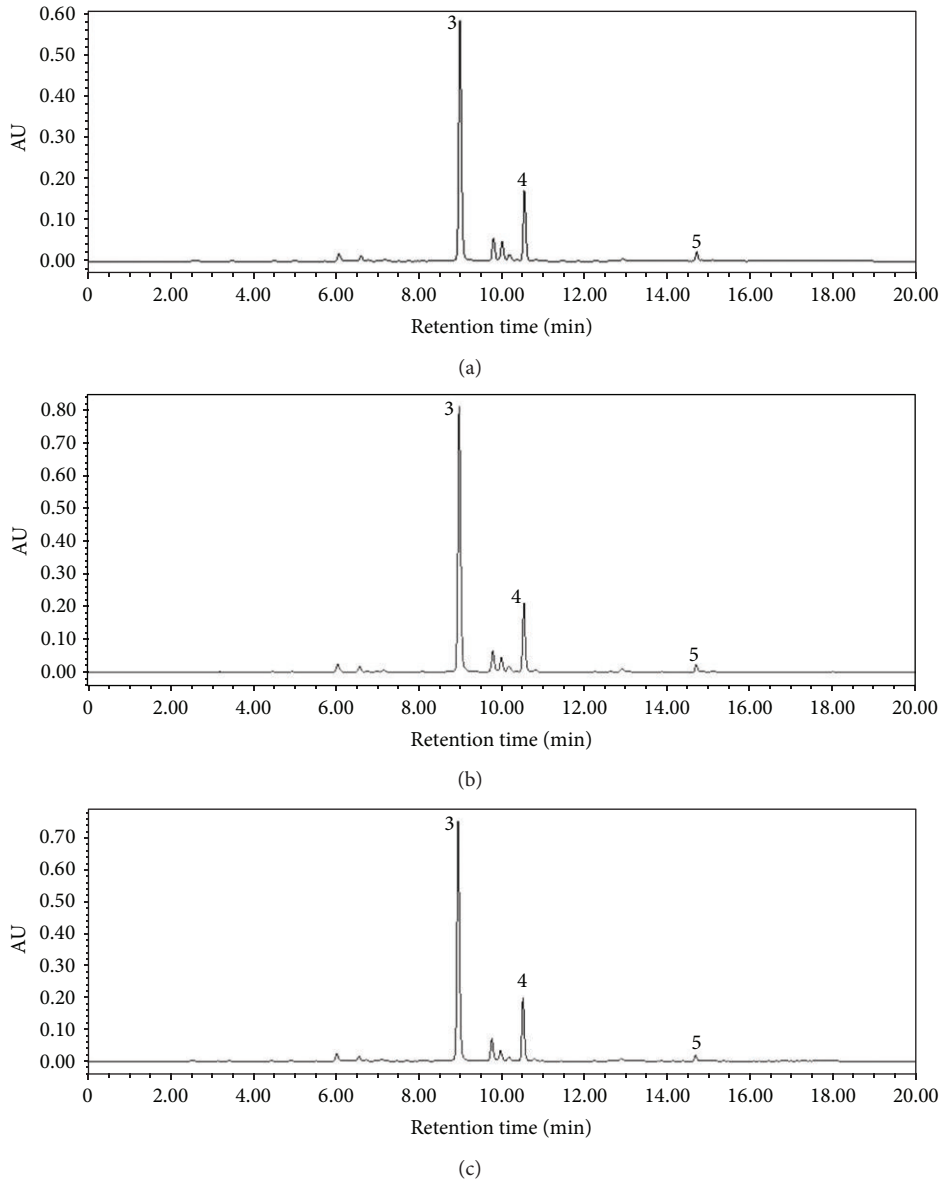

Figure 5: Typical chromatograms of CK (a), TL (b), and TH (c) from root of *S. baicalensis*.

and high-intensity enhanced UV-B radiation have not increased the contents of baicalin, wogonoside, and wogonin in root of *S. baicalensis*.

4. Discussions

HPLC method was used for influence of enhanced UV-B radiation on the chemical composition of plants. Flavonoids including the active ingredient of *S. baicalensis* can be accurately determinated based on this method. *S. baicalensis* was exposed under long-term UV-B radiation to understand the response of flavonoids in whole leaves and roots of plants under enhanced UV-B radiation. There is no significantly difference among the enhanced UV-B radiation group compared with control group, although baicalin content has a trend of increase under low-intensity enhanced UV-B radiation, as well as contents of wogonoside and wogonin under high-intensity enhanced UV-B radiation.

The content of scutellarin in leaves of *S. baicalensis* even decreased in low-intensity enhanced UV-B radiation. The contents of tectoridin and baicalin had no significant difference compared with the control group while they showed a trend of increase under high-intensity enhanced UV-B radiation. Chrysin was not detected in the control group, while chrysin was detected in the low-intensity and high-intensity enhanced UV-B radiation, and chrysin content was

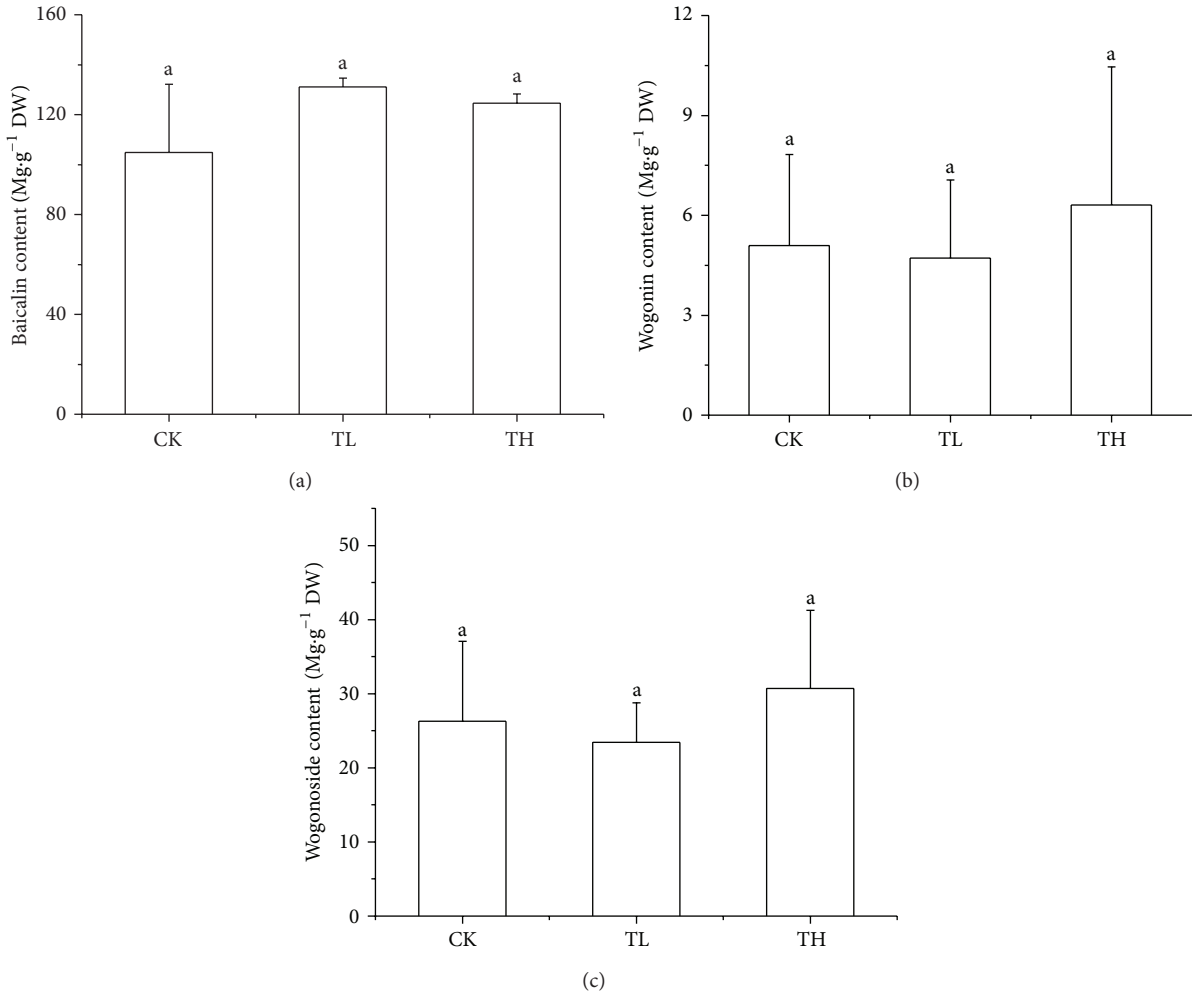

Figure 6: The contents of baicalin, wogonoside, and wogonin of CK, TL, and TH form roots of *S. baicalensis*. Different alphabet followed the data of same index at the same treatment time that indicates significant difference among treatments.

the highest under the low-intensity UV-B radiation. Results indicated that the several flavonoids were affected by different enhanced UV-B radiation, and enhanced UV-B radiation on leaves was stronger than roots. Flavonoids of relative peak area in leaves indicated significant increase of several flavonoids under enhanced UV-B radiation.

The reported literature showed the ratio of flavonoids with *ortho*-dihydroxy to those only with 4′-hydroxy in ring B of the flavonoid skeleton increase [11]. Quercetin and kaempferol were flavonoids with 3′,4′-*ortho*-hydroxy and 4′-hydroxy, respectively. The shift from kaempferol to quercetin was of interest. Increase level of quercetin was significantly higher than kaempferol under UV-B radiation [12]. It was demonstrated that quercetin showed a better scavenger of superoxide than kaempferol *in vitro* [13]. Other studies found the same shift between apigenin and luteolin derivatives [14]. Studies indicated that quercetin can more effectively scavenge hydroxyl radicals than kaempferol [15]. Olsson et al. reported that the contents of quercetin (or luteolin) derivatives had a significant increase after enhanced UV-B exposure in species capable of the shift in compound. These compounds were considered as an indicator of stress, especially if this translates into a greater capacity for antioxidative function.

Several studies have explored the mechanism of accumulation of plant secondary metabolites by enhanced UV-B radiation. Increase of some essential oil under enhanced UV-B radiation could promote development of vegetable oil glands [16]. A well-established UV-B effect thought to be mediated by the postulated UV-B photoreceptor is the induction of phenylpropanoid biosynthetic pathway components leading to the accumulation of sunscreen flavonoids [17].

5. Conclusions

This study is the first application of LC-UV-ESI-Q/TOF-MS method to routine identification and determination of the flavonoids from ultraviolet-B radiation in leaves and roots of *Scutellaria baicalensis* Georgi. Long-term enhanced UV-B radiation caused more effect on leaves than on roots of the plant. An amount of some flavonoids are significantly increased under low-intensity or (and) high-intensity UV-B

radiation, while others do not change significantly. Different changes of different flavonoids under enhanced UV-B radiation indicated that induction on flavonoids by enhanced UV-B radiation is selective.

Conflict of Interests

There are no conflict of interests.

Acknowledgments

This study was supported in part by grants from the National Science Foundation of China (31070362), Special Foundation of Key Laboratory of Resource Biology and Biotechnology in Western China, Ministry of Education (2010JS100), and Innovative Research Team in University of Ministry of Education of China (IRT1174).

References

[1] D. Y. Zhang, J. Wu, F. Ye et al., "Inhibition of cancer cell proliferation and prostaglandin E2 synthesis by *Scutellaria baicalensis*," *Cancer Research*, vol. 63, no. 14, pp. 4037–4043, 2003.

[2] H.-T. Lu, Y. Jiang, and F. Chen, "Application of high-speed counter-current chromatography to the preparative separation and purification of baicalin from the Chinese medicinal plant *Scutellaria baicalensis*," *Journal of Chromatography A*, vol. 1017, no. 1-2, pp. 117–123, 2003.

[3] X. Shang, X. He, X. He et al., "The genus Scutellaria an ethnopharmacological and phytochemical review," *Journal of Ethnopharmacology*, vol. 128, no. 2, pp. 279–313, 2010.

[4] J. Zhu, Z. Wang, Q. Zhang, J. Niu, and F. Li, "A quantitative method for simultaneous assay of four flavones with one marker in *Radix Scutellariae*," *China Journal of Chinese Meteria Medica*, vol. 34, no. 24, pp. 3229–3234, 2009.

[5] C. Y. Ma, B. C. Dai, R. C. Lin et al., "HPLC quantitative analysis and fingeprint study of four flavonoids in *Scutellaria baicalensis*," *Chinese Journal of Pharmaceuticals Analysis*, vol. 23, no. 2, pp. 83–86, 2003.

[6] J. C. Luis, R. M. Pérez, and F. V. González, "UV-B radiation effects on foliar concentrations of rosmarinic and carnosic acids in rosemary plants," *Food Chemistry*, vol. 101, no. 3, pp. 1211–1215, 2006.

[7] P. B. F. Ouwerkerk, D. Hallard, R. Verpoorte, and J. Memelink, "Identification of UV-B light-responsive regions in the promoter of the tryptophan decarboxylase gene from *Catharanthus roseus*," *Plant Molecular Biology*, vol. 41, no. 4, pp. 491–503, 1999.

[8] C. B. Johnson, J. Kirby, G. Naxakis, and S. Pearson, "Substantial UV-B-mediated induction of essential oils in sweet basil (*Ocimum basilicum* L.)," *Phytochemistry*, vol. 51, no. 4, pp. 507–510, 1999.

[9] D. W. Pate, "Possible role of ultraviolet radiation in evolution of Cannabis chemotypes," *Economic Botany*, vol. 37, no. 4, pp. 396–405, 1983.

[10] C. R. Horvath, P. A. Martos, and P. K. Saxena, "Identification and quantification of eight flavones in root and shoot tissues of the medicinal plant Huang-qin (*Scutellaria baicalensis* Georgi) using high-performance liquid chromatography with diode array and mass spectrometric detection," *Journal of Chromatography A*, vol. 1062, no. 2, pp. 199–207, 2005.

[11] K. R. Markham, G. J. Tanner, M. Caasi-Lit, M. I. Whitecross, M. Nayudu, and K. A. Mitchell, "Possible protective role for 3′,4′;-dihydroxyflavones induced by enhanced UV-B in a UV-tolerant rice cultivar," *Phytochemistry*, vol. 49, no. 7, pp. 1913–1919, 1998.

[12] L. C. Olsson, M. Veit, G. Weissenböck, and J. F. Bornman, "Differential flavonoid response to enhanced UV-B radiation in *Brassica napus*," *Phytochemistry*, vol. 49, no. 4, pp. 1021–1028, 1998.

[13] J. P. Hu, M. Calomme, A. Lasure et al., "Structure-activity relationship of flavonoids with superoxide scavenging activity," *Biological Trace Element Research*, vol. 47, no. 1–3, pp. 327–331, 1995.

[14] L. Liu, D. C. Gitz, and J. W. McClure, "Effects of UV-B on flavonoids, ferulic acid, growth and photosynthesis in barley primary leaves," *Physiologia Plantarum*, vol. 93, no. 4, pp. 725–733, 1995.

[15] M. V. Rao, G. Paliyath, and D. P. Ormrod, "Ultraviolet-B- and ozone-induced biochemical changes in antioxidant enzymes of *Arabidopsis thaliana*," *Plant Physiology*, vol. 110, no. 1, pp. 125–136, 1996.

[16] C. B. Johnson, J. Kirby, G. Naxakis, and S. Pearson, "Substantial UV-B-mediated induction of essential oils in sweet basil (*Ocimum basilicum* L.)," *Phytochemistry*, vol. 51, no. 4, pp. 507–510, 1999.

[17] B. Kucera, G. Leubner-Metzger, and E. Wellmann, "Distinct ultraviolet-signaling pathways in bean leaves. DNA damage is associated with β-1,3-glucanase gene induction, but not with flavonoid formation," *Plant Physiology*, vol. 133, no. 4, pp. 1445–1452, 2003.

Hindawi Publishing Corporation
Journal of Analytical Methods in Chemistry
Volume 2014, Article ID 764397, 7 pages
http://dx.doi.org/10.1155/2014/764397

Research Article

Using the Doubly Charged Selected Ion Coupled with MS/MS Fragments Monitoring (DCSI-MS/MS) Mode for the Identification of Gelatin Species

Xian-Long Cheng,[1,2] Feng Wei,[2] Jia Chen,[2] Ming-hua Li,[1] Lei Zhang,[1] Ying-Yong Zhao,[3] Xin-Yue Xiao,[2] Shuang-cheng Ma,[1,2] and Rui-Chao Lin[1,2]

[1] *School of Chinese Pharmacy, Beijing University of Chinese Medicine, No. 6 Wangjing Zhong Huan Nan Lu, Chaoyang District, Beijing 100102, China*
[2] *Institute for the Control of Traditional Chinese Medicine and Ethnic Medicine, National Institutes for Food and Drug Control, State Food and Drug Administration, 2 Tiantan Xili, Beijing 100050, China*
[3] *Key Laboratory of Resource Biology and Biotechnology in Western China, Ministry of Education, The College of Life Sciences, Northwest University, No. 229 Taibai North Road, Xi'an, Shaanxi 710069, China*

Correspondence should be addressed to Shuang-cheng Ma; masc@nifdc.org.cn and Rui-Chao Lin; linrch307@sina.com

Received 18 January 2014; Accepted 11 February 2014; Published 13 March 2014

Academic Editor: Yu-Ming Fan

Copyright © 2014 Xian-Long Cheng et al. This is an open access article distributed under the Creative Commons Attribution License, which permits unrestricted use, distribution, and reproduction in any medium, provided the original work is properly cited.

In electrospray ionization (ESI) mode, peptides and proteins can be multiply charged ions; in this situation a doubly charged selected ion (DCSI) coupled with mass spectrometry (MS/MS) fragments monitoring (DCSI-MS/MS) method is the most suitable scanning mode to detect known peptides in complex samples when an ion-trap mass spectrometer is the instrument used for the analysis. In this mode, the MS detector is programmed to only select a doubly charged ion as a precursor and to perform continuous MS/MS on one or more of the selected precursors, either during a specific time interval or along the whole chromatographic run. Gelatin is a mixture of high molecular weight polypeptides from the hydrolysis of collagen. In this study, the DCSI-MS/MS monitoring mode was applied to the detection of previously characterized species-specific peptides from different gelatins. The proposed methodology makes use of tryptic digestion for sample preparation and peptide separation and identification by rapid resolution liquid chromatography coupled to an ion trap working in the DCSI-MS/MS mode for the analysis. This methodology was applied to the differential classification of five commercial, homological species of gelatins and proved to be an excellent tool for gelatin product authentication.

1. Introduction

The assessment of gelatin authentication and origin is of major concern for standards authorities, not only to assist in the prevention of commercial fraud in the food, cosmetic, and pharmaceutical industries [1, 2], but also to help avoid the safety risks derived from diseases among livestock that might be harmful for human health. The correct identification of gelatin species thus becomes an issue of primary relevance for these industries.

The characterization of external morphological features is a particularly difficult method for gelatin species differentiation because of their apparent similarities and to the fact that they are frequently lost during the manufacturing process. An alternative, molecular method for gelatin species identification based on DNA or protein analysis is tedious and time consuming. Polymerase chain reaction (PCR) method has been used in DNA analysis but again is not available for gelatin identification because of the heavy destruction of DNA in gelatin during processing, although this method has been widely applied in collagen identification [3, 4]. Similarly, the immunochemical method has been used to identify collagen [5], but again the usefulness of this method might be influenced by the extent of the proline hydroxylation which plays an important role in determining

the antigenicity of collagen. As a result of the problems with the methods that we have outlined, proteomics methods have been proposed as alternative tools for the assessment of the authenticity and traceability of collagen species in gelatins [6], and mass spectrometry has been successfully applied to elucidate differences among homological gelatins [7]. In line with these results, we developed an analytical method based on proteomics to distinguish these gelatins effectively. This method will also prevent the possibility of mislabeling and adulterations.

Collagens from different sources contain differential amino-acidic sequences. In previous studies [8], we have characterized the specific peptides from five species of gelatins by means of UPLC-QTOF/MS coupled with PCA. Those specific peptides can be used as specific markers for gelatin product authentication.

The analysis of tryptic peptides, as commonly used in proteomics, is a powerful technique for the identification of proteins [9, 10]. A complex peptide sample is typically first separated into its constituents by using HPLC-DAD (diode array detector) and HPLC/MS/MS [11, 12] procedures. In recent years, the new analytical technique of ultraperformance liquid chromatography has been developed for the study of proteins [13, 14]. This method uses small particle size packing in the column to provide better chromatographic resolution.

A peptide resulting from tryptic digestion normally has a basic residue (arginine or lysine) at its C-terminus and yields a prominent doubly charged ion peak when ionized by ESI. If this ion is chosen as the parent ion for an MS/MS measurement, the production of a series of y-ion daughters (ions resulting from cleavage at the amide bonds and containing the C-terminus) is favored and the resulting spectrum is likely to be easy to interpret [15]. For this reason we selected the doubly charged ion as the parent ion for our analysis.

The objective of this work is the study of gelatins using the doubly charged selected ion coupled with MS/MS fragments monitoring (DCSI-MS/MS) to aid in the identification of gelatins. The gelatins were digested by trypsin, liquid chromatography separation, and peptide identification by MS using the DCSI-MS/MS scanning mode, as a reliable method for fast and effective gelatin identification. In addition, the possibility of detecting the target peptides in these samples with rapid resolution liquid chromatography (RRLC) separation, using an electrospray ionization- (ESI-) ion trap (IT) MS, was tested.

2. Experimental

2.1. Chemicals. Formic acid was purchased from Sigma-Aldrich (St. Louis, MO, USA). Acetonitrile (HPLC grade) was purchased from Merck (Rahway, NJ, USA). Methanol (HPLC grade) was purchased from Fisher Scientific (Pittsburgh, PA, USA). Ultra-high-purity water was prepared by a Milli-Q water purification system (Millipore Corporation, Bedford, Massachusetts). Trypsin (sequencing grade) was obtained from Promega (Madison, WI, USA). A syringe filter (0.22 μm) was purchased from Millipore (Billerica, MA, USA). All other chemicals used were of analytical grade. Five different gelatins were made by lab for analysis. Five of the 20 samples tested were donkey-hide gelatins, belonging to the family Equidae, six samples were bovine-hide gelatins belonging to the family Bovidae, three samples were porcine-hide gelatins belonging to the family Suidae, three samples were deerhorn gelatins belonging to the family Cervidae, and three samples were of Tortoise shell glue, belonging to the family Emydidae. Twenty commercial samples were collected on market.

2.2. Peptide Sample Preparation. First, 100 mg of the gelatin standard was dissolved in 50 mL of a 1% NH_4HCO_3 solution (pH 8.0). The solution was filtered through a 0.22 μm syringe filter. Then, 100 μL of the gelatin solution was drawn, and 10 μL of trypsin solution (1 mg/mL in 1% NH_4HCO_3, pH 8.0) was added. The mixture was incubated at 37°C for 12 hours.

3. Equipment

Chromatographic separation was performed on an Agilent G6320 series LC/MSD Trap Mass Spectrometer system. The actual chromatographic separation was carried out using an Agilent 1200 Series Rapid Resolution LC system (Agilent Technologies, USA), equipped with a binary pump, a microvacuum degasser, a high performance autosampler, a column compartment, a diode array detector, and a MS detector. The samples were separated on an Agilent Zorbax SB-C8 (100 mm × 2.1 mm, 1.8 μm). The mobile phase consisted of solvent A (0.1% formic acid in water, v/v) and solvent B (acetonitrile). The optimized RRLC elution conditions were as follows: 0.0–25.0 min, 5%–20% B; 25.0–40.0 min, 20–50% B; 40.0–41.0 min, 50–99% B; 40.0–45.0 min, 99% B; 45.0–45.1 min, 99.0–5.0% B; 45.1–55.0 min, 5.0%. The flow rate was set at 300 μL/min. The column and autosampler were maintained at 40°C and 10°C, respectively. The injection volume was 5 μL.

Mass spectrometry experiments were performed with the ESI source in positive ion mode. The vaporizer temperature was maintained at 350°C. The temperature of the drying gas was set at 350°C. The flow rate of the drying gas and the pressure of the nebulizing gas were set at 6 L/min and 60 psi, respectively. The capillary voltage was kept at 3.5×10^3 V. Full-scan spectra were acquired over a scan range of m/z 50–2200. Qualitative analyses were programmed to be carried out by using the doubly charged selected ion monitoring (DC-SIM) mode of the doubly charged ion peak from previously characterized peptides [12]. An Agilent ChemStation was used to control and process the data from the Agilent 6320 Series Ion Trap LC-MS.

4. Results and Discussion

4.1. Specificity. Specificity was performed by using one gelatin as a sample, while the other four gelatins were present as blank samples. The chromatographic peak was verified by comparing the retention times and the fragments of

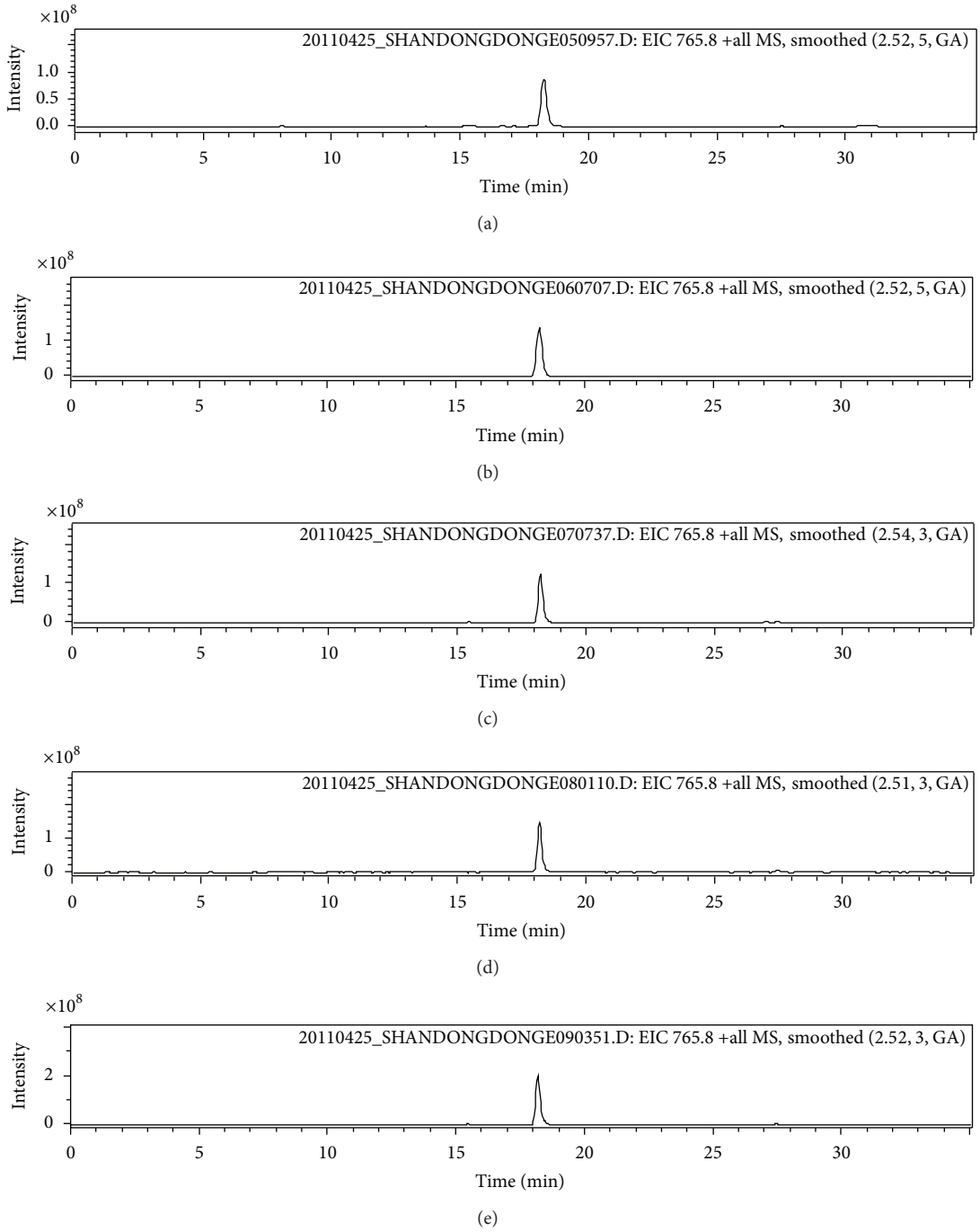

Figure 1: Doubly charged selected ion chromatograms obtained from the tryptic digests analysis of five donkey-hide gelatins.

the peaks, with the retention times and the fragments of the characterized species-specific peptides of every kind of gelatin listed in Table 1.

4.2. Repeatability. Five same samples were digested in the same condition; the marker peptides in these five same samples could be detected; the selected ions chromatograms for the five samples from the family Equidae are shown in Figure 1.

4.3. Stability. The freeze and thaw stability of tryptic samples was detected. The samples were frozen at −20°C, thawed at room temperature, and then, when completely thawed, refrozen for 24 hours under the same conditions with at least a 12-hour interval between each cycle. This freeze-thaw cycle was repeated three times before the analysis of the samples was carried out using the method described above. Long-term stabilities were measured by leaving samples at −20°C or at ambient temperature for a certain time period (20 days

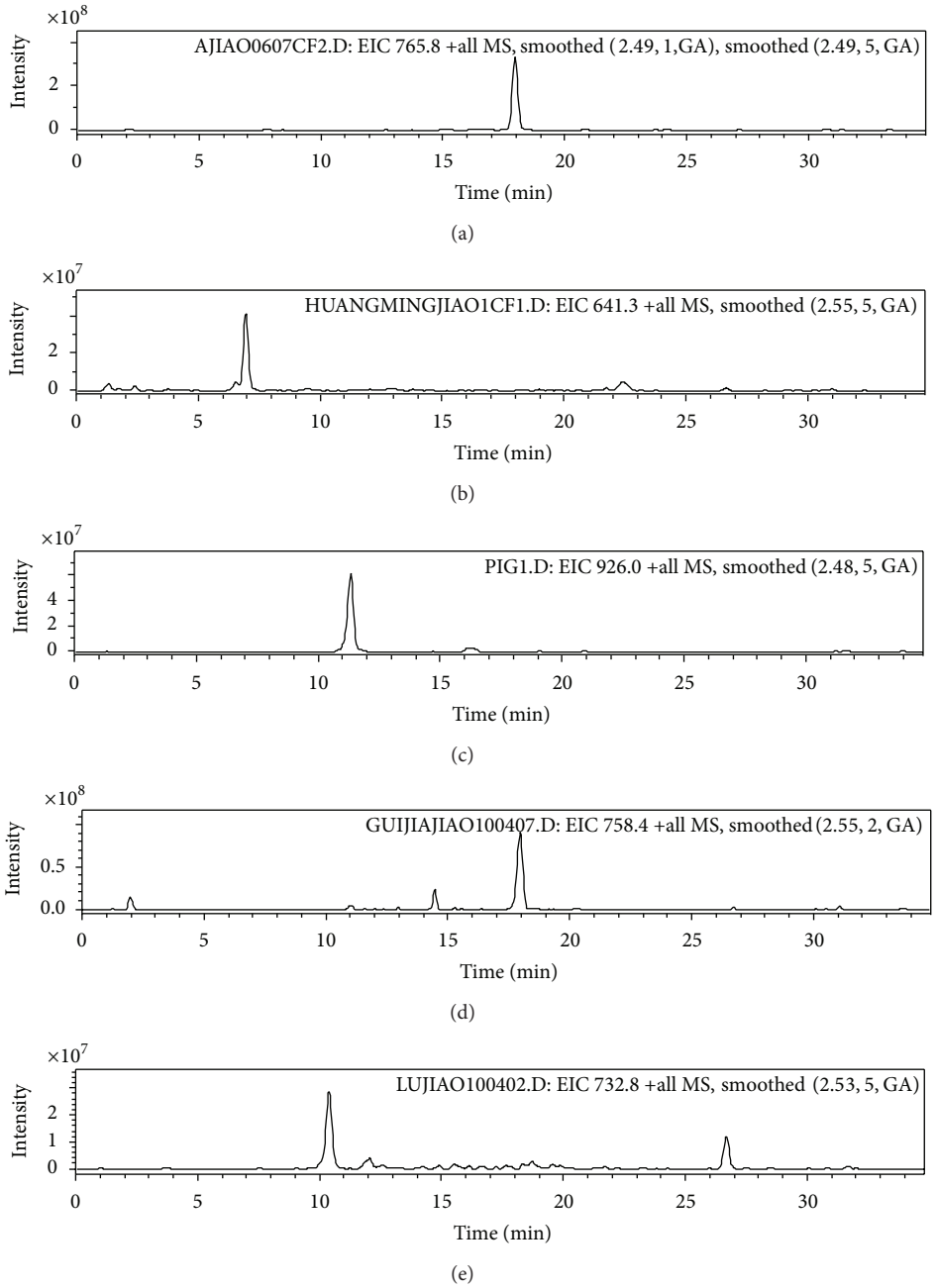

Figure 2: Doubly charged selected ion chromatograms obtained from the tryptic digest analysis of (a) donkey-hide gelatin, (b) bovine-hide gelatin, (c) pig-hide gelatin, (d) tortoise shell glue, and (e) deerhorn glue.

or 24 hours, resp.), after digestion. The results show that the characterized species-specific peptides of samples kept at −20°C for 20 days and then thawed at room temperature can still be detected.

4.4. Species Identification by DCSI-MS/MS in Gelatins. The complex peptide pools obtained by tryptic digestion of gelatins were subjected to LC-MS/MS, analyzing only five precursor ions at *m/z* 765.8, *m/z* 641.8, *m/z* 924.5, *m/z* 758.8, and *m/z* 732.8, which were the doubly charged ions of the previously described species-specific peptides [12]. Once the MS/MS spectra of these precursor ions were recorded, chromatogram traces for the different fragment ions could be obtained. The fragmented ions produced by precursor ions were determined by the sequence of the marker peptide, so the averaged MS/MS spectra obtained around this retention time gave a perfect agreement with the peptide pattern, even without knowledge of sequence of the marker peptides. Figure 2 shows the selected ion chromatography of five gelatins obtained by DC-SMIM. Figure 3(a) is the doubly charged ion *m/z* 765.8 fragmentation spectra representing the presence of the characteristic species-specific peptide of

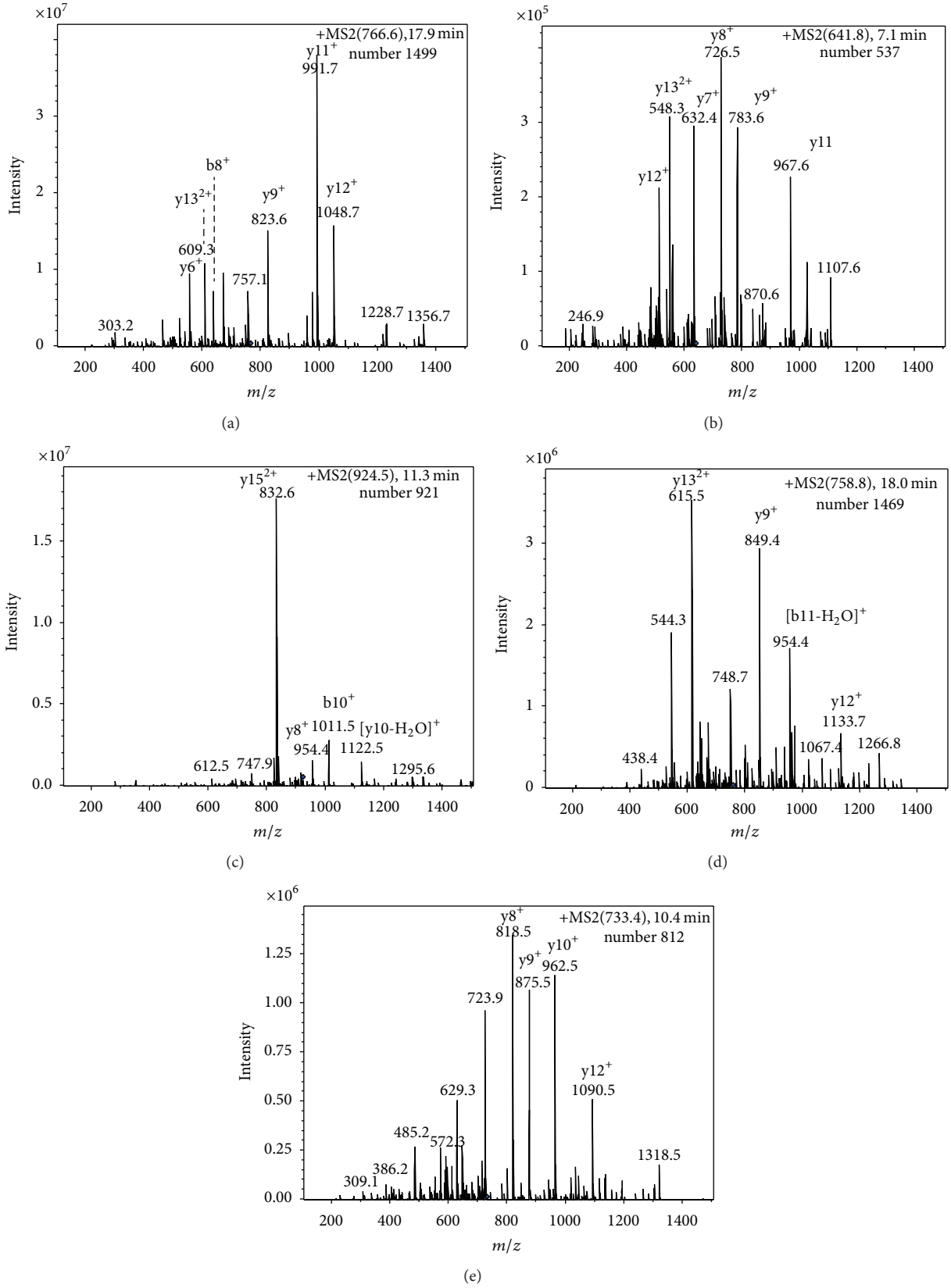

Figure 3: MS/MS fragmentation spectra of the ions at *m/z* (a) 765.8, (b) 641.8, (c) 924.5, (d) 758.8, and (e) 732.8 obtained by DCSI-MS/MS analysis, showing the fragment peaks that matched the expected peptide sequences. Gelatins were digested with trypsin.

Table 1: Retention times and fragments of characterized species-specific peptides from each gelatin.

m/*z* observed	Retention times	Fragments	Sequence	Originated from
765.8	17.9	1084.7, 991.7, 823.6, 609.3	GEAGPAGPAGPIGPVGAR	Donkey-hide gelatin
641.8	7.1	1107.6, 967.6, 783.6, 726.5, 632.4, 548.3	GEAGPSGPAGPTGAR	Bovine-hide gelatin
924.5	11.3	1122.5, 1011.5, 832.6, 747.9,	GEPGPTGVQGPPGPAGEEGK	Pig-hide gelatin
758.8	18.0	1133.7, 954.4, 849.4, 748.7, 615.5, 544.3	GDGGPP(OH)GITGFPGASGR	Glue of tortoise shell
733.4	10.4	1090.5, 962.5, 875.5, 818.5, 723.9, 629.3	SGETGASGPP(OH)GFAGEK	Deerhorn glue

donkey-hide gelatin. Four spectra proving the presence of the corresponding characteristic species-specific peptides for the remaining gelatins are shown in Figures 3(b)–3(e).

Commercial samples were also effectively identified after matching specific peptides in these samples with the corresponding reference samples. Ten of twenty commercial samples were donkey-hide gelatins, five were bovine-hide gelatins, three were deerhorn gelatins, and two were Tortoise shell glue. This method enables the researcher to identify the exact species correctly and efficiently.

5. Conclusions

The results presented in this paper confirm the validity of our previously presented approach, which showed that the characterized species-specific peptides of gelatins can be used to distinguish one gelatin from a second or to identify individual gelatins in a mixture. In our work, five doubly charged ions at *m*/*z* 765.8, *m*/*z* 641.3, *m*/*z* 924.5, *m*/*z* 758.8, and *m*/*z* 732.8, which are the respective species-specific peptides of donkey-hide gelatin, bovine-hide gelatin, pig-hide gelatin, tortoise shell glue, and deer-horn glue, were selected as monitor ions. Our results show that using the method we outline in this paper based on the high separation capability of RRLC and the peptide identification ability of MS using the DCSI-MS/MS scanning mode to detect and monitor diagnostic peptides from five different gelatins is simple, rapid, and exclusive. The method is shown to be suitable for identifying five gelatins in a mixture.

Conflict of Interests

The authors declare that there is no conflict of interests.

Acknowledgments

This study was supported in part by grants from the Important Program of Ministry of Science and Technology of the People's Republic of China (no. 2014ZX09304307-002), the National Natural Science Foundation of China (nos. 81202909 and 81274025) and the Project "Study on the inspection and determination method of drug" (no. 20124244008) from General Administration of Quality Supervision, Inspection and Quarantine of China.

References

[1] G. Y. Li, S. Pukunaga, K. Takenouchi, and F. Nakamura, "Comparative study of the physiological properties of collagen, gelatin and collagen hydrolysate as cosmetic materials," *International Journal of Cosmetic Science*, vol. 27, no. 2, pp. 101–106, 2005.

[2] D. Shoshani, E. Markovitz, Y. Cohen, A. Heremans, and A. Goldlust, "Skin test hypersensitivity study of a cross-linked, porcine collagen implant for aesthetic surgery," *Dermatologic Surgery*, vol. 33, supplement 2, pp. S152–S158, 2007.

[3] K. Tasanen, R. Palatsi, and A. Oikarinen, "Demonstration of increased levels of type I collagen mRNA using quantitative polymerase chain reaction in fibrotic and granulomatous skin diseases," *British Journal of Dermatology*, vol. 139, no. 1, pp. 23–26, 1998.

[4] S. G. Kauschke, A. Knorr, M. Heke et al., "Two assays for measuring fibrosis: reverse transcriptase-polymerase chain reaction of collagen α1 (III) mRNA is an early predictor of subsequent collagen deposition while a novel serum N-terminal procollagen (III) propeptide assay reflects manifest fibrosis in carbon tetrachloride- treated rats," *Analytical Biochemistry*, vol. 275, no. 2, pp. 131–140, 1999.

[5] R. S. Sawhney, "Immunological identification of types I and III collagen in bovine lens epithelium and its anterior lens capsule," *Cell Biology International*, vol. 29, no. 2, pp. 133–137, 2005.

[6] H. Lam and R. Aebersold, "Building and searching tandem mass (MS/MS) spectral libraries for peptide identification in proteomics," *Methods*, vol. 54, no. 4, pp. 424–431, 2011.

[7] G. Zhang, T. Liu, Q. Wang et al., "Mass spectrometric detection of marker peptides in tryptic digests of gelatin: a new method to differentiate between bovine and porcine gelatin," *Food Hydrocolloids*, vol. 23, no. 7, pp. 2001–2007, 2009.

[8] X.-L. Cheng, F. Wei, X.-Y. Xiao et al., "Identification of five gelatins by ultra performance liquid chromatography/time-of-flight mass spectrometry (UPLC/Q-TOF-MS) using principal component analysis," *Journal of Pharmaceutical and Biomedical Analysis*, vol. 62, pp. 191–195, 2012.

[9] C. Solazzo, W. W. Fitzhugh, C. Rolando, and C. Tokarski, "Identification of protein remains in archaeological potsherds by proteomics," *Analytical Chemistry*, vol. 80, no. 12, pp. 4590–4597, 2008.

[10] E. C. Huang and J. D. Henion, "LC/MS and LC/MS/MS Determination of protein tryptic digests," *Journal of the American Society for Mass Spectrometry*, vol. 1, no. 2, pp. 158–165, 1990.

[11] W. Fremout, M. Dhaenens, S. Saverwyns et al., "Tryptic peptide analysis of protein binders in works of art by liquid chromatography-tandem mass spectrometry," *Analytica Chimica Acta*, vol. 658, no. 2, pp. 156–162, 2010.

[12] M. Buckley, M. Collins, J. Thomas-Oaies, and J. C. Wilson, "Species identification by analysis of bone collagen using matrix-assisted laser desorption/ionisation time-of-flight mass spectrometry," *Rapid Communications in Mass Spectrometry*, vol. 23, no. 23, pp. 3843–3854, 2009.

[13] C. Esteve, C. del Río, M. L. Marina, and M. C. García, "Development of an ultra-high performance liquid chromatography analytical methodology for the profiling of olive (*Olea europaea* L.) pulp proteins," *Analytica Chimica Acta*, vol. 690, no. 1, pp. 129–134, 2011.

[14] R. A. Everley and T. R. Croley, "Ultra-performance liquid chromatography/mass spectrometry of intact proteins," *Journal of Chromatography A*, vol. 1192, no. 2, pp. 239–247, 2008.

[15] D. L. Tabb, L. L. Smith, L. A. Breci, V. H. Wysocki, D. Lin, and J. R. Yates III, "Statistical characterization of ion trap tandem mass spectra from doubly charged tryptic peptides," *Analytical Chemistry*, vol. 75, no. 5, pp. 1155–1163, 2003.

Hindawi Publishing Corporation
Journal of Analytical Methods in Chemistry
Volume 2014, Article ID 951075, 9 pages
http://dx.doi.org/10.1155/2014/951075

Research Article

One Single Amino Acid for Estimation the Content of Total Free Amino Acids in *Qingkailing Injection* Using High-Performance Liquid Chromatography-Diode Array Detection

Li Zhang, Xue Wang, Jiankun Su, Haiyu Liu, Zhixin Zhang, Lingling Qin, Cheng He, Long Peng, Mingxing Guo, and Xiaoyan Gao

Science Experiment Center for Traditional Chinese Medicine, Beijing University of Chinese Medicine, No. 11 North Third Ring Road, Chaoyang District, Beijing 100029, China

Correspondence should be addressed to Xiaoyan Gao; gaoxiaoyan0913@sina.com

Received 7 January 2014; Accepted 11 February 2014; Published 13 March 2014

Academic Editor: Shuang-Qing Zhang

Copyright © 2014 Li Zhang et al. This is an open access article distributed under the Creative Commons Attribution License, which permits unrestricted use, distribution, and reproduction in any medium, provided the original work is properly cited.

Qingkailing injection (QKLI), a modern traditional Chinese medicine preparation, has been widely used in clinics due to its fast and significant efficacy in treatment of high fever. The free amino acids (AAs) were considered to be the most abundant active ingredients indisputably. So developing an accurate and simple determination method to measure the contents of total free AAs in *QKLI* is very crucial. In current study, the accurate and simple method of using one single standard AA for simultaneous quantification of multiple AAs (One for M) in *QKLI* was developed. Particularly, the calculation methods and the robustness of relative correction factors (RCFs) were investigated systematically. No statistically significant difference between these two quantification methods of One for M and classic regression equation was found by the t-test ($P = 95\%$, $P > 0.05$). The results showed that the precision (RSD < 4.88%), the robustness (RSD < 4.04%), and the average recoveries (94.11%–107.94%) of this newly proposed method all met the requirements for content determination. This One for M method will provide a scientific reference for the quantitative determination of AAs in other traditional Chinese medicines and their preparations owing to its accuracy and simplicity.

1. Introduction

Qingkailing injection (QKL), which is modified from a well-known classic formulation An-Gong-Niu-Huang pill, has become one of the essential Chinese patent medicines for its wide clinical application in the treatment of liver damage, inflammation, viral infections, and cardiovascular diseases, especially hyperpyrexia [1–5]. The formula of *QKLI* is composed by eight medicinal materials or their extracts, in which amino acids (AAs) are the main bioactive components which come from three drugs, including *Margaritifera Concha, Bubal Cornu,* and *Isatidis Radix* [6–9]. By now, the content of total nitrogen derived from free AAs is the key control index in the complex production process of *QKLI*. In the monograph of Chinese Pharmacopoeia (2010 edition), the Kjeldahl nitrogen determination method, a classic method for analyzing the content of total nitrogen, was used to evaluate the total content of AAs in *QKLI* indirectly [10]. Some disadvantages of this nitrogen determination method, including time-consuming, complicated operation and the consumption of large amounts of solvents, are not facilitative to accomplish the determination of the total nitrogen. What is more, this Kjeldahl's method could not distinguish the nitrogen between the free AAs and the binding AAs or the inorganic nitrogen and the organic nitrogen. To ensure the security and the efficiency of *QKLI*, the accurate determination of multiple AAs and evaluation of the content ratio of them are essential. So, developing an accurate and simple determination method of multiple AAs used in production process of *QKLI* and quality control to its preparation is imperative.

Though the determination methods of AAs were reported in many literatures, most of them mainly focused on the optimization of the instruments [11–16], derivatization reagents [17–20], and columns [21, 22]. The method of using one single standard substance for simultaneous determination of

multiple AAs (One for M) has not been reported. As we all know, AAs occurring in herbal medicines are mostly in the form of homologues and have similar chemical structures, implying that there are no obvious differences in their derivatization efficiencies and chromatographic behaviors. Therefore, it is more suitable to employ One for M method to simultaneously determine the content of multiple AAs.

Up to now, a number of studies have been reported on the determination of multiple active components in the herbal medicines by One for M [23–30]. But the key node of One for M, namely, the calculation method of RCFs, has not been investigated adequately in previous researches. In our previous study, One for M method was adopted to carry out an assay of seven anthraquinone ingredients in rhubarb [31]. With further research, we found that the effect of intercept and slope of calibration curve on RCFs could not be ignored. So, in this study, we went into depth study on the calculating methods of RCFs and made a comparison among them. Then we selected the best one by investigating the relative deviation of the contents between the methods of One for M and classic calibration curve in ten batches of *QKLI*. Afterwards, the t-test was performed to validate the feasibility of the present method. At the same time, the robustness of RCFs was also investigated systemically for enhancing the applicability of the proposed method, including the effects of different instruments, columns, and HPLC conditions.

In our previous work, a HPLC method was developed and validated for the simultaneous determination of twenty AAs in *QKLI* based on a pre-column derivatization with phenylisothiocyanate (PITC) [32]. In current study, fourteen AAs with higher contents and good resolution were chosen for the methodology study, which accounted for about 97% of total free AAs in *QKLI*. Above all, we presented an accurate and fast One for M method for the simultaneous quantification of fourteen AAs with Gly as the internal standard, aiming at realizing a better quality control to *QKLI*.

2. Experimental

2.1. Instrumentation. Analyses were performed on an Agilent 1100 liquid chromatography system (Agilent Technologies, Palo Alto, CA, USA) comprising a binary solvent delivery system, an online degasser, an autosampler, a column temperature controller and a diode-array detector (DAD) coupled with an analytical workstation (HP, USA), and an Alliance 2695 LC system (Waters Corp, Milford, MA, USA) comprising a quaternary solvent delivery system, a vacuum degasser, an autosampler, a column temperature controller, and a photodiode array detector (PDA) coupled with an analytical workstation (Empower 3). Chromatographic separation was operated on three different chromatographic columns: Diamond C_{18} (4.6 mm × 250 mm, 5 μm), Phenomenex Luna C_{18} (4.6 mm × 250 mm, 5 μm), and Hypersil BDS C_{18} (4.6 mm × 250 mm, 5 μm).

2.2. Reagents and Materials. The 14 AAs standards including glycine (Gly), aspartic acid (Asp), alanine (Ala), ornithine (Orn), glutamic acid (Glu), lysine (Lys), arginine (Arg), proline (Pro), valine (Val), tyrosine (Tyr), isoleucine (Ile), leucine (Leu), and tryptophan (Try) (with the purity higher than 99.5%) were all purchased from Xinjingke biotechnology company (Beijing, China). Sixteen batches of *QKLI* were obtained from YaBao pharmaceutical Group Co., Ltd. (Beijing, China).

HPLC-grade acetonitrile was supplied by Fisher Scientific (Fair Lawn, NJ, USA). Phenylisothiocyanate (PITC, lot code: 10113227) was purchased from Alfa Aesar Chemical Co. Ltd (Tianjin, China), and the purity was higher than 97%. Triethanolamine (TEA, analytical grade) was purchased from Fuchen Chemical (Tianjin, China). Other reagents were all analytical grades and obtained from Chemical Works (Beijing, China). Ultrapure water (18.2 MΩ) was generated from Milli-Q water purification (Millipore, France).

2.3. Preparation of Standard Solution. Each of the 14 AAs was accurately weighed (Asp 49.94 mg, Glu 99.30 mg, Ser 49.87 mg, Gly 100.82 mg, Arg 50.25 mg, Ala 99.33 mg, Pro 200.29 mg, Tyr 34.67 mg, Val 50.08 mg, Ile 30.35 mg, Leu 99.63 mg, Phe 49.50 mg, Orn 50.48 mg, and Lys 30.23 mg). The stock solution was prepared by dissolving the above 14 standards in 50 mL volumetric flask with 0.1 mol/L hydrochloric acid and stored in refrigerator at 4°C until being used.

2.4. Sample Preparation. *QKLI* 2 mL was accurately placed into 25 mL volumetric flask, and then 6 mL of phenylisothiocyanate (PITC) acetonitrile solution (0.1 mol/L) and 6 mL of triethylamine (TEA) acetonitrile solution (1 mol/L) were added. After 60 min of ultrasonic bath (60 Hz), the solution was taken out, cooled to room temperature, and diluted with 50% acetonitrile aqueous solution to 25 mL. 10 mL of the above solution was placed in the separating funnel; after the addition of 10 mL of n-hexane, the mixture was then shaken thoroughly and the underlayer solution was filtered through a 0.45 μm membrane filter for injection.

2.5. Chromatographic Conditions. Analyses were primarily performed on an Agilent 1100 liquid chromatographic system with a Diamond C_{18} column (4.6 mm × 250 mm, 5 μm). The flow rate was 1.0 mL/min and sample injection volume was 1 μL. Detection wavelength was set at 254 nm. The column temperature was maintained at 40°C. The mobile phase consisted of 0.1 mol/L acetate- (pH was adjusted to 6.5 with glacial acetic acid) acetonitrile (93 : 7) (A) and acetonitrile-water (4 : 1) (B). The gradient program was as follows: 0–2 min, 0% B; 2–5 min, 0–10% B; 15–25 min, 10–30% B; 25–33 min, 30–45% B; 33–33.1 min, 45–100% B; 33.1–36 min, 100% B; 36–36.1 min, 100–0% B; and 36.1–43 min, 0% B.

The chromatographic profiles of the blank control solution, the reference solution, and *QKLI* are shown in Figure 1. The blank control solution was obtained by preparing 0.1 mol/L hydrochloric acid according to the sample processing produce.

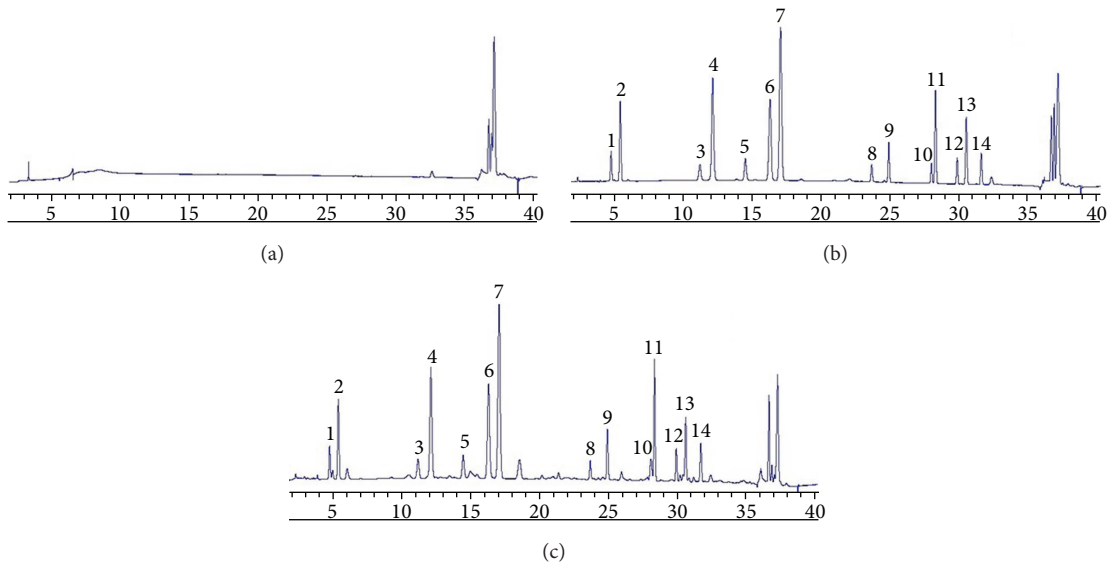

Figure 1: Representative HPLC chromatograms obtained from (a) the blank control solution, (b) the mixed standards solution, and (c) *QKLI* sample solution. Numbers 1–14 were identified as Asp (1), Glu (2), Ser (3), Gly (4), Arg (5), Ala (6), Pro (7), Tyr (8), Val (9), Ile (10), Leu (11), Phe (12), Orn (13), and Lys (14).

3. Principles of One for M

Method 1 (the calibration of RCF based on external standard method). The absorption of analyte (peak area, A) was linearly proportional to sample content (concentration, C) in a linearity range and their relation could be shown with the formula below:

$$A = f \times C. \tag{1}$$

(1) The standard solutions of analytes were prepared and analyzed according to the HPLC conditions mentioned above; then the correction factors (CFs) were calculated by the following equation:

$$f_i = \frac{A_i}{C_i}. \tag{2}$$

(2) The RCFs of each analyte relative to the selected internal standard were calculated by the formula

$$F = \frac{A_i/C}{A_s/C_s}. \tag{3}$$

(3) When this One for M method was used, the standard solution of internal standard was reprepared and its CF calculated:

$$f_{s'} = \frac{A_{s'}}{C_{s'}}. \tag{4}$$

The concentrations of other analytes could be calculated by their RCFs:

$$C = \frac{A}{f_{s'} \times F}. \tag{5}$$

Method 2 (the calibration of RCF based on the slope of standard curve). (1) The standard solution of each analyte was analyzed under the conditions detailed above and established the calibration curves:

$$A = a_i C + b_i, \tag{6}$$

where A and C are the peak area and concentration of compounds; a_i is the slope; and b_i is the interception.

When a_i is much larger than b_i, b_i can be ignored and then the standard equation can be simplified into:

$$A = a_i C. \tag{7}$$

(2) The RCFs were calculated as the ratio of the equation slope for each analytes relative to the chosen internal standard

$$F_i = \frac{a_i}{a_s}. \tag{8}$$

(3) Reestablish the calibration curve of internal standard and obtain the slop $a_{s'}$, and then the quantification of each sample was carried out according to the following equation:

$$C = \frac{A}{a_{s'} \times F}. \tag{9}$$

Method 3 (the calibration of RCF based on the slope of standard curve and correction interception). (1) Established the calibration curves of each analytes, respectively:

$$A = a_i C + b_i. \tag{10}$$

(2) Calculated the ratio of the slope of the linear calibration curves for each analyte relative to the internal standard as the RCFs:

$$F_i = \frac{a_i}{a_s}. \tag{11}$$

Table 1: Calibration curves, LOQ, and LOD of the fourteen investigated AAs.

AAs	Linear regression data			LOQ (μg)	LOD (μg)
	Regressive equation	Test range (mg/mL)	r		
Asp	$Y = 509.433X - 16.066$	0.050–1.000	0.9998	0.017	0.005
Glu	$Y = 449.506X - 5.904$	0.099–1.986	1.0000	0.040	0.012
Ser	$Y = 642.902X - 4.916$	0.050–1.000	0.9999	0.020	0.006
Gly	$Y = 890.173X - 8.861$	0.101–2.016	1.0000	0.015	0.004
Arg	$Y = 398.247X - 4.785$	0.050–1.005	1.0000	0.040	0.012
Ala	$Y = 796.495X - 7.740$	0.099–1.987	1.0000	0.030	0.009
Pro	$Y = 659.777X - 6.110$	0.200–4.006	0.9999	0.020	0.006
Tyr	$Y = 419.329X - 3.329$	0.035–0.693	0.9999	0.015	0.005
Val	$Y = 595.691X - 2.190$	0.050–1.002	1.0000	0.015	0.004
Ile	$Y = 555.808X - 1.043$	0.030–0.607	1.0000	0.010	0.003
Leu	$Y = 560.738X - 1.376$	0.100–1.993	1.0000	0.013	0.004
Phe	$Y = 455.008X - 1.167$	0.050–0.990	1.0000	0.030	0.009
Orn	$Y = 619.760X - 4.322$	0.050–1.010	0.9999	0.012	0.003
Lys	$Y = 869.350X - 1.930$	0.030–0.605	0.9999	0.010	0.003

(3) Reestablish the calibration curve of internal standard and the contents of other components could be calculated through their RCFs and b_i:

$$C = \frac{A - b_i}{a_{s'} \times F}. \quad (12)$$

Method 4 (the calibration of RCF based on the slope and interception of standard curve). (1) Develop the calibration curves of the each analyte, respectively:

$$A = a_i C + b_i. \quad (13)$$

(2) Calculate the ratio of the equation slopes for each analyte relative to the internal standard as the RCFs:

$$F_i = \frac{a_i}{a_s}. \quad (14)$$

(3) The correction factors of interception (B_i) were calculated as the difference of the interception for each analyte relative to the internal standard

$$B_i = \frac{b_i}{b_s}. \quad (15)$$

(4) Reestablished the calibration curve of internal standard and the contents of other components were calculated as

$$C = \frac{A - (B_i - b_{s'})}{a_{s'} \times F}. \quad (16)$$

There are four methods to calculate the RCFs, so four determination results of analytes can be obtained by One for M method. The choice of RCFs calculation method depends on the accuracy and the robustness, namely, the relative deviation of the analytes content between One for M method and calibration curve method.

4. Results and Discussion

4.1. Methodology Investigation on Determination of 14 AAs by Classic Calibrate Curve

4.1.1. Calibration Curves, Limits of Quantification, and Detection. The stock solution of mixed standards was diluted to appropriate concentrations with 0.1 mol/mL HCl for the establishment of calibration curves. The calibration curves were obtained by plotting the ratio of peak area (Y) of each analyte versus the concentrations (X, mg/mL) of calibration standards through the linear least-squares regression analysis. All calibration curves exhibited good linearity with the correlation coefficients (r) higher than 0.995. The limits of quantification (LOQ) and detection (LOD) for each AA were measured based on a signal-to-noise (S/N) ratio at about 10 and 3, respectively. The data is listed in Table 1.

4.1.2. Precision. Precision was evaluated by analysis of three different concentrations (low, medium, and high) with six replicates on the same day and three consecutive days. Precision was expressed as the intra- and interday relative standard deviation (RSD). The RSDs of intra- and interday were ranged from 0.75 to 2.20% and from 0.20 to 4.88%. The details are given in Table 2.

4.1.3. Accuracy. The accuracy was expressed as the recovery by the standard addition method. The mixed standard solution at high, medium, and low concentration levels was added into a certain amount of the *QKLI* sample ($n = 6$); the resultant samples were processed and analyzed. The results were acceptable with the average recoveries of fourteen AAs ranged from 94.11% to 107.94% and the RSDs from 0.14 to 4.49%. All data is depicted in Table 3.

Table 2: Intra- and interday precision of the fourteen investigated AAs.

AAs	Concentration (mg/mL)	Intraday ($n = 6$) RSD%	Interday ($n = 6$) RSD%	AAs	Concentration (mg/mL)	Intraday ($n = 6$) RSD%	Interday ($n = 6$) RSD%
Asp	0.101	1.63	2.11	Tyr	0.080	0.79	3.39
	0.303	2.18	2.14		0.241	1.16	4.75
	0.505	2.20	3.99		0.401	1.96	2.07
Glu	0.293	1.42	3.08	Val	0.127	1.00	3.21
	0.880	2.19	2.10		0.380	1.22	3.41
	1.467	2.14	4.36		0.634	2.11	1.15
Ser	0.069	0.75	1.34	Ile	0.063	0.84	2.21
	0.207	1.48	3.33		0.190	1.13	4.38
	0.345	2.06	2.36		0.316	2.14	2.37
Gly	0.305	0.78	2.68	Leu	0.109	0.92	2.01
	0.916	1.32	3.45		0.328	1.13	4.88
	1.527	2.02	1.60		0.547	2.04	2.50
Arg	0.141	1.23	0.20	Phe	0.166	1.02	3.58
	0.422	1.74	2.86		0.498	0.98	2.01
	0.703	1.90	4.09		0.831	1.98	4.41
Ala	0.303	0.84	3.74	Orn	0.300	1.08	3.96
	0.909	1.25	3.34		0.901	0.96	3.23
	1.514	2.06	1.29		1.501	1.97	4.02
Pro	0.655	0.92	4.23	Lys	0.076	1.21	3.91
	1.964	1.36	3.42		0.228	0.92	2.57
	3.274	2.06	1.65		0.380	2.02	4.47

4.2. Relative Correction Factors (RCFs). The four methods mentioned above were applied to calculate the RCFs with the Gly as the single standard (Table 4).

4.2.1. Evaluation of RCFs. To confirm an optimal calculation method of the RCFs, six batches of *QKLI* were processed and analyzed. The Gly (standard substance) was determined directly using the calibration curve method and the content of the other 13 AAs was calculated according to their RCFs and the calibration curve, respectively. Except for Method 1, the results obtained from other three methods were satisfactory (see Supplementary Tables 1–4 available online at http://dx.doi.org/10.1155/2014/951075). Furthermore, the result of t-test ($P > 0.05$) indicated that there are no statistically significant differences between the calibration curve method and One for M Methods 2, 3, and 4. However, the calculation procedures of Methods 3 and 4 are more complicated for the requirement of two calculation parameters. Therefore, Method 2 was considered to be the preferred method used to calculate the RCFs.

4.2.2. Robustness Validation of RCFs. The robustness test was designed to determine some potential and changeable factors on analytic procedures in different conditions.

Different instruments and columns were the most important factors to evaluate the ruggedness and robustness of RCF [33]. In our study, two instruments (Waters Alliance 2695 with PDA and Agilent 1100 with DAD) and three columns (Diamond C_{18}, Phenomenex Luna C_{18}, and Hypersil BDS C_{18}) were used to explore. The RCFs of 13 AAs on each instrument and column are listed in Supplementary Table 5. As it showed, the RSDs of RCFs were all lower than 3.96% when analyzed on the same instrument with different columns, indicating that the different types of columns had no significant effects on RCFs. However, the RCF of Pro had a big difference in the same column on different instruments, which probably due to the methylene structure of Pro is different from others.

The RCFs were investigated at different flow rates (0.9, 1.0, 1.1 mL/min) by Agilent 1100 LC system and Diamond C_{18} (4.6 mm × 250 mm, 5 μm) column. As a result, the RSDs of all AAs were within 0.24%–1.98% expected for the Asp and Ile were 2.49% and 2.78%, higher than 2% slightly. Presumably the retention time changed with the flow rates, which increasing the effect of the peak around them on their peak area. The peak area was closely related to the calculation of RCF. But the methods still met the analytical requirements with the RSDs less than 5%, indicating that the flow rate was a nonsignificant factor.

The resolution of the instrument varied with the column temperature, thereby affected the peak area of the compound, and ultimately influenced the RCF. So the different column temperatures (35°C, 40°C, and 45°C) were investigated and

Table 3: The average recoveries of the fourteen investigated AAs ($n = 6$).

Analytes	Original (mg)	Spiked (mg)	Found (mg)	Recovery[a] (%)	RSD (%)
Asp	0.149	0.100	0.256	106.72	2.41
		0.200	0.365	107.94	2.39
		0.300	0.460	103.56	3.25
Glu	0.531	0.291	0.830	102.84	4.49
		0.582	1.152	106.73	1.96
		0.873	1.471	107.60	2.44
Ser	0.148	0.070	0.217	97.76	1.25
		0.141	0.281	94.50	0.14
		0.211	0.371	105.44	4.23
Gly	0.632	0.305	0.945	103.02	0.26
		0.609	1.266	104.16	2.57
		0.914	1.603	106.32	1.10
Arg	0.264	0.140	0.412	105.39	2.51
		0.281	0.544	99.58	1.53
		0.421	0.714	106.89	1.10
Ala	0.622	0.303	0.942	105.61	2.79
		0.606	1.270	107.05	3.70
		0.909	1.581	105.57	1.90
Pro	1.445	0.656	2.102	100.17	2.63
		1.313	2.829	105.48	1.04
		1.969	3.721	107.69	2.50
Tyr	0.136	0.079	0.219	105.27	2.95
		0.159	0.291	98.17	2.71
		0.238	0.384	104.35	3.80
Val	0.273	0.128	0.407	104.87	3.85
		0.256	0.543	105.62	1.50
		0.384	0.683	106.90	3.01
Ile	0.115	0.063	0.181	103.84	2.92
		0.127	0.236	95.68	0.94
		0.190	0.320	107.80	3.71
Leu	0.607	0.297	0.908	101.73	2.15
		0.593	1.221	103.56	1.25
		0.890	1.517	102.30	3.68
Phe	0.233	0.110	0.338	94.87	4.12
		0.220	0.441	94.11	2.16
		0.331	0.586	106.77	2.06
Orn	0.200	0.166	0.371	103.11	2.24
		0.332	0.556	107.18	1.07
		0.497	0.726	105.64	3.94
Lys	0.133	0.076	0.214	106.01	3.91
		0.153	0.291	103.14	2.19
		0.229	0.374	105.37	2.05

[a]Recovery (%) = 100 × (found amount − original amount)/spiked amount; the data presented as average of three determinations.

the RSDs ranged from 0.48% to 4.05%, revealing that the RCF was steadily under different column temperatures.

Table 4: Relative correction factors (RCFs) of the 13 AAs.

AAs	Relative response factors					
	Method I	Method II	Method III		Method IV	
	F	F	F	bi	F	Bi
Asp	0.531	0.551	0.551	−0.466	0.551	−9.425
Glu	0.492	0.501	0.501	1.498	0.501	−7.462
Ser	0.662	0.696	0.696	−1.768	0.696	−10.728
Arg	0.441	0.450	0.450	0.744	0.450	−8.215
Ala	0.896	0.891	0.891	8.858	0.891	−0.101
Pro	0.749	0.730	0.730	20.829	0.730	11.870
Tyr	0.471	0.470	0.470	1.501	0.470	−7.458
Val	0.677	0.666	0.666	4.178	0.666	−4.781
Ile	0.637	0.629	0.629	1.882	0.629	−7.077
Leu	0.646	0.633	0.633	8.324	0.633	−0.636
Phe	0.533	0.514	0.514	4.430	0.514	−4.529
Orn	0.913	0.932	0.932	1.226	0.932	−7.733
Lys	0.982	0.987	0.987	2.056	0.987	−6.904

The above results showed that Method 2, the calculation method of RCF based on the slope of standard curve, had good robustness (RSD $<$ 5%) in different instruments, columns, flow rates, and column temperatures.

Above all, Method 2 was chosen to calculate the RCFs.

4.3. Method Validation of One for M. To validate the One for M method, ten batches of *QKLI* were processed for HPLC analyzed. The content of the fourteen AAs was calculated (Table 5). No significant difference was found between the classic calibrate determine method and One for M method (Method 2) using the t-test ($P = 95\%$, $P > 0.05$), indicating that the newly developed method was a satisfactory method for quality control of traditional Chinese medicines.

4.4. Discussion. The relative correction factor (RCF), which is the most crucial parameter in One for M method, greatly determines the accuracy of the results. Four different calculation methods of RCF were compared in the current study and the calibration method based on the slope of standard curve was selected as the best one, considering the accuracy of the results and the simplicity of the method. Therefore, the slopes of the analytes and internal standard would directly affect the accuracy of the analytic results. The slope of the standard curve can be affected by various factors, such as the purity of reference, the accuracy of measurement method, and the influence of instrument. All AA references reached enough purity (>99.5%) in this study and the accuracy of measurement method was confirmed very well. By applying different instruments, columns, and chromatographic conditions, the effect of instrument was eliminated and the robustness of RCF was also verified. The AAs must be analyzed after derivatizing due to the lack of chromophore. Phenylisothiocyanate (PITC) was selected as the derivatization reagent. The detection wavelength was set at 254 nm which is in the B absorption band of the benzene

Table 5: Contents of 14 AAs in ten batches of *QKLI* by two methods.

AAs	013105A		RD[a] (%)	110101A		RD[a] (%)	115202A		RD[a] (%)	210204A		RD[a] (%)	111103A		RD[a] (%)
	a	b		a	b		a	b		a	b		a	b	
Gly	—	1.039	—	—	1.028	—	—	0.997	—	—	0.983	—	—	1.046	—
Asp	0.273	0.269	1.29	0.324	0.321	0.81	0.315	0.312	0.88	0.338	0.336	0.70	0.339	0.337	0.69
Glu	1.055	1.074	−1.74	1.008	1.026	−1.72	0.922	0.937	−1.67	0.954	0.970	−1.69	0.996	1.013	−1.71
Ser	0.284	0.284	−0.04	0.296	0.296	−0.04	0.288	0.288	−0.04	0.254	0.254	−0.03	0.273	0.273	−0.04
Arg	0.424	0.429	−1.19	0.434	0.440	−1.20	0.711	0.720	−1.31	0.661	0.670	−1.30	0.611	0.619	−1.28
Ala	1.200	1.211	−0.86	1.133	1.142	−0.81	1.074	1.082	−0.76	1.078	1.087	−0.77	1.180	1.190	−0.85
Pro	2.284	2.254	1.34	2.471	2.440	1.26	2.179	2.149	1.38	2.357	2.326	1.31	2.832	2.800	1.15
Tyr	0.234	0.233	0.57	0.270	0.269	0.39	0.251	0.250	0.48	0.196	0.194	0.83	0.237	0.236	0.56
Val	0.537	0.542	−0.91	0.511	0.515	−0.83	0.483	0.486	−0.73	0.506	0.510	−0.81	0.555	0.560	−0.95
Ile	0.264	0.263	0.32	0.249	0.248	0.49	0.232	0.231	0.72	0.246	0.245	0.53	0.273	0.272	0.23
Leu	1.209	1.212	−0.24	1.124	1.126	−0.15	1.075	1.075	−0.08	1.070	1.071	−0.08	1.185	1.188	−0.22
Trp	0.408	0.403	1.20	0.377	0.372	1.35	0.368	0.362	1.40	0.378	0.373	1.34	0.404	0.399	1.22
Orn	0.353	0.355	−0.58	0.322	0.324	−0.63	0.323	0.325	−0.63	0.314	0.316	−0.64	0.328	0.330	−0.62
Lys	0.245	0.254	−3.50	0.218	0.226	−3.41	0.234	0.243	−3.46	0.228	0.236	−3.44	0.244	0.253	−3.50
AAs	115203A		RD[a] (%)	210401A		RD[a] (%)	012602A		RD[a] (%)	210301A		RD[a] (%)	115702A		RD[a] (%)
	a	b		a	b		a	b		a	b		a	b	
Gly	—	1.077	—	—	1.115	—	—	1.145	—	—	1.125	—	—	1.138	—
Asp	0.359	0.357	0.55	0.356	0.354	0.57	0.375	0.373	0.46	0.372	0.370	0.48	0.397	0.395	0.34
Glu	1.016	1.034	−1.72	0.978	0.995	−1.70	0.966	0.983	−1.70	0.997	1.015	−1.71	1.094	1.114	−1.76
Ser	0.332	0.332	−0.06	0.301	0.301	−0.05	0.275	0.275	−0.04	0.279	0.279	−0.04	0.324	0.324	−0.05
Arg	0.821	0.832	−1.34	0.659	0.668	−1.30	0.596	0.604	−1.28	0.483	0.489	−1.23	0.576	0.583	−1.27
Ala	1.167	1.177	−0.84	1.199	1.209	−0.86	1.233	1.244	−0.88	1.184	1.194	−0.85	1.254	1.265	−0.90
Pro	2.367	2.337	1.30	2.489	2.458	1.26	2.919	2.886	1.13	2.251	2.221	1.35	2.225	2.195	1.36
Tyr	0.257	0.256	0.45	0.217	0.216	0.68	0.289	0.288	0.32	0.213	0.211	0.71	0.247	0.246	0.50
Val	0.525	0.529	−0.87	0.538	0.543	−0.91	0.530	0.535	−0.88	0.533	0.537	−0.89	0.566	0.571	−0.98
Ile	0.251	0.250	0.47	0.259	0.258	0.37	0.258	0.257	0.39	0.263	0.262	0.33	0.279	0.278	0.17
Leu	1.161	1.163	−0.19	1.166	1.168	−0.19	1.205	1.208	−0.24	1.167	1.170	−0.20	1.243	1.246	−0.27
Trp	0.390	0.385	1.29	0.393	0.388	1.27	0.408	0.403	1.20	0.408	0.403	1.20	0.431	0.426	1.11
Orn	0.362	0.365	−0.56	0.349	0.351	−0.58	0.366	0.368	−0.56	0.380	0.382	−0.54	0.382	0.384	−0.53
Lys	0.257	0.267	−3.53	0.250	0.259	−3.51	0.257	0.267	−3.53	0.265	0.275	−3.56	0.268	0.278	−3.56

[a]Relative deviation = (a − b)/b.

a: the content were calculated by One for M method; b: the content were determined by the traditional calibration equation method.

for there is no conjugation between the benzene and its side-chain of their product. The measurement results were stable and had no effect on the SCF, so the detection wavelength was not investigated in the current study. The response signals of analytes would varied with the detection wavelength when the analyres have different absorbent structure. Thus the absorption wavelength, as an important factor, need to be investigated in other researches of One for M.

In the experiment, the compound with excellent separation, high content, good stability, and suitable peak position that was in the middle of the chromatogram was preferentially selected as the internal standard. Based on the determination of AAs in several batches of *QKLI* and the calculation of RCFs, five AAs including Ser, Gly, Arg, Ala, and Pro were selected as internal standard. When the Ser and Pro were chosen as internal standard, the RDs calculated by two of four calculation methods were beyond ±5% while part of the RSD% of AAs was greater than 5% under different columns or column temperature when Arg and Ala were selected as internal standard, respectively. The four AAs mentioned above could not provide a precise result or relatively stable RCF. Eventually, Gly was used as internal standard to simultaneously determine other thirteen AAs for the satisfactory calculation results and stable RCFs.

5. Conclusions

Under the condition of one standard, One for M method can realize the simultaneous determination of multiple active ingredients in the herbal medicines with better reproducibility and accuracy. Using HPLC-PDA method, in the present research, fourteen AAs in ten batches of *QKLI* were quantified successfully by the One for M method. This method, with shorter analytical time, lower cost, and higher accuracy, can be employed as a rapid, practical technique to control

the quality of the complex traditional herbal medicines and their preparations.

Disclosure

Li Zhang and Xue Wang are cofirst authors.

Conflict of Interests

The authors declare that there is no conflict of interests regarding the publication of this paper.

Acknowledgments

This work was supported in part by National Natural Science Foundation of China (81173649/H2817) and in part by the National S & T Major Project-Created Major New Drugs Projects (2010ZX09502-002).

References

[1] K.-H. Lee, H.-K. Wang, H. Itokawa, and S. L. Morris-Natschke, "Current perspectives on Chinese medicines and dietary supplements in China, Japan and the United States," *Journal of Food and Drug Analysis*, vol. 8, no. 4, pp. 219–228, 2000.

[2] J. H. Yang, "Clinical applications of Qingkailing injection," *Journal of Traditional Chinese Medicine*, vol. 16, no. 12, pp. 10–21, 1994.

[3] M. J. Liu, "Overview on clinical application of Qingkailing injection," *Journal of Emergency in Traditional Chinese Medicine*, vol. 14, no. 6, pp. 578–579, 2005.

[4] X. Chen, O. M. Zack Howard, X. Yang, L. Wang, J. J. Oppenheim, and T. Krakauer, "Effects of Shuanghuanglian and Qingkailing, two multi-components of traditional Chinese medicinal preparations, on human leukocyte function," *Life Sciences*, vol. 70, no. 24, pp. 2897–2913, 2002.

[5] S. Yan, G. Luo, Y. Wang, and Y. Cheng, "Simultaneous determination of nine components in Qingkailing injection by HPLC/ELSD/DAD and its application to the quality control," *Journal of Pharmaceutical and Biomedical Analysis*, vol. 40, no. 4, pp. 889–895, 2006.

[6] X. Y. Gao, *Study on the methods of online process monitoring and quality control of Qingkailing injection [Ph.D. thesis]*, Beijing University of Chinese Medicine, Beijing, China, 2006.

[7] X.-Y. Gao, Q. Fan, N. Li, X.-Y. Shi, and Y.-J. Qiao, "Characterization and determination of nitrogen in preparation of Qingkailing injection and its intermediate products," *Zhongguo Zhongyao Zazhi*, vol. 33, no. 14, pp. 1673–1676, 2008.

[8] Y. J. Bai, X. Y. Gao, H. G. Zhang, F. Y. Gao, and J. Q. Lu, "Determination of nineteen amino acids in Qingkailing injection by using HPLC-ELSD method," *China Journal of Chinese Materia Mdeica*, vol. 34, pp. 3301–3303, 2009.

[9] X. Y. Gao, J. K. Su, X. Wang, and J. Q. Lu, "Determination of amino acids in Qingkailing Injection by using phenylisothiocyanate method," *China Journal of Chinese Materia Mdeica*, vol. 35, pp. 554–558, 2012.

[10] The State Pharmacopoeia Commission of People's Republic of China, *Pharmacopoeia of the People's Republic of China*, vol. 1, China Medical Science Press, Beijing, China, 1997.

[11] S. Akamatsu and T. Mitsuhashi, "Development of a simple analytical method using capillary electrophoresis-tandem mass spectrometry for product identification and simultaneous determination of free amino acids in dietary supplements containing royal jelly," *Journal of Food Composition and Analysis*, vol. 30, pp. 47–51, 2013.

[12] T. Mohabbat and B. Drew, "Simultaneous determination of 33 amino acids and dipeptides in spent cell culture media by gas chromatography-flame ionization detection following liquid and solid phase extraction," *Journal of Chromatography B: Analytical Technologies in the Biomedical and Life Sciences*, vol. 862, no. 1-2, pp. 86–92, 2008.

[13] K. Hamase, Y. Miyoshi, K. Ueno et al., "Simultaneous determination of hydrophilic amino acid enantiomers in mammalian tissues and physiological fluids applying a fully automated micro-two-dimensional high-performance liquid chromatographic concept," *Journal of Chromatography A*, vol. 1217, no. 7, pp. 1056–1062, 2010.

[14] M. T. Kelly, A. Blaise, and M. Larroque, "Rapid automated high performance liquid chromatography method for simultaneous determination of amino acids and biogenic amines in wine, fruit and honey," *Journal of Chromatography A*, vol. 1217, no. 47, pp. 7385–7392, 2010.

[15] S. Jia, Y. P. Kang, J. H. Park, J. Lee, and S. W. Kwon, "Simultaneous determination of 23 amino acids and 7 biogenic amines in fermented food samples by liquid chromatography/quadrupole time-of-flight mass spectrometry," *Journal of Chromatography A*, vol. 1218, no. 51, pp. 9174–9182, 2011.

[16] L. Wang, R. Xu, B. Hu et al., "Analysis of free amino acids in Chinese teas and flower of tea plant by high performance liquid chromatography combined with solid-phase extraction," *Food Chemistry*, vol. 123, no. 4, pp. 1259–1266, 2010.

[17] M. P. Arrieta and M. S. Prats-Moya, "Free amino acids and biogenic amines in Alicante Monastrell wines," *Food Chemistry*, vol. 135, pp. 1511–1519, 2012.

[18] V. Lozanov, S. Petrov, and V. Mitev, "Simultaneous analysis of amino acid and biogenic polyamines by high-performance liquid chromatography after pre-column derivatization with N-(9-fluorenylmethoxycarbonyloxy)succinimide," *Journal of Chromatography A*, vol. 1025, no. 2, pp. 201–208, 2004.

[19] A. Jámbor and I. Molnár-Perl, "Quantitation of amino acids in plasma by high performance liquid chromatography: simultaneous deproteinization and derivatization with 9-fluorenylmethyloxycarbonyl chloride," *Journal of Chromatography A*, vol. 1216, no. 34, pp. 6218–6223, 2009.

[20] L. Chen, Q. Chen, Z. Zhang, and X. Wan, "A novel colorimetric determination of free amino acids content in tea infusions with 2,4-dinitrofluorobenzene," *Journal of Food Composition and Analysis*, vol. 22, no. 2, pp. 137–141, 2009.

[21] H. Yu, Y.-S. Ding, S.-F. Mou, P. Jandik, and J. Cheng, "Simultaneous determination of amino acids and carbohydrates by anion-exchange chromatography with integrated pulsed amperometric detection," *Journal of Chromatography A*, vol. 966, no. 1-2, pp. 89–97, 2002.

[22] M. Zhao, Y. Ma, L.-L. Dai et al., "A high-performance liquid chromatographic method for simultaneous determination of 21 free amino acids in tea," *Food Analytical Methods*, vol. 6, pp. 79–75, 2013.

[23] H. Cai, J. Chen, and P. Li, "Simultaneous assay of four isoflavonoids in Astragali Radix by QAMS," *Zhongguo Zhongyao Zazhi*, vol. 35, no. 20, pp. 2712–2717, 2010.

[24] J. Zhu, Z. Wang, Q. Zhang, J. Niu, and F. Li, "A quantitative method for simultaneous assay of four flavones with one marker in Radix Scutellariae," *Zhongguo Zhongyao Zazhi*, vol. 34, no. 24, pp. 3229–3234, 2009.

[25] J.-J. Zhu, Z.-M. Wang, Y.-H. Kuang, Q.-W. Zhang, Q.-P. Gao, and N. Ma, "A quantitative method using one marker for simultaneous assay of ginsenosides in Panax ginseng and P. notoginseng," *Acta Pharmaceutica Sinica*, vol. 43, no. 12, pp. 1211–1216, 2008.

[26] J. J. Zhu, Z. M. Wang, X. Y. Ma, W. H. Feng, and Q. W. Zhang, "A quantitative method for simultaneous determination of four anthraquinones with one marker in rhei radix et ehizoma," *Chinese Herbal Medicines*, vol. 4, no. 2, pp. 157–163, 2012.

[27] A. P. Li, X. Yang, Y. H. Ding, and J. B. Zhao, "HPLC method for simultaneous measurement of seven water-soluble ingredients with single markerin Danshen injection," *Chinese Journal of Pharmaceutical Analysis*, vol. 32, no. 9, pp. 1534–1540, 2012.

[28] Y. Q. Lin, L. H. Xu, S. H. Wang, and M. R. Zhuang, "Quantitative analysis on multi-components by single marker for simultaneous determination of six caffeoylquinic acids in Yinhuang Tablets," *Chinese Traditional and Herbal Drugs*, vol. 43, no. 4, pp. 706–710, 2012.

[29] H. Wang, G. J. Provan, and K. Helliwell, "HPLC determination of catechins in tea leaves and tea extracts using relative response factors," *Food Chemistry*, vol. 81, no. 2, pp. 307–312, 2003.

[30] P. Sun, X. Wang, L. Alquier, and C. A. Maryanoff, "Determination of relative response factors of impurities in paclitaxel with high performance liquid chromatography equipped with ultraviolet and charged aerosol detectors," *Journal of Chromatography A*, vol. 1177, no. 1, pp. 87–91, 2008.

[31] X.-Y. Gao, Y. Jiang, J.-Q. Lu, and P.-F. Tu, "One single standard substance for the determination of multiple anthraquinone derivatives in rhubarb using high-performance liquid chromatography-diode array detection," *Journal of Chromatography A*, vol. 1216, no. 11, pp. 2118–2123, 2009.

[32] X. Y. Gao, J. K. Su, X. Wang, and J. Q. Lu, "Determination of amino acids in Qingkailing Injection by using phenylisothiocyanate method," *Journal of Beijing University of Traditional Chinese Medicine*, vol. 35, pp. 554–558, 2012.

[33] J.-J. Hou, W.-Y. Wu, J. Da et al., "Ruggedness and robustness of conversion factors in method of simultaneous determination of multi-components with single reference standard," *Journal of Chromatography A*, vol. 1218, no. 33, pp. 5618–5627, 2011.

Hindawi Publishing Corporation
Journal of Analytical Methods in Chemistry
Volume 2014, Article ID 575246, 4 pages
http://dx.doi.org/10.1155/2014/575246

Research Article

A New Method for the Analysis of Bacterial Endotoxins in Ultrapure Paraffin Oil

Dandan Chen

National Institutes for Food and Drug Control, Beijing 100050, China

Correspondence should be addressed to Dandan Chen; chendandan0506@126.com

Received 1 January 2014; Accepted 2 February 2014; Published 9 March 2014

Academic Editor: Yu-Ming Fan

Copyright © 2014 Dandan Chen. This is an open access article distributed under the Creative Commons Attribution License, which permits unrestricted use, distribution, and reproduction in any medium, provided the original work is properly cited.

The paper demonstrates the feasibility of the gel-clot method for the analysis of bacterial endotoxins in water extracts of ultrapure paraffin oil which is a water insoluble oily medical device. Because ultrapure paraffin oil is water insoluble oily liquid, the ultrapure paraffin oil (10 mL) was shaken with 10 mL water for 15 minutes at 2000 rpm, the endotoxin present was extracted to the aqueous phase without interference inhibition/enhancement of the product, the recovery of the endotoxin added to the ultrapure paraffin oil was determined. A validation study confirmed that endotoxins present in ultrapure paraffin oil which is water insoluble liquid medical device pass over into the aqueous phase at concentrations of 20, 10, and 5 EU/mL with recoveries of 94.2% to 111%. So the conclusion is that the gel-clot test is suitable for detecting bacterial endotoxins in ultrapure paraffin oil which is a water insoluble oily medical device.

1. Introduction

Ultrapure paraffin oil is used for covering culture solution during artificial fertilization in vitro and micromanipulation of reproduction technique in vitro. The major component of the ultrapure paraffin oil is light paraffin oil. This product has been classified as a class III medical device according to the Chinese Classification Rules of Medical Devices. According to the quality specification of this product the bacterial endotoxin level must be less than 0.25 EU/mL.

The reaction between the Tachypleus Amebocyte Lysate (TAL) and the bacterial endotoxin normally occurs in water solution; that is why water insoluble oily medical devices cannot be analysed directly. There is no reference to this situation in the United States Pharmacopeia [1, 2]. Also no relevant literature has been published on this issue. To this end, the major purpose of this report is to introduce a new method to analyse bacterial endotoxins present in ultrapure paraffin oil and other water insoluble oily medical devices. In this study, the agglutination interference test and the recovery test of soluble extraction of ultrapure paraffin oil have been studied in detail. This is a fundamental and methodological research of bacterial endotoxin analysis for water insoluble oily medical devices with gel-clot test.

2. Materials and Methods

2.1. Materials. The ultrapure paraffin oil (lot number: 503687) was obtained from VITROLIFE SWEDEN AB. The Tachypleus Amebocyte Lysate with a sensitivity of 0.125 EU/mL (TAL-01, lot number: 1301172) or 0.01~10 EU/mL (lot number: 1203020) and endotoxin-free water (EF-water, lot number: 1207040) were obtained from Zhanjiang Endosafe Biological Ltd. The Tachypleus Amebocyte Lysate with a sensitivity of 0.125 EU/mL (TAL-02, lot number: 130102) was obtained from Zhanjiang Bokang Ocean Biological Co. Ltd. Control standard endotoxins (100 EU per pack, lot number: 150601–201176) were provided by the National Institute for the Control of Food and Pharmaceutical Products, Beijing, China.

2.2. Preparation. All equipment and material used in this study were treated at 250°C for more than 1 hour in order to destroy exogenous bacterial endotoxins.

2.3. Confirmation of the Labelled Sensitivity of the Tachypleus Amebocyte Lysate. The confirmation was performed according to the requirement of the Chinese Pharmacopoeia 2010, Appendix II, XIE Bacterial Endotoxin Test Regulation [3, 4].

2.4. Calculation of the Maximum Valid Dilution Ratio. In order to determine the concentration of possible bacterial endotoxins in the ultrapure paraffin oil the latter was mixed with water and shaken to extract the endotoxin into the aqueous phase. The limit value in the bottom aqueous phase (L') and the endotoxin in the ultrapure paraffin oil have the following relationship:

formula (1): $L_{\text{ultrapure paraffin oil}} \times V_{\text{ultrapure paraffin oil}} \times$ recovery of the endotoxin (%) $= L'_{\text{water}} \times V_{\text{water}}$

formula (2): $L'_{\text{water}} = (L \times V_{\text{ultrapure paraffin oil}} \times$ recovery of the endotoxin$)/V_{\text{water}}$

According to the regulation of the gel-clot method of the Chinese Pharmacopoeia, the recovery does not need to agree with the calculation of the limit value if the recovery is within 50–200%. Otherwise, the limit value has to be calculated based on the recovery. The limit of ultrapure paraffin oil is 0.25 EU/mL according to the company standard. In the test, 10 mL ultrapure paraffin oil was taken and added to 10 mL endotoxin-free water and shaken for 15 min at 2000 rpm. The limit value in the top aqueous phase is 0.25 EU/mL if the recovery is within 50%–200%. The sensitivity of the marketed Tachypleus Amebocyte Lysate is usually within 0.5–0.03 EU/mL. So the maximum valid dilution ratio of the sample which is corresponding to different sensitivities of Tachypleus Amebocyte Lysate is

$$\text{MVD}_{0.25} = \frac{0.25}{0.25} = 1; \qquad \text{MVD}_{0.125} = \frac{0.25}{0.125} = 2;$$
$$\text{MVD}_{0.06} = \frac{0.25}{0.06} = 4; \qquad \text{MVD}_{0.03} = \frac{0.25}{0.03} = 8. \tag{1}$$

2.5. Interference of the Aqueous Phase Extraction Solution. As the ultrapure paraffin oil is water insoluble oily liquid, its endotoxin must be water-extracted before analysis can be made. In order to determine possible interference factors, 10 mL ultrapure paraffin oil was mixed with 10 mL endotoxin-free water and shaken for 15 min at 2000 rpm. The bottom aqueous phase was then diluted twice with endotoxin-free water followed by endotoxin analysis according to the regulation of the Chinese Pharmacopoeia 2010, Appendix II, "The bacterial endotoxin test sample for the interference test" [5]. Control standard endotoxins were prepared at different concentrations, 0.25, 0.125, 0.06, and 0.03 EU/mL, with endotoxin-free water. The endotoxin-free water and the twice diluted water phase were used as negative controls. Tachypleus Amebocyte Lysate preparations with a sensitivity of 0.125 EU/mL from two different suppliers were applied for comparison.

2.6. Recovery of Bacterial Endotoxin in the Aqueous Extract. The extraction rate of endotoxin from the ultrapure paraffin oil to the aqueous phase is defined by the absolute recovery, which must be within 50%–200% in accordance with the requirements of the Chinese Pharmacopoeia. Otherwise the $L' = (L \times V_{\text{ultrapure paraffin oil}})/(V_{\text{water}} \times \text{recovery})$ value has to be calculated based on the recovery, to ensure the accuracy of the analysis.

The determination is based on three endotoxin standards at 5, 10, and 20 EU/mL and one ultrapure paraffin oil water extract batch, respectively. 10 mL endotoxin-free water was added to 10 mL of each sample followed by shaking for 15 min at 2000 r/min. The bottom aqueous phase was then diluted 25, 50, 100, and 200 times with EF-water and the recovery was measured using the dynamic turbidimetric analysis method.

2.7. Analysis of the Concentration of Bacterial Endotoxin in the Ultrapure Paraffin Oil. 10 mL endotoxin-free water was added to 10 mL sample followed by shaking for 15 min at 2000 rpm. The bottom aqueous phase was then analysed for endotoxin according to the gel-clot method of the Chinese Pharmacopoeia 2010, appendix XIE. The endotoxin level must be lower than 0.25 EU/mL. Bacterial endotoxin analysis of twice diluted extracts was performed using a Tachypleus Amebocyte Lysate with a sensitivity of 0.125 EU/mL [6, 7].

3. Results

3.1. Confirmation of the Labelled Sensitivity of the Tachypleus Amebocyte Lysate. Table 1 shows the results of the confirmation of the sensitivity of two batches of Tachypleus Amebocyte Lysate. The values obtained indicate that the sensitivity of both batches meets the requirement. TAL-01 ($\lambda = 0.125$) was obtained from Zhanjiang Endosafe Biological Ltd. TAL-02 ($\lambda = 0.125$) was obtained from Zhanjiang Bokang Ocean Biological Co. Ltd. Plus sign shows a positive result. Minus sign shows a negative result.

3.2. Interference Test of the Aqueous Phase Extract. The result of the interference test is shown in Table 2. The results indicate a E_s within 0.5λ–2.0λ and a E_t within $0.5E_s$–$2.0E_s$ (E_s: bacterial endotoxin of standard, E_t: bacterial endotoxin of samples), and it confirms that twice dilution or more will not interfere with the bacterial endotoxin test. Plus sign shows a positive result. Minus sign shows a negative result.

3.3. Recovery of Bacterial Endotoxin in the Aqueous Extract. The results of bacterial endotoxin recovery in aqueous extracts of the ultrapure paraffin oil are shown in Table 3.

The data indicate that the recovery of the endotoxin from the ultrapure paraffin oil extract meets the requirement of the gel-clot method of the Chinese Pharmacopoeia which is in the range of 50%–200%.

3.4. Analysis of Bacterial Endotoxin of Ultrapure Paraffin Oil. All the analysis results matched the requirements. Result was shown in Table 4.

4. Discussion

Because of the water insolubility of the ultrapure paraffin oil, extraction with water is an indispensable part of the bacterial endotoxin test. However, two considerations should be taken into account. Although ultrapure paraffin oil is water insoluble, there may still be some residues in the extracted aqueous phase, so it is important to confirm that

Table 1: The results of confirmation of the labelled sensitivity.

TAL	Concentration of bacterial endotoxin (EU/mL)				Negative control	λ
	0.25	0.125	0.06	0.03		
TAL-01	++++	++++	− − −−	− − −−	− −	0.125
TAL-02	++++	++++	− − −−	− − −−	− −	0.125

Table 2: Results of interference test of the ultrapure paraffin oil aqueous phase extract.

TAL	Endotoxin concentration (EU/mL)				Negative control	Results (EU/mL)
	0.25	0.125	0.06	0.03		
TAL-01						
BET	++++	++++	− − −−	− − −−	− −	$E_s = 0.125$
Sample	++++	++++	− − −−	− − −−	− −	$E_t = 0.125$
TAL-02						
BET	++++	++++	− − −−	− − −−	− −	$E_s = 0.125$
Sample	++++	++++	− − −−	− − −−	− −	$E_t = 0.125$

Table 3: Recovery of bacterial endotoxin in the aqueous extracts.

Added bacterial endotoxin (EU/mL)	Measured value (EU/mL)	Recovery (%)
20	19.1	95.5
10	11.1	111
5	4.71	94.2

Table 4: Bacterial endotoxin analysis of ultrapure paraffin oil aqueous extracts.

Test sample	Positive product control	Positive control	Negative control
− −	++	++	− −

the extraction solution will not interfere with the clot between the Tachypleus Amebocyte Lysate and the endotoxin.

Also, since the limit value of the endotoxin in the aqueous phase has the following relationship with the limit value of the endotoxin in the ultrapure paraffin oil, $L'_{\text{water}} = (L_{\text{ultrapure paraffin oil}} \times V_{\text{ultrapure paraffin oil}} \times \text{Percent recovery of the endotoxin})/V_{\text{water}}$, the recovery of the endotoxin of the ultrapure paraffin oil must also be considered; otherwise the result of the test will not correlate with the endotoxin in the ultrapure paraffin oil. If the recovery of endotoxin in the ultrapure paraffin oil is within 50%–200% after extraction, then it does not need to be recovered based on the method in Chinese Pharmacopoeia (converted at 100%). If not within 50%–200%, the limit value of the endotoxin in the aqueous phase should be calculated based on the recovery [8]. Due to the different concentrations of endotoxin, their proportion in the ultrapure paraffin oil phase and the aqueous phase and the recovery will be different. This is why the recovery test should be done with different concentrations of endotoxin.

Till present, there are few studies of test methods for bacterial endotoxins in water insoluble oily medical devices. In this study, an interference test was applied to the aqueous phase extracted from the ultrapure paraffin oil to confirm that it did not interfere with the clot formation between the Tachypleus Amebocyte Lysate and the endotoxin. To this end, ultrapure paraffin oil with different endotoxin concentrations was prepared and the recovery was tested using a dynamic turbidimetric method. All results were within 86.8%–96.8% and thus met the requirement of 50%–200% in the Chinese Pharmacopeia. This also indicates that the test method in this study is able to accurately determine the endotoxin concentration in ultrapure paraffin oil by analysis of the aqueous phase extract.

5. Conclusions

In this study, we have shown that it is possible to analyse the concentration level of bacterial endotoxin in water extracts of ultrapure paraffin oil using the gel-clot method and verified the limit value of <0.25 EU/mL. At the same time, this study can be regarded as a supplement analysis method for water insoluble oily medical devices to the United States Pharmacopeia chapter number 85 "Analysis of bacterial endotoxin" and chapter number 161 "Blood and other liquid transfusion device and similar medical device."

Conflict of Interests

The author declares that there is no conflict of interests regarding the publication of this paper.

References

[1] United States Pharmacopeia. chapter no. 85 Analysis of bacterial endotoxin.

[2] United States Pharmacopeia. chapter no. 161 Blood and other liquid transfusion device and similar medical device.

[3] *Chinese Pharmacopoeia*, Appendix XIE, 2010.

[4] Y. Zhang et al., "New method for bacterial endotoxin test of absorptive medical film," *Modern Preventive Medicine*, vol. 34, pp. 3442–3446.

[5] X. Zheng, Y. M. Zhao, and C. Liu, "Bacterial endotoxin test f or puerarin injection," *China Pharmacy*, vol. 18, pp. 1254–1255, 2007.

[6] Z. X. Pan and Q. Song, "Study on ditermination of bacterial endotoxin of omeprazole sodium for injection," *Chinese Journal of Pharmaceutical Analysis*, vol. 28, pp. 275–277.

[7] J. Gao et al., "Study on of bacterial endotoxin test for neostigmine methylsulfate injection," *Journal of Pharmaceutical Analysis*, vol. 28, pp. 1141–1143, 2008.

[8] Y. C. Hu, N. Li, and J. P. Zhou, "Study on gelation clot method of bacterial endotoxin test in test orerone undecanoate injection," *Chinese Journal of Pharmaceutical Analysis*, vol. 30, pp. 2425–2429, 2010.

Hindawi Publishing Corporation
Journal of Analytical Methods in Chemistry
Volume 2014, Article ID 241505, 12 pages
http://dx.doi.org/10.1155/2014/241505

Research Article

A Metabolomic Strategy to Screen the Prototype Components and Metabolites of *Shuang-Huang-Lian Injection* in Human Serum by Ultra Performance Liquid Chromatography Coupled with Quadrupole Time-of-Flight Mass Spectrometry

Mingxing Guo,[1] Baosheng Zhao,[1] Haiyu Liu,[1] Li Zhang,[1] Long Peng,[1] Lingling Qin,[1] Zhixin Zhang,[1] Jian Li,[2] Chengke Cai,[3] and Xiaoyan Gao[1]

[1] *Science Experiment Center for Traditional Chinese Medicine, Beijing University of Chinese Medicine, No. 11, North Third Ring Road, Chaoyang District, Beijing 100029, China*
[2] *School of Basic Medical Sciences, Beijing University of Chinese Medicine, No. 11, North Third Ring Road, Chaoyang District, Beijing 100029, China*
[3] *School of Chinese Material Medica, Beijing University of Chinese Medicine, South of Wangjing Middle Ring Road, Chaoyang District, Beijing, 100102, China*

Correspondence should be addressed to Chengke Cai; cck98@126.com and Xiaoyan Gao; gaoxiaoyan0913@sina.com

Received 22 December 2013; Accepted 19 January 2014; Published 26 February 2014

Academic Editor: Ying-Yong Zhao

Copyright © 2014 Mingxing Guo et al. This is an open access article distributed under the Creative Commons Attribution License, which permits unrestricted use, distribution, and reproduction in any medium, provided the original work is properly cited.

Shuang-huang-lian injection (*SHLI*) is a famous Chinese patent medicine, which has been wildly used in clinic to treat acute respiratory tract infection, pneumonia, influenza, and so forth. Despite the widespread clinical application, the prototype components and metabolites of *SHLI* have not been fully elucidated, especially in human body. To discover and screen the constituents or metabolites of Chinese medicine in biofluids tends to be more and more difficult due to the complexity of chemical compositions, metabolic reactions and matrix effects. In this work, a metabolomic strategy to comprehensively elucidate the prototype components and metabolites of *SHLI* in human serum conducted by UPLC-Q-TOF/MS was developed. Orthogonal partial least squared discriminant analysis (OPLS-DA) was applied to distinguish the exogenous, namely, drug-induced constituents, from endogenous in human serum. In the S-plot, 35 drug-induced constituents were found, including 23 prototype compounds and 12 metabolites which indicated that *SHLI* in human body mainly caused phase II metabolite reactions. It was concluded that the metabolomic strategy for identification of herbal constituents and metabolites in biological samples was successfully developed. This identification and structural elucidation of the chemical compounds provided essential data for further pharmacological and pharmacokinetics study of *SHLI*.

1. Introduction

Shuang-huang-lian injection (SHLI) is a typical Chinese herbal injection that is made from the extracts of *Flos Lonicerae Japonicae, Radix Scutellariae,* and *Fructus Forsythiae*. It has been widely used for the treatment of acute upper respiratory tract infections [1, 2]. Baicalin, chlorogenic acid, and forsythin are the marker compounds representing *Radix Scutellariae*, *Flos Lonicerae Japonicae,* and *Fructus Forsythiae*, respectively, for the quality control of this medicine [3]. Though several published papers have reported the determination of major active components and metabolites in *Shuang-huang-lian (SHL)* preparations [4–6], there is no substantial evidence to confirm the holistic existing form of *SHLI* in vivo, especially in human body. Therefore, systematically, screening the constituents and metabolites of *SHLI* in human blood is of great significance for interpreting its material basis for pharmacological effects. Currently, the ingredients of *SHL* formula have been detected in rat blood [7]. However, the recent study suggests that

species differences in key hepatic efflux transporters are sufficiently profound to warrant careful re-examination of conclusions and to design future studies with caution [8]. Some data have revealed that rat liver contains much more (~10-fold) apical multidrug resistance-associated protein 2 (Mrp2) resulting in a much higher capacity for the biliary excretion of organic anions in rats than human or other preclinical species [9]. Therefore, to reveal the pharmacological mechanism of *SHLI*, comprehensive analysis of the constituents and metabolites in human body is more scientific and rational.

The process of metabolite detection and identification is typically a labor-intensive and time-consuming process. This process has been simplified by the use of radio-labeled compounds and/or spectroscopic techniques such as mass spectrometry and NMR spectroscopy [10–13]. Of these analysis techniques, liquid chromatography coupled with electrospray ionization mass spectrometer has been widely used to detect and identify trace levels of drugs and metabolites in various biological samples due to its high sensitivity and selectivity [14–16]. Ultra performance liquid chromatography (UPLC) applied for short run times combined with a quadrupole/time of flight-mass spectrometer (Q/TOF-MS) which offers high mass accuracy has become a major tool that provides a significant source of global constituent and metabolite profiling data [17–19]. Given the chemical complexity of *SHLI* in vivo, UPLC-Q-TOF/MS provides faster separations for complex blood samples and valuable structural insights into the characterization of *SHLI* metabolites.

A straightforward approach for identifying exogenous metabolites in vivo is to compare the LC-MS chromatograms of biological samples collected before and after xenobiotic treatment. However, without using effective analysis method, it is difficult to identify exogenous metabolites through visual examination of LC-MS chromatograms that contain information from thousands of chemical species [20]. A metabolomic strategy has been developed to handle the acquired data and to search for the discriminating features from biosample sets. A xenobiotic and its metabolites only appear in the samples after xenobiotic treatment, and so when using metabolomic strategy, the differences between the control group and the xenobiotic-treated group are mainly defined by the presence of the xenobiotic and its metabolites. With appropriate data processing, the separation of the control group and the xenobiotic-treated group can be achieved in the score plot of a multivariate model, and exogenous metabolites can be conveniently identified by analyzing ions contributing to the separation of the two groups. Employing this approach, the present study aims to develop a metabolomic strategy to comprehensively elucidate the prototype components and metabolites of *SHLI* in human serum conducted by UPLC-Q-TOF/MS.

2. Experiment

2.1. Materials. *SHLI* was achieved from the Second Chinese Medicine Factory of Harbin Pharm. Group CO., Ltd. (No. 1204014). HPLC grade formic acid was obtained from Sigma Chemical Co., Ltd. (St. Louis, MO, USA). Methanol (HPLC grade) was acquired from Fisher Corporation (Michigan, USA). Water was purified with a Milli-Q system (Millipore, Bedford, USA).

2.2. Subjects and Clinical Trial Design. The study was approved by an independent ethics committee at Beijing University of Chinese Medicine, before recruitment commenced. Before the initiation of study procedures, all volunteers gave their written informed consent for participation in the study. Thirteen healthy volunteers, without taking any medication, participated in the study. They were aged between 25 and 40 years and with weight between 50 and 80 kg. After overnight fasting, early-morning blood samples (20 mL each) were collected from the medial cubital vein into evacuated tubes and marked as the control group (C group). Then participants were intravenous infusion of 60 mg/kg of *SHLI* (dissolved with 500 mL saline solution). The blood samples were collected at 0.5 h after *SHLI* administration and marked as *SHLI* dosed group (*SHLI* group). The blood supernatant was allowed to clot overnight at room temperature, and the clotted material was removed by centrifugation (3000 rpm, 15 min). The serum was collected and stored at −80°C.

2.3. Pretreatment Procedure for SHLI. The *Shuang-huang-lian* lyophilized powder for injection (0.1 g) was weighed and dissolved with 100 mL water. Then, it was filtered by a 0.22 μm filter before UPLC-Q-TOF/MS analysis.

2.4. Pretreatment Procedure for Serum Samples. All serum samples were thawed at room temperature followed by methanol protein precipitation. Serum (200 μL) was added with 600 μL methanol, vortexed for 30 s, and centrifuged at 14000 g for 10 min at 4°C. Then, supernatant (400 μL) was transferred to a clean tube and evaporated to dryness under a gentle stream of nitrogen. The residue was redissolved with 100 μL ultra high purity water and transferred to an autosampler vial.

2.5. UPLC-Q-TOF/MS Analysis. Separation and detection of the components and metabolites of *SHLI* were performed on a Waters Acquit UPLC chromatographic system (Waters Corp., Milford, USA) equipped with a Evoe G2 Q/TOF (Waters MS Technologies, Manchester, UK). An electrospray ionization source (ESI) interface was used in both positive and negative ion modes. Acquit UPLC HSS T3 column (2.1 mm × 100 mm, 1.8 μm, Waters, UK) was applied for all analyses. The mobile phase was composed of A (0.1% formic acid in water) and B (methanol) with a linear gradient elution: 0–1 min, maintained at 0% B; 1–5 min, from 0% B to 40% B; 5–8 min, from 40% B to 100% B; 8–13 min, maintained at 0% B; 13.0–13.1 min, isocratic of 0% B; 13.1–15 min, maintained at 0% B. The flow rate was 0.30 L/min. The analytic column and autosampler were maintained at temperatures of 45°C and 4°C, respectively. Then, 1 μL of sample solution was injected for each run. Data were collected from m/z 50 to m/z 1200. For positive ion mode, the capillary and cone voltage were

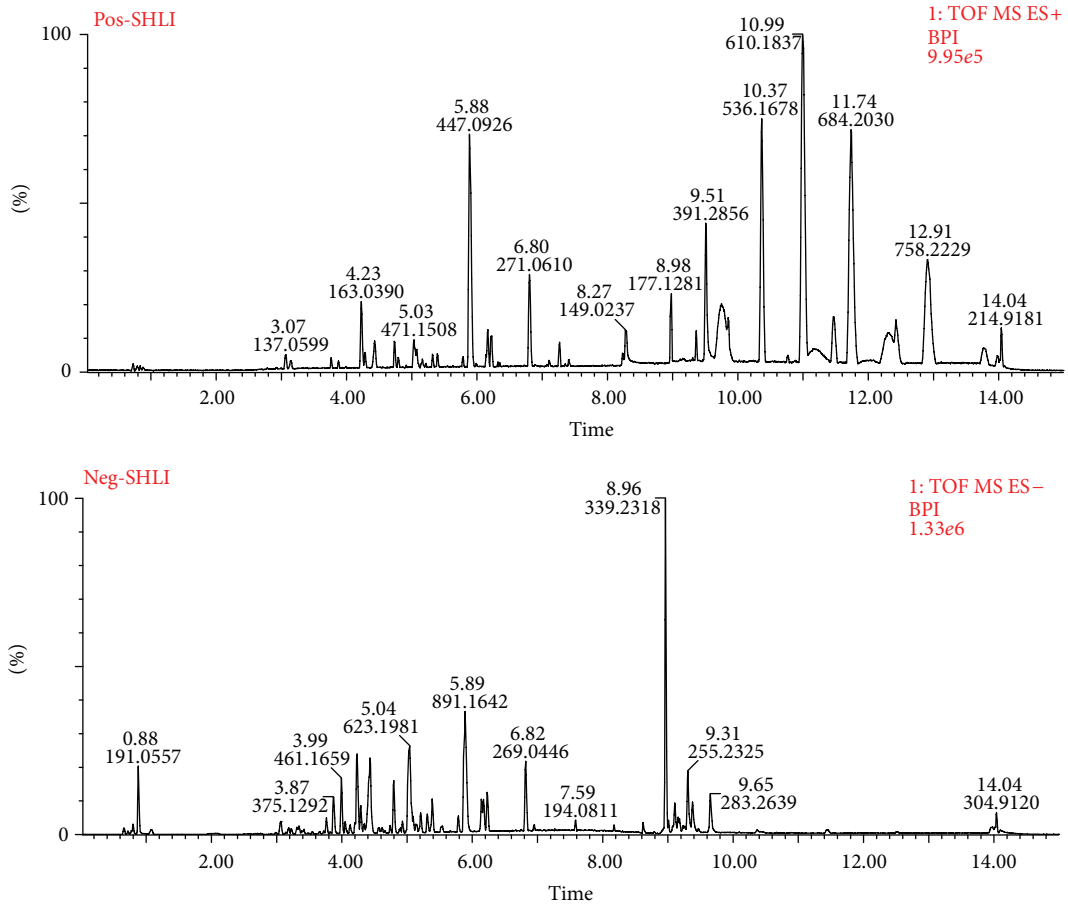

Figure 1: UPLC-Q-TOF/MS BPI chromatograms of *SHLI* in positive ion mode and negative ion mode.

set at 3 kV and 35 V. For negative ion mode, the capillary and cone voltage were set at 2.5 kV and 35 V. The conservation gas was set at 700 L/h at a temperature of 350°C. The source temperature was set at 100°C. The cone gas was set at 50 L/h. Leucine-enkephalin was used as the lock mass solution to ensure the accuracy and reproducibility.

2.6. Data Processing and Statistical Analysis. The ES+ and ES− raw data was analyzed by MarkerLynx XS software (Waters Corp., Milford, USA). For extracting data from the raw file and detecting potential markers, the retention time range was set at 0–13 min, the mass range at 50–1000 amu, and the mass tolerance as 0.01. For detecting chromatographic peaks in the Apex Track Peak, peak width at 5% height was set at 1.00, and the peak-to-peak baseline noise was 0.00. For collecting parameters, the marker intensity threshold was set at 1000 cps, the mass window was 0.02 amu, and retention time window was 0.20 min. The noise elimination level was 6. This process provided alignment of drift (retention time and accurate mass) in data and ensured that a chromatographic peak was identified with the same parameters in each sample. Subsequently, a list of intensities or peak areas of the peaks was then generated for the first chromatogram, using the ER-*m/z* pairs as identifiers. The procedure was applied for each UPLC/MS analysis. The ion intensities or peak area for each peak detected was also normalized within each sample to the sum of the peak intensities in that sample. The three-dimensional data were introduced into the EZinfo 2.0 software (Waters Corporation, Milford, MA, USA) for orthogonal partial least-squares-discriminate analysis (OPLS-DA).

3. Results and Discussion

3.1. Identification and Analysis of Chemical Components in SHLI. Global profiling of both positive and negative ion modes was analyzed by UPLC-Q-TOF/MS. The typical base peak intensity (BPI) chromatograms (positive ion mode and negative ion mode) of *SHLI* were shown in Figure 1. In total, 38 constituents were detected and tentatively characterized in *SHLI* (Table 1). MS^E technique, a new technique used in deducing the splitting disciplinary of MS, was applied to data collection. MS^E technique could provide parallel alternating scans for acquisition at low collision energy to obtain precursor ion information or at a ramping of high collision energy to obtain a full-scan accurate mass of fragments, precursor ions, and neutral loss information [21, 22]. Here, the high precision MS/MS fragments

Table 1: UPLC-Q-TOF/MS identification of the constituents in *SHLI*.

NO.	t_R (min)	Positive ion MS	Negative ion MS	Formula	Identification	Positive ion MS/MS	Negative ion MS/MS	Class
1	0.88	193.0722	191.0557	$C_7H_{12}O_6$	Quinic acid	112.0521	127.0400 85.0288	Quinic acid
2	3.77	355.1033	353.0873	$C_{16}H_{18}O_9$	Chlorogenic acid	163.0395 145.0279 135.0454	191.0549 179.0341 135.0449	Quinic acid
3	3.87	—	375.1287	$C_{16}H_{24}O_{10}$	Isomer of loganic acid	—	213.0765 169.0867 151.0759	Iridoid
4	3.90	623.2080	—	$C_{29}H_{34}O_{15}$	Isomer of suspensaside A	191.0568 149.0232	461.1674 443.1554 205.0319	Phenylethanoid glycoside
5	3.97	—	461.1659	$C_{20}H_{30}O_{12}$	Forsythoside E	—	315.1076 205.0718 135.0448	Phenylethanoid glycoside
6	4.20	—	375.1287	$C_{16}H_{24}O_{10}$	Loganic acid	—	213.0778 169.0853 151.0773	Iridoid
7	4.24	355.1023	353.0866	$C_{16}H_{18}O_9$	3-O-Caffeoylquinic acid	163.0393 145.0286	191.0569 179.0365	Quinic acid
8	4.29	—	353.0873	$C_{16}H_{18}O_9$	4-O-Caffeoylquinic acid	—	173.0450 135.0453	Quinic acid
9	4.35	—	639.1925	$C_{29}H_{36}O_{16}$	Suspensaside	—	621.1841 469.1273	Phenylethanoid glycoside
10	4.43	375.1288	373.1129	$C_{16}H_{22}O_{10}$	Secologanic acid	213.0749 195.0638	193.0494 149.0605	Iridoid
11	4.45	391.1255	389.1074	$C_{16}H_{22}O_{11}$	Monotropein	211.0586 177.0546 151.0395	209.0455 165.0554 149.0605	Iridoid
12	4.58	—	639.1918	$C_{29}H_{36}O_{16}$	Isomer of suspensaside	—	445.1318 205.0318 179.0346	Phenylethanoid glycoside
13	4.72	—	403.1239	$C_{17}H_{24}O_{11}$	Isomer of secoxyloganin	—	241.1177	Iridoid
14	4.73	359.1348	—	$C_{16}H_{22}O_9$	Sweroside	197.0812 151.0400	—	Iridoid
15	4.80	625.2124	623.1982	$C_{29}H_{36}O_{15}$	Acteoside	471.1504 325.0927 163.0398	461.1671 443.1567 203.0428	Phenylethanoid glycoside
16	4.89	—	755.2399	$C_{34}H_{44}O_{19}$	Forsythoside B	—	593.2103 447.1500 315.1137	Phenylethanoid glycoside
17	4.93	623.1986	621.1816	$C_{29}H_{34}O_{15}$	Suspensaside A	191.0571 149.0234	487.1371 469.1180	Phenylethanoid glycoside
18	5.03	625.2133	623.1970	$C_{29}H_{36}O_{15}$	Forsythoside A	471.1512 325.0919 163.0398	461.1671 443.1567 205.0321	Phenylethanoid glycoside
19	5.06	405.1387	403.1236	$C_{17}H_{24}O_{11}$	Secoxyloganin	243.0880 211.0612	371.0979 223.0611	Iridoid
20	5.09	—	515.1174	$C_{25}H_{24}O_{12}$	3,4-Dicaffeoylquinic acid	—	353.0906 191.0561 135.0446	Quinic acid
21	5.13	—	515.1174	$C_{25}H_{24}O_{12}$	3,5-Dicaffeoylquinic acid	—	353.0906 173.0355 135.0446	Quinic acid

Table 1: Continued.

NO.	t_R (min)	Positive ion MS	Negative ion MS	Formula	Identification	Positive ion MS/MS	Negative ion MS/MS	Class
22	5.21	—	519.1863	$C_{26}H_{32}O_{11}$	Pinoresinol 4-O-glucoside	—	357.1336 151.0398 136.0164	Lignan
23	5.30	463.0876	461.0730	$C_{21}H_{18}O_{12}$	Luteolin 7-galacturonide	287.0552 269.0462 241.0493	285.0399 211.0400 113.0238	Flavonoid
24	5.32	—	447.0927	$C_{21}H_{20}O_{11}$	5,6-Dihydroxy flavanone-7-O-glucuronide	—	285.0399 267.0309 239.0356	Flavonoid
25	5.35	—	621.1788	$C_{29}H_{34}O_{15}$	Suspensaside A	—	487.1510 179.0351	Phenylethanoid glycoside
26	5.37	611.1599	609.1453	$C_{27}H_{30}O_{16}$	Rutin	465.1016 303.1489	300.0253 271.0236 255.0290	Flavonoid
27	5.38	517.1344	515.1186	$C_{25}H_{24}O_{12}$	4,5-Dicaffeoylquinic acid	499.1206 355.1702 337.0856	353.0866 191.0553 173.0451	Quinic acid
28	5.54	—	757.2550	$C_{34}H_{46}O_{19}$	Centauroside	—	525.1569 493.1695 179.0511	Iridoid
29	5.78	—	533.2020	$C_{27}H_{34}O_{11}$	Phillyrin	—	371.1484 356.1257 121.0295	Lignan
30	5.88	447.0925	445.0771	$C_{21}H_{18}O_{11}$	Baicalin	271.0603	269.0455 241.0503	Flavonoid
31	6.01	477.1027	475.0876	$C_{22}H_{19}O_{12}$	5,2′-Dihydroxy-6′-methoxyflavone-7-O-glucuronide	301.0713	443.0556 299.0546	Flavonoid
32	6.17	431.0978	429.0815	$C_{21}H_{18}O_{10}$	Chrysin 7-glucuronide	255.0658	253.0505	Flavonoid
33	6.23	461.1079	459.0927	$C_{22}H_{20}O_{11}$	Wogonoside	285.0767 270.0534	283.0611 268.0375 239.0345	Flavonoid
34	6.38	—	445.0779	$C_{21}H_{18}O_{11}$	Norwogonin-7-O-glucuronide	—	269.0422	Flavonoid
35	6.81	271.0608	269.0446	$C_{15}H_{10}O_5$	Baicalein	271.0623 253.0498 123.0083	251.0362 223.0379 195.0447	Flavonoid
36	7.26	285.0761	283.0602	$C_{16}H_{12}O_5$	Wogonin	270.0489	268.0377 162.9845	Flavonoid
37	7.35	255.0654	—	$C_{15}H_{10}O_4$	Chrysin	153.0173	—	Flavonoid
38	7.40	285.0762	283.0601	$C_{16}H_{12}O_5$	Isomer of wogonin	270.0489	268.0409	Flavonoid

information obtained from the MS^E technique were also listed in Table 1 to explain the structure information of the chemical constituents. All the constituents and the fragmentation information were consistent with previous reports [23, 24].

3.2. Analysis of Human Serum by Metabolomic Strategy. Figure 2 represented the typical BPI chromatograms (positive ion mode and negative ion mode) of human serum samples before and after *SHLI* administration. The prototype components and metabolites of *SHLI* in human serum were almost submerged by the endogenous metabolites due to the high level of endogenous signals. Interferences from biological matrices remain a major challenge to detection of metabolites in vivo. Without the presence of a radiolabeled isotope or a data-mining tool, it would be almost impossible to identify low level exogenous metabolites. In our work, a metabolomic strategy was employed to phenotype the differences between C group and *SHLI* group. The LC/MS

Table 2: The prototype components and metabolites in human serum after *SHLI* dosed in both positive and negative mode.

NO.	t_R (min)	Positive ion MS	Negative ion MS	Formula	Identification	Positive ion MS/MS	Negative ion MS/MS	Relegation
1	0.88	193.0722	191.0557	$C_7H_{12}O_6$	Quinic acid	112.0521	127.0400 85.0288	Prototype component
2	3.77	355.1033	353.0873	$C_{16}H_{18}O_9$	Chlorogenic acid	163.0395 145.0279 135.0454	191.0549 179.0341 135.0449	Prototype component
3	3.87	—	375.1287	$C_{16}H_{24}O_{10}$	Isomer of loganic acid	—	213.0765 169.0867 151.0759	Prototype component
4	4.20	—	375.1287		Loganic acid	—	213.0778 169.0853 151.0773	Prototype component
5	4.24	—	353.0873	$C_{16}H_{18}O_9$	3-O-Caffeoylquinic acid	—	191.0569 179.0365	Prototype component
6	4.29	—	353.0873	$C_{16}H_{18}O_9$	4-O-Caffeoylquinic acid	—	173.0450 135.0453	Prototype component
7	4.37	478.1365	—	$C_{22}H_{23}NO_{11}$	Isorhamnetin 7-glucosamine	316.0847 298.0745 280.0654	—	Metabolite of flavonoids
8	4.42	—	475.1816	$C_{21}H_{32}O_{12}$	Kanokoside A	—	313.0276 193.0493 123.0452	Metabolite of iridoids
9	4.43	375.1288	373.1129	$C_{16}H_{22}O_{10}$	Secologanic acid	213.0749 195.0638	193.0494 149.0605	Prototype component
10	4.45	—	389.1074	$C_{16}H_{22}O_{11}$	Monotropein	—	209.0455	Prototype component
11	4.57	—	369.0815	$C_{16}H_{18}O_{10}$	Ferulic acid 4-O-glucuronide	—	193.0490 178.0263	Metabolite of quinic acids
12	4.72	—	403.1239	$C_{17}H_{24}O_{11}$	Isomer of secoxyloganin	—	241.1177	Prototype component
13	4.73	359.1348	—	$C_{16}H_{22}O_9$	Sweroside	197.0812 151.0400	—	Prototype component
14	5.03	—	731.1866	$C_{31}H_{40}O_{18}S$	Methylated and sulfated forsythiaside	—	651.2212 457.1421	Metabolite of phenylethanoid glycosides
15	5.06	405.1387	403.1236	$C_{17}H_{24}O_{11}$	Secoxyloganin	243.0880 211.0612	371.0979 223.0611	Prototype component
16	5.09	—	515.1174	$C_{25}H_{24}O_{12}$	3,4-Dicaffeoylquinic acid	—	353.0906 191.0561 135.0446	Prototype component
17	5.16	623.1266	621.1092	$C_{27}H_{26}O_{17}$	Genistein 4′,7-O-diglucuronide	447.0916 271.0607	445.0765 357.1336 269.0444	Metabolite of flavonoids
18	5.20	—	827.2600	$C_{37}H_{48}O_{21}$	2-(3,4-Dihydroxyphenyl)ethyl6-deoxy-mannopyranosyl-glucopyranosyl-2-O-acetyl-4-O-[3-(3,4-dihydroxyphenyl)-2-propenoyl]-glucopyranoside	—	520.1801 429.1375 437.0904	Metabolite of phenylethanoid glycosides
19	5.21	—	519.1863	$C_{26}H_{32}O_{11}$	Pinoresinol 4-O-glucoside	—	357.1336 151.0398 136.0164	Prototype component
20	5.47	623.1250	621.1088	$C_{27}H_{26}O_{17}$	Baicalein 6,7-diglucuronide	447.0922 271.0605	445.0774 269.0452	Metabolite of flavonoids
21	5.54	609.1461	607.1299	$C_{27}H_{28}O_{16}$	Luteolin 7-glucuronide-4′-rhamnoside	447.0919 271.0610	431.0965	Metabolite of flavonoids

Table 2: Continued.

NO.	t_R (min)	Positive ion MS	Negative ion MS	Formula	Identification	Positive ion MS/MS	Negative ion MS/MS	Relegation
22	5.54	—	757.2550	$C_{34}H_{46}O_{19}$	Centauroside	—	525.1569 493.1695 179.0511	Prototype components
23	5.69	—	287.0234	$C_{11}H_{12}O_7S$	5′-(3′,4′-Dihydroxyphenyl)-gamma-valerolactone sulfate	—	207.0651 179.0334 135.0437	Metabolite of flavonoids
24	5.78	—	533.2020	$C_{27}H_{34}O_{11}$	Phillyrin	—	371.1484 356.1257 121.0295	Prototype component
25	5.88	447.0925	445.0771	$C_{21}H_{18}O_{11}$	Baicalin	271.0603	269.0455 241.0503	Prototype component
26	6.17	431.0969	429.0815	$C_{21}H_{18}O_{10}$	Chrysin 7-glucuronide	255.0645	253.0505	Prototype component
27	6.23	461.1079	459.0927	$C_{22}H_{20}O_{11}$	Wogonoside	285.0760	283.0611 268.0375 239.0345	Prototype component
28	6.38	—	445.0779	$C_{21}H_{18}O_{11}$	Norwogonin-7-O-glucuronide	—	269.0449 131.0625	Prototype component
29	6.41	—	349.0014	$C_{15}H_{10}O_8S$	Baicalein 7-sulfate	—	269.0449	Metabolite of flavonoids
30	6.43	—	363.0174	$C_{16}H_{12}O_8S$	Wogonin 7-sulfate	—	283.0606	Metabolite of flavonoids
31	6.46	—	283.0607	$C_{16}H_{12}O_5$	7,5-Dihydroxy-6-methoxyflavone	—	268.0371	Metabolite of flavonoids
32	6.81	271.0608	269.0446	$C_{15}H_{10}O_5$	Baicalein	271.0623 253.0498 123.0083	251.0362 223.0379 195.0447	Prototype component
33	7.26	285.0761	283.0602	$C_{16}H_{12}O_5$	Wogonin	270.0489	268.0377 162.9845	Prototype component
34	7.35	255.0654	—	$C_{15}H_{10}O_4$	Chrysin	153.0173	—	Prototype component
35	7.41	285.0761	283.0601	$C_{16}H_{12}O_5$	Wogonin	270.0502	268.0409	Prototype component

data were processed using MarkerLynx XS to detect peaks and generate a three-dimensional data with t_R-m/z pairs and the corresponding intensities. Statistical analysis by OPLS-DA was subsequently performed on the entire dataset. Figure 3 showed the OPLS-DA score plots of human serum samples before and after *SHLI* injection. Clear separation was observed between the two groups, which indicated that the drug-induced constituents were contributed to the clustering.

3.3. Identification and Analysis of Prototype Components and Metabolites. In order to discover the multiple prototype components and metabolites of *SHLI* in human serum, S-plot, a tool for visualization and interpretation of multivariate classification models, was used. In the S-plot, each point represented an ion detected by UPLC-Q-TOF/MS. Variables that were the farthest from the origin in the S-plot were representative of the most significant changes between the two groups. Based on this, even subtle differences in the two groups could be easily extracted. Figure 4 showed the ions in S-plot that were most responsible for distinguishing the C and *SHLI* groups and had a higher level in *SHLI* group.

The S-plot responsible for the variances in the data was a combination of metabolites derived from the *SHLI* administration and endogenous molecules which were ubiquitous to serum and were interfered by *SHLI*. From a drug metabolite identification perspective, it was important that the disturbance endogenous molecules could be eliminated, and the prototype components and metabolites could be easily screened between *SHLI*-treated group and the control group. This comparison was achieved by using the trend plot. From the trend plots, the variables that only existed in the dosed serums were marked as the prototype components or the metabolites of *SHLI*. Figure 5 showed the visualized trend plot of 7.41-285.0762 in positive mode between C group and *SHLI* group. The ion only appeared in the *SHLI* group. Therefore, 7.41-285.0762 might be a prototype component or a metabolite of *SHLI*.

Based on the metabolomic strategy, 35 exogenous components in human serum were found, among them, 23 prototype

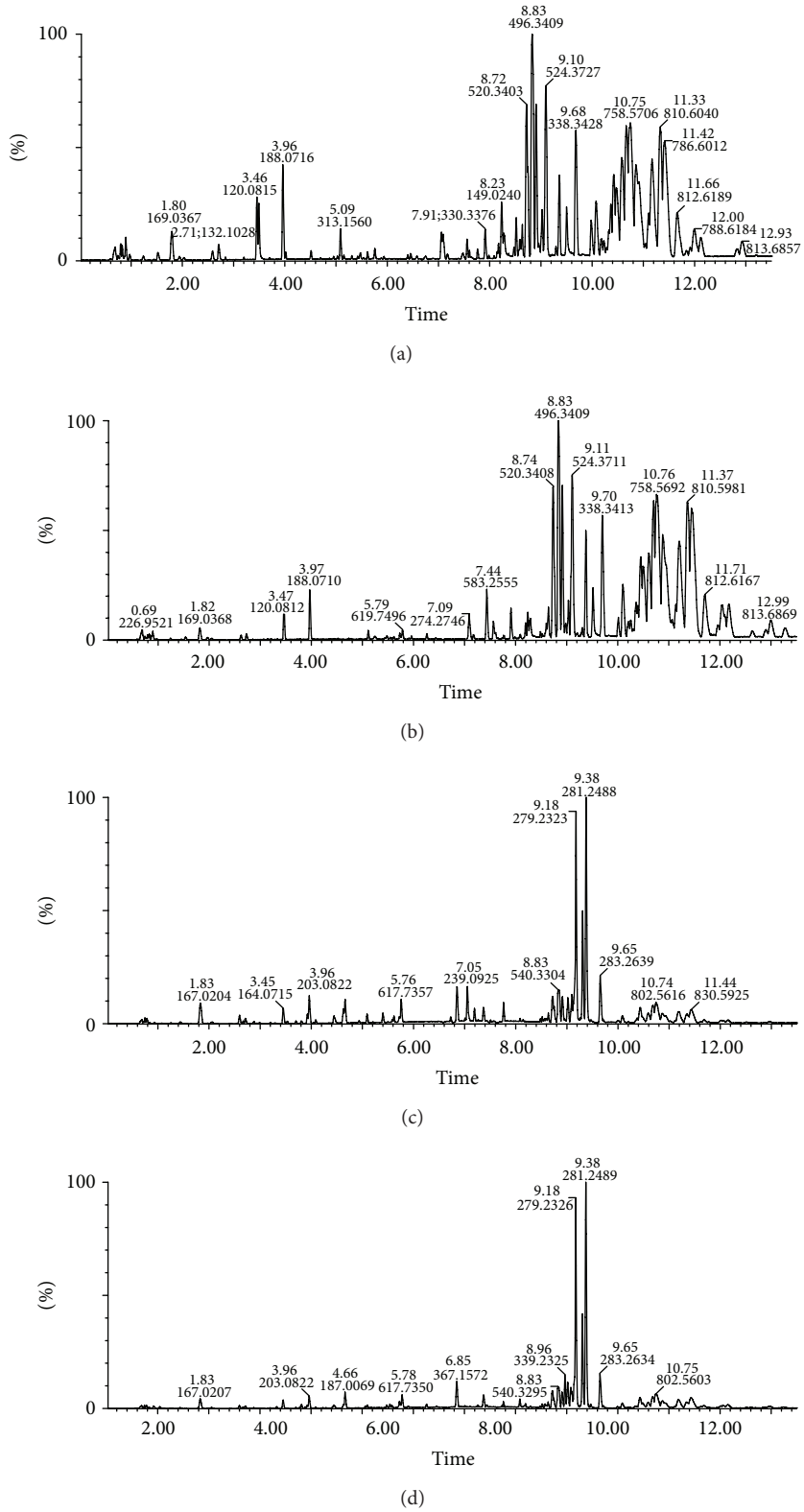

Figure 2: UPLC-Q-TOF/MS BPI chromatograms of human serum samples (a) before *SHLI* administration in positive ion mode, (b) after *SHLI* administration in positive ion mode, (c) before *SHLI* administration in negative ion mode, and (d) after *SHLI* administration in negative ion mode.

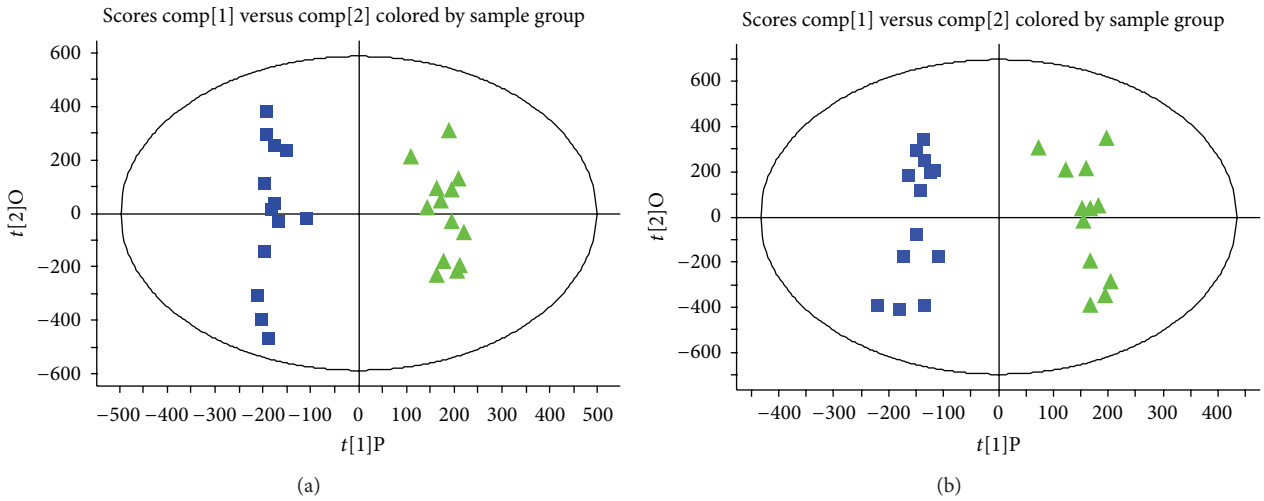

Figure 3: Score plots of OPLS-DA in human serum samples between C group (■) and *SHLI* group (▲) in (a) positive ion mode and (b) negative ion mode.

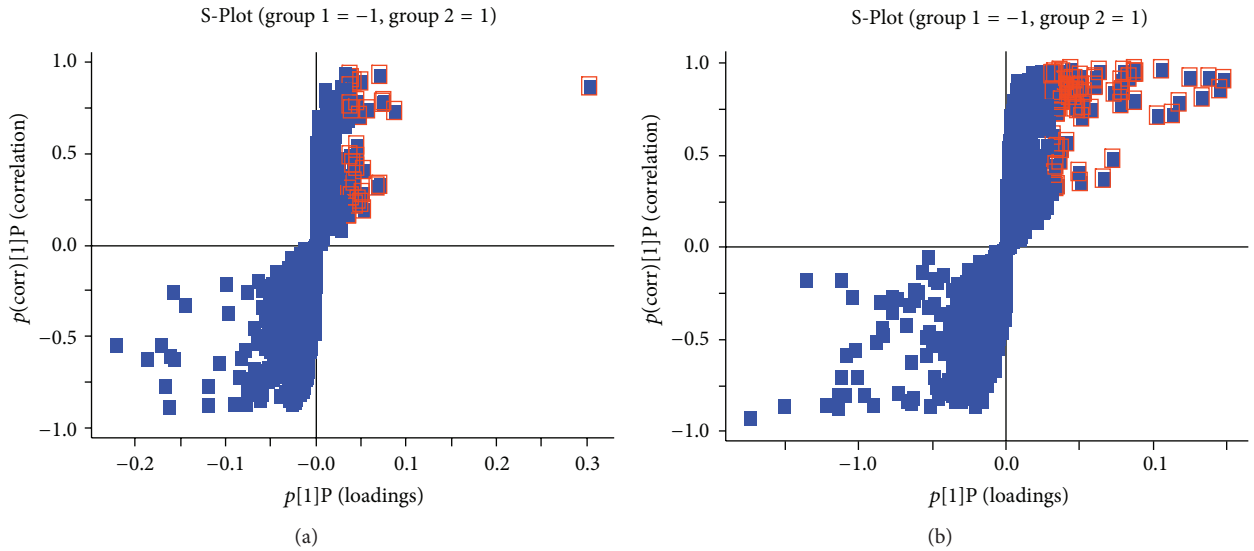

Figure 4: S-plots of human serum samples between C and *SHLI* groups in (a) positive ion mode and (b) negative ion mode. The ions marked with box were at the higher level in *SHLI* group.

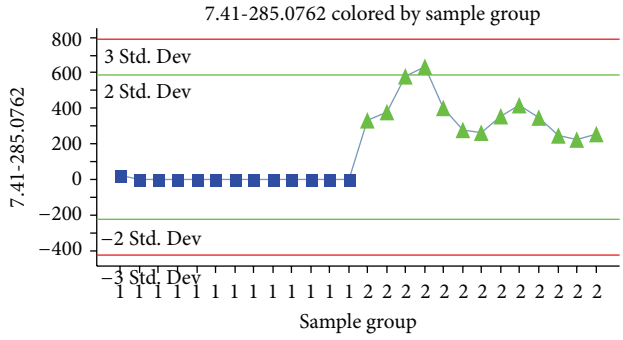

Figure 5: The trend plot of 7.41-285.0762 in positive mode between C group (■) and *SHLI* group (▲).

components of *SHLI* and 12 metabolites were identified and their information was shown in Table 2.

3.4. Characterization Analysis of Human Serum Prototype Components and Metabolites of SHLI. In our study, the prototype components and metabolites of *SHLI* were identified by comparing the accurate mass and MS^E fragment information obtained from the MS^E technique. Figure 6 showed typical MS/MS spectra of the prototype component 6.23-461.1079 and the flavonoid metabolite 6.46-363.0174. In positive ion mode, the ion at *m/z* 483.0906 was $[M + Na]^+$ion. The dominant fragment ion of *m/z* 285.0763 was produced by loss of *m/z* 176 (glucuronide-H_2O) fragment from $[M + H]^+$ in positive ion mode. The characteristic and abundant

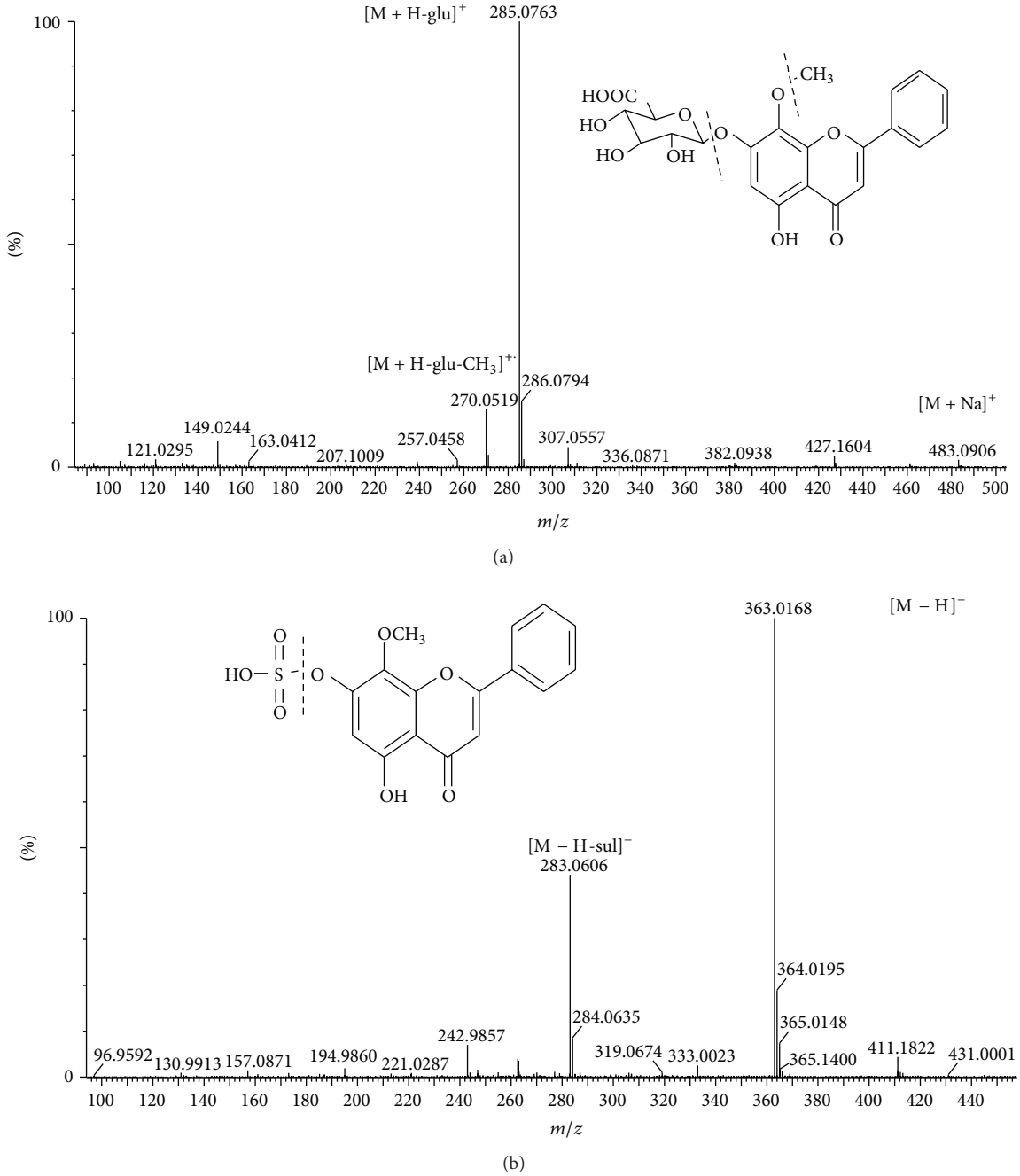

Figure 6: MS/MS spectra and structures of (a) prototype compound wogonoside in positive ion mode and (b) flavonoids metabolite wogonin 7-sulfate in negative ion mode identified in human serum after *SHLI* administration. In the tag, glu was the abbreviation of glucuronide-H_2O and sul was the abbreviation of sulfate-H_2O.

fragment ion $[M + H\text{-}CH_3]^{+\bullet}$ was generated by loss of $CH_3^{\bullet}$ for the flavones with a methoxyl group on the side chains of an aromatic ring. Its molecular formula was speculated to be $C_{22}H_{21}O_{11}$ based on the analysis of its elemental composition. Then the ion at *m/z* 483.0906 was inferred as wogonoside. The ion at *m/z* 363.0168 was $[M - H]^-$ ion. The major fragment ion of *m/z* 283.0606 was generated by loss of *m/z* 80 (sulfate-H_2O) fragment from $[M - H]^-$ in negative ion mode. The molecular formula was speculated to be $C_{16}H_{12}O_8S$, and the fragmentation information and the molecular formula were consistent with wogonin 7-sulfate. Other metabolites were determined by the same method described above and some of them were also supported by the databases such as HMDB (http://www.hmdb.ca/) and METLIN (http://masspec.scripps.edu/). As a result, 23 prototype components and 12 metabolites of *SHLI* were identified.

3.5. Correlative Analysis of the Prototype Components and Metabolites of SHLI. The prototype herb components could be further metabolized by various drug metabolizing enzymes. Drug metabolism is classified into phase I and phase II reactions. Phase I reactions are mediated primarily by the cytochrome P450 family of microsomal enzymes [25]. Compounds are factionalized by oxidation, hydrolysis, or reduction, leading to the introduction of, for example, hydroxyl, amino, carboxyl, or thiol groups into the molecule. Most compounds undergo phase I oxidation prior to phase II conjugation, but molecules with sites amenable to conjugation may undergo phase II reactions directly. The most relevant phase II drug conjugation reactions are methylation, sulfation, glucuronidation, and glutathione conjugation. There were three types of components found in human serum after *SHLI* administration: (i) compounds found in their native form; (ii) phase I metabolites formed by chemical modifications, such as hydroxylation (M + OH) and hydration (M + H_2O), and (iii) phase II metabolites formed by conjugation, such as methylation (M + CH_3), glucuronidation (M + $C_6H_8O_6$), sulfation (M + HSO_3), and other conjugation reactions. In human serum, a large number of phase II metabolites were found. Among them, 8 flavonoids metabolites, 2 phenylephrine glycosides metabolites, 1 iridoid metabolite, and 1 quinic acid metabolite were found.

Some researchers have reported the metabolites of *SHL* formula in rat plasma [8]. We compared the metabolites differences in human and rats after *SHLI* administration and found great differences on the types and quantities of the metabolites after *SHLI* or *SHL* formula administrated between human and rats. The metabolites of *SHLI* found in rats and human were listed in Supplementary Material (see Table S1 in Supplementary Material available online at http://dx.doi.org/10.1155/2014/241505). Large number of phase I metabolites were detected in rats such as dihydrosecologanic acid and 3,4-dihydroxyphenylethanol, while little was found in the human serum. Besides, sulfated metabolites which were common in human serum were less detected in the rat plasma. Such a discrepancy might be attributed to different species (human or rats), prescription (*SHLI* or *SHL* formula), or blood collection time (1 h or shorter time). Further studies of the biological properties of these metabolites would be helpful to understand the pharmacological mechanism of *SHLI*.

4. Conclusion

In this paper, we developed an unbiased approach for screening the prototype components and metabolites of *SHLI* in human serum based on metabolomic technique. Employing UPLC-Q-TOF-MS combined with multivariate statistical analysis, 23 prototype components and 12 metabolites of *SHLI* were rapidly and sensitively identified, which suggested that the metabolomic approach was an effective tool to discover, screen, and analyze the multiple prototype components and metabolites from complicated traditional Chinese preparations in vivo. *SHLI* in human body mainly caused phase II metabolite reactions such as sulfation, methylation, glucuronidation, and other complex conjugation reactions. This identification and structural elucidation of the chemical compounds provided essential data for further pharmacological and pharmacokinetics study of *SHLI*. The human serum metabolomic approach avoids the laborious process of predicting possible metabolites and provides information on unexpected reactive metabolites and a type of validated rapid and higher throughput methodology for the identification of constituents of traditional Chinese medicine.

Conflict of Interests

The authors declare that they have no conflict of interests regarding the publication of this paper.

Acknowledgments

This work was supported in part by National Science and Technology Major Projects for "Major New Drugs Innovation and Development" (Grant no. 2011ZX09201-201-15), National Science Foundation of China (Grant no. 81173562), and in part by the Foundation of Independent Topics at Beijing University of Chinese Medicine (Grant no. 2013-JYBZZ-XS-064).

References

[1] H. Zhang, Q. Chen, W. Zhou et al., "Chinese medicine injection Shuanghuanglian for treatment of acute upper respiratory tract infection: a systematic review of randomized controlled trials," *Evidence-Based Complementary and Alternative Medicine*, vol. 2013, Article ID 987326, 7 pages, 2013.

[2] Y. Cao, L. Wang, X. Yu, and J. Ye, "Development of the chromatographic fingerprint of herbal preparations Shuang-Huang-Lian oral liquid," *Journal of Pharmaceutical and Biomedical Analysis*, vol. 41, no. 3, pp. 845–856, 2006.

[3] The State Commission of Chinese Pharmacopoeia, *Pharmacopoeia of People's Republic of China*, part 1, Chemical Industry Press, Beijing, China, 2005.

[4] Y. M. Zhang, D. Yan, P. Zhang et al., "Quality control of Shuanghuanglian freeze-dried powder for injection based on its HPLC-ELSD fingerprints and biological profiles," *Acta Pharmaceutica Sinica*, vol. 45, no. 1, pp. 93–97, 2010.

[5] L. Liu, Z. Suo, and J. Zheng, "Simultaneous determination of four compounds in Sanjing Shuanghuanglian oral liquid by high performance liquid chromatography-diode array detection-electrochemical detection," *Chinese Journal of Chromatography*, vol. 24, no. 3, pp. 247–250, 2006.

[6] H. Cao and Y. Zhu, "Content determination of chlorogenic acid and baicalin in Shuanghuanglian oral solution by HPLC," *Drug Stands in China*, vol. 8, no. 2, pp. 44–46, 2007.

[7] G. L. Yan, A. H. Zhang, H. Sun et al., "An effective method for determining the ingredients of Shuanghuanglian formula in blood samples using high-resolution LC-MS coupled with background subtraction and a multiple data processing approach," *Journal of Separation Science*, vol. 36, no. 19, pp. 3191–3199, 2013.

[8] M. J. Zamek-Gliszczynski, K. A. Hoffmaster, K. I. Nezasa, M. N. Tallman, and K. L. R. Brouwer, "Integration of hepatic drug

transporters and phase II metabolizing enzymes: mechanisms of hepatic excretion of sulfate, glucuronide, and glutathione metabolites," *European Journal of Pharmaceutical Sciences*, vol. 27, no. 5, pp. 447–486, 2006.

[9] H. Ishizuka, K. Konno, T. Shiina et al., "Species differences in the transport activity for organic anions across the bile canalicular membrane," *Journal of Pharmacology and Experimental Therapeutics*, vol. 290, no. 3, pp. 1324–1330, 1999.

[10] G. B. Scarfe, J. C. Lindon, J. K. Nicholson et al., "Investigation of the metabolism of 14C/13C-practolol in rat using directly coupled radio-HPLC-NMR-MS," *Xenobiotica*, vol. 30, no. 7, pp. 717–729, 2000.

[11] J. Iwabu, J. Watanabe, K. Hirakura, Y. Ozaki, and K. Hanazaki, "Profiling of the compounds absorbed in human plasma and urine after oral administration of a traditional Japanese (Kampo) medicine, daikenchuto," *Drug Metabolism and Disposition*, vol. 38, no. 11, pp. 2040–2048, 2010.

[12] I. Iswaldi, D. Arráez-Román, A. M. Gómez-Caravaca et al., "Identification of polyphenols and their metabolites in human urine after cranberry-syrup consumption," *Food and Chemical Toxicology*, vol. 55, pp. 484–492, 2013.

[13] G. Tan, W. Liao, X. Dong et al., "Metabonomic profiles delineate the effect of traditional Chinese medicine Sini decoction on myocardial infarction in rats," *PLoS ONE*, vol. 7, no. 4, Article ID e34157, 2012.

[14] O. Corcoran and M. Spraul, "LC-NMR-MS in drug discovery," *Drug Discovery Today*, vol. 8, no. 14, pp. 624–631, 2003.

[15] M. S. Lee and E. H. Kerns, "LC/MS applications in drug development," *Mass Spectrometry Reviews*, vol. 18, no. 3-4, pp. 187–279, 1999.

[16] Y. Wu, "The use of liquid chromatography-mass spectrometry for the identification of drug degradation products in pharmaceutical formulations," *Biomedical Chromatography*, vol. 14, no. 6, pp. 384–396, 2000.

[17] X. Wang, W. Sun, H. Sun et al., "Analysis of the constituents in the rat plasma after oral administration of Yin Chen Hao Tang by UPLC/Q-TOF-MS/MS," *Journal of Pharmaceutical and Biomedical Analysis*, vol. 46, no. 3, pp. 477–490, 2008.

[18] S. L. Li, S. F. Lai, J. Z. Song et al., "Decocting-induced chemical transformations and global quality of Du-Shen-Tang, the decoction of ginseng evaluated by UPLC-Q-TOF-MS/MS based chemical profiling approach," *Journal of Pharmaceutical and Biomedical Analysis*, vol. 53, no. 4, pp. 946–957, 2010.

[19] L. Li, G. A. Luo, Q. L. Liang, P. Hu, and Y. M. Wang, "Rapid qualitative and quantitative analyses of Asian ginseng in adulterated American ginseng preparations by UPLC/Q-TOF-MS," *Journal of Pharmaceutical and Biomedical Analysis*, vol. 52, no. 1, pp. 66–72, 2010.

[20] C. Chen, F. J. Gonzalez, and J. R. Idle, "LC-MS-based metabolomics in drug metabolism," *Drug Metabolism Reviews*, vol. 39, no. 2-3, pp. 581–597, 2007.

[21] Y. Y. Zhao, X. L. Cheng, F. Wei, X. Bai, and R. C. Lin, "Application of faecal metabonomics on an experimental model of tubulointerstitial fibrosis by ultra performance liquid chromatography/high-sensitivity mass spectrometry with MS^E data collection technique," *Biomarkers*, vol. 17, no. 8, pp. 7221–7729, 2012.

[22] P. D. Rainville, C. L. Stumpf, J. P. Shockcor, R. S. Plumb, and J. K. Nicholson, "Novel application of reversed-phase UPLC-oaTOF-MS for lipid analysis in complex biological mixtures: a new tool for lipidomics," *Journal of Proteome Research*, vol. 6, no. 2, pp. 552–558, 2007.

[23] J. Han, M. Ye, H. Guo, M. Yang, B. R. Wang, and D. A. Guo, "Analysis of multiple constituents in a Chinese herbal preparation Shuang-Huang-Lian oral liquid by HPLC-DAD-ESI-MSn," *Journal of Pharmaceutical and Biomedical Analysis*, vol. 44, no. 2, pp. 430–438, 2007.

[24] Q. Z. Luo, J. B. Luo, and Y. Z. Wang, "Qualitative analysis of the main chemical constituents of Shuanghuanglian injection powder and their origin by HPLC-ESI/MS/MS spectrometry," *Acta Pharmaceutica Sinica*, vol. 44, no. 12, pp. 1391–1396, 2009.

[25] M. J. Zamek-Gliszczynski, K. A. Hoffmaster, K. I. Nezasa, M. N. Tallman, and K. L. R. Brouwer, "Integration of hepatic drug transporters and phase II metabolizing enzymes: mechanisms of hepatic excretion of sulfate, glucuronide, and glutathione metabolites," *European Journal of Pharmaceutical Sciences*, vol. 27, no. 5, pp. 447–486, 2006.

Hindawi Publishing Corporation
Journal of Analytical Methods in Chemistry
Volume 2014, Article ID 378242, 5 pages
http://dx.doi.org/10.1155/2014/378242

Research Article

Analysis of Photosynthetic Characteristics and UV-B Absorbing Compounds in Mung Bean Using UV-B and Red LED Radiation

Fang-Min Li,[1] Zhi-Guo Lu,[2] and Ming Yue[1]

[1] *Key Laboratory of Resource Biology and Biotechnology in Western China, Ministry of Education, The School of Life Science, Northwest University, Xi'an, Shaanxi 710069, China*
[2] *The College of Physics, Northwest University, Xi'an, Shaanxi 710069, China*

Correspondence should be addressed to Ming Yue; lifm@nwu.edu.cn

Received 12 December 2013; Accepted 7 January 2014; Published 12 February 2014

Academic Editor: Feng Wei

Copyright © 2014 Fang-Min Li et al. This is an open access article distributed under the Creative Commons Attribution License, which permits unrestricted use, distribution, and reproduction in any medium, provided the original work is properly cited.

Mung bean has been reported to have antioxidant, antidiabetic, anti-inflammatory, and antitumor activities. Various factors have important effects on the types and contents of plant chemical components. In order to study quality of mung bean from different light sources, mung bean seedlings were exposed to red light-emitting diodes (LEDs) and ultraviolet-B (UV-B). Changes in the growth parameters, photosynthetic characteristics, the concentrations of chlorophyll a and chlorophyll b and the content of UV-B absorbing compounds were measured. The results showed that photosynthetic characteristics and chlorophyll a and chlorophyll b concentrations were enhanced by red LEDs. The concentrations of UV-B absorbing compounds were enhanced by UV-B on the 20th day, while photosynthetic characteristics, plant length, and the concentrations of chlorophyll a and chlorophyll b were reduced by UV-B on the 40th day; at the same time the values of the stem diameter, plant fresh weight, dry weight, and the concentrations of UV-B absorbing compounds were enhanced. It is suggested that red LEDs promote the elongation of plant root growth and photosynthetic characteristics, while UV-B promotes horizontal growth of stems and the synthesis of UV-B absorbing compounds.

1. Introduction

Mung bean (*Phaseolus radiatus* L.) is a leguminous species grown in different parts of the world, primarily especially in Asia including China, India, Burma, and Thailand. Mung bean commonly is a common source of protein in the Asian diet or nutrient supplements [1]. Mung bean has been reported to possess antioxidant, antidiabetic, anti-inflammatory, antitumor and antimelanocytes, and antiangiotensin I-converting enzyme activities [2–8]. Mung bean contains free phenolic acids, bound phenolic acids, total phenolic, and anthocyanin. Correlation analyses between bioactivities and phytochemicals demonstrated that antioxidant bioactivity may be mainly contributed to phenolic compounds, whereas anthocyanins play an important role in the antidiabetic bioactivities [3]. Other reports showed that flavonoids including vitexin and isovitexin were the dominant components in mung bean [2, 9] and the content of vitexin was much higher than that of isovitexin in ethanol extracts [10]. It has been reported that mung bean has a strong antioxidant activity and isovitexin and vitexin contribute to most of the 1,1-diphenyl-2-picrylhydrazyl, ferric-reducing antioxidant power or 2,2′-azinobis-(3-ethylbenzthiazoline-6-sulphonate) radical scavenging ability [2].

Various factors including geographical location, climate change, temperature, and illumination time have important effects on the types and contents of plant chemical components, which are related to their bioactivity, functionality, and applications. Light quality is one of the most important factors in the regulation of plant growth, morphogenesis, photosynthesis, metabolism, and gene expression [11, 12]. For the photobiological research, ultraviolet-visible spectrum between 200 nm and 800 nm wavelength plays an important role in changes of chemical compounds of the organisms by irradiating them, especially compounds with ultraviolet (UV) absorption property [13, 14].

Compared to the ordinary fluorescent light source, the light-emitting diode (LED) light sources can provide a single wavelength of light quality with high photoelectric conversion efficiency, fixed wavelength, and low heat. LED light

Table 1: The treatments of the experiment.

Treatment	Ordinary fluorescent light	Red LEDs	UV-B radiation
CK	Ordinary fluorescent light	/	/
L	Ordinary fluorescent light	Red LEDs	/
U	Ordinary fluorescent light	/	UV-B radiation

The lamps were suspended above the plant at the height of 40 cm perpendicular to the ground.

source is considered to be a new important light source in the field of plant physiology and plant cultivation. Previous studies indicated that the LED light sources were used in the research of photomorphogenesis [15], chlorophyll synthesis [16], and photosynthesis [17]. Recently the studies of this field attract more and more researchers focusing on the work [18, 19].

Many studies indicated that there were the practical problems of insufficient light intensity and limited spectral wavelength during the process of plant cultivation in the laboratory [20–22]. It is necessary to find effective ways to replace or assist the ordinary fluorescent light source, to improve research method for the plant, and to promote the plant quality. In this study, we used the red LEDs and ultraviolet-B (UV-B) radiation as additional light sources for the process of plant cultivation in the laboratory to determine the role of the different qualities of light source on growth and photosynthetic characteristics of mung bean.

2. Materials and Methods

2.1. Plant Materials. Mung bean (*Phaseolus radiatus* L. cv. Qindou 20) seeds were selected for uniform size. Mung bean seeds were obtained from Yangling Breeding Center of National Bean Engineering Research Center of China (Shaanxi, China).

2.2. Supplementary Light Treatments. The ordinary fluorescent light source (power 40 W) was purchased from Philips Inc. The light directly irradiated the seedling of mung bean from am 7:00 to pm 7:00 each day. The UV-B radiation was provided by filter Qin brand (Baoji Lamp Factroy, China) 30 W fluorescence sunlamps. They were filtered with 0.13 mm thick cellulose diacetate (transmission down to 290 nm) for UV-B radiation. The dose of UV-B irradiation was 0.861 kJ/m^2 per day. The supplementary light treatments were shown in Table 1. The lamps were suspended above the plant at the height of 40 cm perpendicular to the ground.

Firstly, seeds were sterilized for 10 min by 0.1% $HgCl_2$ and were grown in Petri dish (diameter 18 cm) after being washed for 50 min by flowing water. Until seeds were germinated, they were transplanted in basin (diameter 25 cm) which was filled with the ratio of peat : vermiculite : perlite for 3 : 1 : 1. One week after seed germination, the supplementary light treatments carried out seed germination. On the 20th day and 40th day of supplementary light treatments, organisms were sampled, respectively, for various analyses.

2.3. Effects Test

2.3.1. Growth Parameter. The morphology including plant height, fresh weight, dry weight, root length, and stem diameter was measured. Mung bean seedlings were oven dried at 80°C until constant weight and being weighed using electronic scale as biomass (g).

2.3.2. Photosynthetic Characteristics. Photosynthetic characteristics were measured with a photosynthesis meter (Photosynthesis Meter I-301, CID. Inc.). The water use efficiency was the ratio of photosynthesis and transpiration. The results of stomatal conductance, photosynthesis and water use efficiency were the mean values of the day.

2.3.3. Determination of Chlorophyll a (chl a) and Chlorophyll (chl b) and UV-B Absorbing Compounds. The method for the measure of the concentration of chl a and chl b was extracted by acetone and determined following the reported methods [23]. Intact leaf samples of seedlings (fresh weight 0.5 g), which were at 5-6 leaves stage of development, were placed in a mortar and followed by the addition of silica of 0.2 g, $CaCO_3$ of 0.2 g, and 15 mL 80% acetone. After thorough grinding, the samples were filtrated with two layers of filter paper by pump air and fixed to 25 mL with 80% acetone, and then the absorbance at 663 and 645 nm was determined, respectively. Chlorophyll concentration was calculated and expressed as mg/g FW.

Fresh samples of 0.5 g were taken from the epicotyls and extracted in 10 mL acidified methanol (methanol-water-hydrochloric acid, 79 : 20 : 1, v/v) for UV-B absorbing compounds, according to the procedure of Mirecki and Teramura [24]. The hydrochloric acid was 36% HCl. Extract absorbance at 300 nm was measured with a spectrophotometer (UV-2100; Shimadzu, Columbia, MD, USA) and the absorbance was arbitrarily used for analysis.

2.4. Statistical Analysis. All experiments were performed in six times repeatedly. Statistical analyses were performed with SPSS 11.5 for windows. The results were expressed as the means ± standard error (SE) of triplicate. The data were subjected to one-way analysis of variance (ANOVA) and the significance of difference between samples means was calculated by Duncans' multiple range test and P values less than 0.05 were considered significant.

3. Results

3.1. Growth Parameters. It was observed that the values of the growth parameters of mung bean seedlings were irradiated for 20th day by red LEDs and UV-B was not significantly different compared with that of the ordinary fluorescent light (Table 2). However, the red LEDs treatment caused a significant increase ($P < 0.05$) of the values of plant height, fresh weight, dry weight, and root length compared with that of the ordinary fluorescent light for 40th day. With the UV-B radiation for 40th day, an obvious decrease ($P < 0.05$) of

Table 2: Effects of red LEDs and UV-B on the growth parameter of the mung bean.

Duration	Treatment	Fresh weight g/seedling	Dry weight g/seedling	Plant height cm/seedling	Root length cm/seedling	Stem diameter mm/seedling
20 d	CK	220.3	55.6	28.2 ± 2.1	6.38 ± 0.64	4.69 ± 0.45
	L	231.4	57.3	29.4 ± 2.6	6.59 ± 0.42	5.03 ± 0.61
	U	228.8	54.9	27.3 ± 2.4	6.08 ± 0.55	5.21 ± 0.36
40 d	CK	373.6	89.2	43.7 ± 2.7	7.69 ± 0.68	6.39 ± 0.74
	L	491.8$^{\#}$	110.6$^{\#}$	44.5 ± 3.0	9.04 ± 0.77$^{\#}$	6.65 ± 0.43
	U	460.7$^{\#}$	108.5$^{\#}$	38.2 ± 3.5$^{\#}$	7.32 ± 0.48	7.69 ± 0.63$^{\#}$

Note: different letters followed the data of same index at the same treatment time indicate significant difference among treatments. Means with pound sign ($^{\#}$) were significantly different at the $P < 0.05$ level ($n = 6$) according to Duncan's multiple range test ($^{\#}P < 0.05$).

Table 3: Effects of red LEDs and UV-B on the photosynthetic characteristics of the mung bean.

Duration	Treatment	Photosynthesis (μmol/m^2/s)	Stomatal conductance (mmol/m^2/s)	Water use efficiency WUE
20 d	CK	4.85	77.3	6.5
	L	5.62*	90.6*	9.8*
	U	4.63	75.9	7.0
40 d	CK	6.23	110.7	13.3
	L	7.49$^{\#}$	142.3$^{\#}$	19.6$^{\#}$
	U	5.33$^{\#}$	90.8$^{\#}$	9.1$^{\#}$

Note: different letters followed the data of same index at the same treatment time indicate significant difference among treatments. Means with asterisk (*) or pound sign ($^{\#}$) were significantly different at the $P < 0.05$ level ($n = 6$) according to Duncan's multiple range test ($^{*}P < 0.05$; $^{\#}P < 0.05$).

plant height was observed, while it induced a marked increase ($P < 0.05$) in fresh weight, dry weight, and stem diameter.

3.2. Photosynthetic Characteristics. The red LEDs treatment induced a significant increase ($P < 0.05$) in the values of the photosynthetic characteristics for the two durations (Table 3). However, a significant decrease ($P < 0.05$) was observed in the values of the photosynthetic characteristics of the UV-B radiation for 40th day.

3.3. Determination of chl a and chl b. The concentrations of chl a and chl b may affect the values of the photosynthetic characteristics to a certain extent. It was obvious that the red LEDs treatment induced statistically significant increases ($P < 0.05$) not only in the values of the photosynthetic characteristics (Table 3) but also in the concentrations of chl a and chl b (Figure 1) for the two durations. Compared with the ordinary fluorescent light, the UV-B radiation did not cause significant differences.

3.4. Determination of UV-B Absorbing Compounds. With the treatment of UV-B radiation, the concentrations of UV-absorbing compounds were increased dramatically and the same trend of results was shown in Figure 2. UV-B radiation-treated seedlings resulted in a notably increase in the concentrations of UV-absorbing compounds for the two durations ($P < 0.05$). However, red LEDs did not cause significant difference in comparison to the ordinary fluorescent light.

4. Discussion

LEDs are a promising irradiation source for plant growth in space for long life, minimal mass, volume, and being a solid state device. The red LEDs (wavelength 650 nm) were used as a supplementary light source for the greenhouse tomato in 1982, which was reported earlier by Japan's Mitsubishi Corporation [25]. During the process of laboratory cultivation, it has been reported that the ordinary fluorescent light lacked the ultraviolet part of the solar spectrum background, which was essential growth factor to play an important biological role [20, 26].

However, it was difficult to use a mixed-use LED light sources during the process of plant cultivation completely [27]. Therefore, we used red LED and UV-B as supplementary light sources for the ordinary fluorescent light to study the role of these light sources in plant cultivation. Our results showed that these light sources were obviously increased for growth and photosynthetic characteristics of mung bean. The red LED light source promoted the growth of the mung bean root (Table 2), which was useful to absorb the nutrients and water of the soil.

Chlorophyll concentrated in the chloroplast grana is the main pigment to capture the energy for photosynthesis in green plants. The results showed that the red LED light source can significantly increase the concentrations of the chlorophyll (Figure 1), which effectively promoted the photosynthesis and water use efficiency (Table 3). On the contrary, UV-B radiation induced a notably decrease in

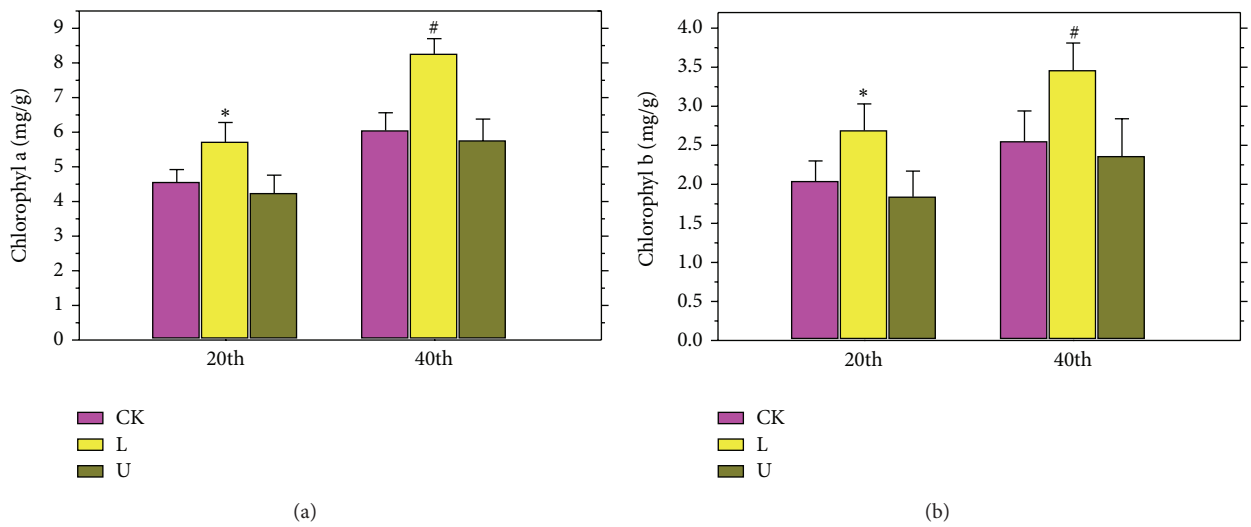

Figure 1: Effects of red LED and UV-B on the chl a (a) and chl b (b) of the mung bean. CK in figure refers to use ordinary fluorescent light as treat light sources. L in the figure refers to using both ordinary fluorescent light and red LEDs. U in the figure refers to using both ordinary fluorescent light and UV-B radiation light. Data are means and SE of six replicate plants. Error bars represent standard errors. Means with different letters above bars were significantly different at the $P < 0.05$ level ($n = 6$) according to Duncan's multiple range test ($^{*}P < 0.05$; $^{\#}P < 0.05$).

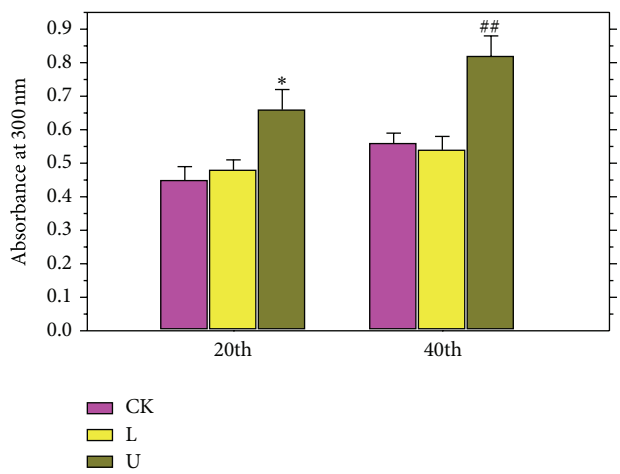

Figure 2: Effects of red LED and UV-B on the UV-B absorbing compounds of the mung bean. CK in the figure refers to use ordinary fluorescent light as treat light sources. L in Figure refers to the use of both ordinary fluorescent light and red LEDs. U in the figure refers to using both ordinary fluorescent light and UV-B radiation light. Data are means and SE of six replicate plants. Error bars represent standard errors. Means with different letters above bars were significantly different at the $P < 0.05$ level ($n = 6$) according to Duncan's multiple range test ($^{*}P < 0.05$; $^{\#\#}P < 0.01$).

the photosynthesis and water use efficiency. It was suggested that the UV-B treatment will reduce the stomatal opening degree of mung bean and then affect the gas exchange in photosynthesis.

UV absorption compounds in leaves are an important class of pigments including flavonoid, flavonol, cinnamon, and anthocyanin, which determine the color changes of many plants and are very sensitive to light. They play an important role in protective effect as a class of secondary metabolites [28, 29], which are related to antioxidant, antidiabetic, anti-inflammatory, antitumor and antimelanocytes and antiangiotensin I-converting enzyme activities [2–8]. The previous studies have reported that vitexin and isovitexin were major flavonoid in the ethanol extract of mung bean and vitexin content was much higher than isovitexin in ethanol extracts from mung bean sprout [3, 9]. However, another report showed that no significant difference in levels of vitexin and isovitexin was observed in mung bean sprout of the same cultivar tested in the experiments [2]. Since UV absorption compounds have an absorption peak in UV-B radiation scope, it could be found that the UV-B treatment caused a significant increase in UV absorption compounds (Figure 2). Compared with the ordinary fluorescent light, red LEDs did not induce significant differences in UV absorption compounds. Red LED and UV-B as supplementary light sources have an important effect on plant growth and chemical components.

Conflict of Interests

The authors declare that there is no conflict of interests.

Acknowledgments

This work was supported by the National Natural Science Foundation of China (no. 31100288), Changjiang Scholars and Innovative Research Team in University (no. IRT1174), and Opening Foundation of Key Laboratory of Resource

Biology and Biotechnology in Western China of Ministry of Education (Northwest University).

References

[1] L. Wongekalak, P. Sakulsom, K. Jirasripongpun, and P. Hongsprabhas, "Potential use of antioxidative mungbean protein hydrolysate as an anticancer asiatic acid carrier," *Food Research International*, vol. 44, no. 3, pp. 812–817, 2011.

[2] H. Li, D. Cao, J. Yi, J. Cao, and W. Jiang, "Identification of the flavonoids in mungbean (*Phaseolus radiatus* L.) soup and their antioxidant activities," *Food Chemistry*, vol. 135, no. 4, pp. 2942–2946, 2012.

[3] Y. Yao, X. Yang, J. Tian, C. Liu, X. Cheng, and G. Ren, "Antioxidant and antidiabetic activities of black mung bean (*Vigna radiata* L.)," *Journal of Agricultural and Food Chemistry*, vol. 61, no. 34, pp. 8104–8109, 2013.

[4] M. Lee, M. Kim, S. Kim, H. Wi, H. Park, and W. Choi, "Effects of mung-bean and black-bean ethanol extracts on inflammation related to obesity in the high fat induced obesity model," *The FASEB Journal*, vol. 27, no. 3, pp. 865–870, 2013.

[5] B. J. Kim, J. H. Kim, M. Y. Heo, and H. P. Kim, "Antioxidant and anti-inflammatory activition of the mung bean," *Cosmetics and Toiletries*, vol. 113, no. 1, pp. 71–74, 1998.

[6] J. Souček, J. Škvor, P. Poučková, J. Matoušek, T. Slavík, and J. Matoušek, "Mung bean sprout (*Phaseolus aureus*) nuclease and its biological and antitumor effects," *Neoplasma*, vol. 53, no. 5, pp. 402–409, 2006.

[7] G. H. Li, J. Z. Wan, G. W. Le, and Y. H. Shi, "Novel angiotensin I-converting enzyme inhibitory peptides isolated from Alcalase hydrolysate of mung bean protein," *Journal of Peptide Science*, vol. 12, no. 8, pp. 509–514, 2006.

[8] S. K. Yeap, H. M. Yusof, N. E. Mohamad et al., "In vivo immunomodulation and lipid peroxidation activities contributed to chemoprevention effects of fermented mung bean against breast cancer," *Evidence-Based Complementary and Alternative Medicine*, vol. 2013, Article ID 708464, 7 pages, 2013.

[9] X. F. Peng, Z. P. Zheng, K. W. Cheng et al., "Inhibitory effect of mung bean extract and its constituents vitexin and isovitexin on the formation of advanced glycation endproducts," *Food Chemistry*, vol. 106, no. 2, pp. 475–481, 2008.

[10] Y. Yao, F. Chen, M. F. Wang, J. S. Wang, and G. X. Ren, "Antidiabetic activity of Mung bean extracts in diabetic KK-Ay mice," *Journal of Agricultural and Food Chemistry*, vol. 56, no. 19, pp. 8869–8873, 2008.

[11] N. Fukuda, K. Y. Mitsuko, M. Ubukawa, K. Takayanagi, and S. Sase, "Effects of light quality, intensity and duration from different artificial light sources on the growth of petunia (Petunia x hybrida Vilm.)," *Journal of the Japanese Society for Horticultural Science*, vol. 71, no. 4, pp. 509–516, 2002.

[12] J. Chory and D. Y. Wu, "Weaving the complex web of signal transduction," *Plant Physiology*, vol. 125, no. 1, pp. 77–80, 2001.

[13] S. H. Lee, R. K. Tewari, E. J. Hahn, and K. Paek, "Photon flux density and light quality induce changes in growth, stomatal development, photosynthesis and transpiration of Withania Somnifera (L.) Dunal. plantlets," *Plant Cell, Tissue and Organ Culture*, vol. 90, no. 2, pp. 141–151, 2007.

[14] Q. B. Fu, J. M. Wang, G. N. Lin, H. Suo, and C. Zhao, "Short-wave near-infrared spectrometer for alcohol determination and temperature correction," *Journal of Analytical Methods in Chemistry*, vol. 2012, Article ID 728128, 7 pages, 2012.

[15] R. C. Jao and W. Fang, "An adjustable light source for photo-phyto related research and young plant production," *Applied Engineering in Agriculture*, vol. 19, no. 5, pp. 601–608, 2003.

[16] P. R. Poudel, I. Kataoka, and R. Mochioka, "Effect of red- and blue-light-emitting diodes on growth and morphogenesis of grapes," *Plant Cell, Tissue and Organ Culture*, vol. 92, no. 2, pp. 147–153, 2008.

[17] C. Chui, A. Aoki, Y. Takeuchi et al., "Antimicrobial effect of photodynamic therapy using high-power blue light-emitting diode and red-dye agent on Porphyromonas gingivalis," *Journal of Periodontal Research*, vol. 48, no. 6, pp. 696–705, 2013.

[18] I. Aguilo-Aguayo, F. Charles, C. M. G. C. Renard, D. Page, and F. Carlin, "Pulsed light effects on surface decontamination, physical qualities and nutritional composition of tomato fruit," *Postharvest Biology and Technology*, vol. 86, pp. 29–36, 2013.

[19] P. I. Gkika, N. Krigas, G. Menexes, I. G. Eleftherohorinos, and E. Maloupa, "Effect of temperature and light on seed germination of *Erysimum naxense* and *Erysimum krendlii*," *Central European Journal of Biology*, vol. 8, no. 12, pp. 1194–1203, 2013.

[20] Y. L. Wang, X. L. Wang, and M. Yue, "Effects of supplementary radiation of UV-B and red light on fruit quality of tomato in winter plastic greenhouse," *Acta Botany Boreal-Occident Sinica*, vol. 20, no. 4, pp. 590–595, 2000.

[21] F. M. Li, J. Wang, Y. P. Chen, Z. R. Zou, X. Wang, and M. Yue, "Combined effects of enhanced ultraviolet-B radiation and doubled CO2 concentration on growth, fruit quality and yield of tomato in winter plastic greenhouse," *Frontiers of Biology in China*, vol. 2, no. 4, pp. 414–418, 2007.

[22] H. Y. Li, L. Liu, M. Y. Li, and X. R. Zhang, "Effects of pH, temperature, dissolved oxygen, and flow rate on phosphorus release processes at the sediment and water interface in storm sewer," *Journal of Analytical Methods in Chemistry*, vol. 2013, Article ID 104316, 7 pages, 2013.

[23] Z. Q. Zhang, *The Experimental Handbook of Plant Physiology*, Scientific and Technical Publishers, Shanghai, China, 1985.

[24] R. M. Mirecki and A. H. Teramura, "Effects of ultraviolet-B irradiance on soybean V. The dependence of plant sensitivity on the photosynthetic photon flux density during and after leaf expansion," *Plant Physiology*, vol. 74, no. 3, pp. 475–480, 1984.

[25] D. J. Barta, T. W. Tibbitts, R. J. Bula, and R. C. Morrow, "Evaluation of light emitting diode characteristics for a space-based plant irradiation source," *Advances in Space Research*, vol. 12, no. 5, pp. 141–149, 1992.

[26] J. Kaakinen, P. Vähäoja, T. Kuokkanen, and K. Roppola, "Studies on the effects of certain soil properties on the biodegradation of oils determined by the manometric respirometric method," *Journal of Automated Methods and Management in Chemistry*, vol. 2007, Article ID 34601, 7 pages, 2007.

[27] K. Xu, Y. P. Guo, and S. L. Zhang, "Effect of light quality on photosynthesis and chlorophyll fluorescence in strawberry leaves," *Scientia Agricultura Sinica*, vol. 38, no. 2, pp. 369–375, 2005.

[28] Y. P. Cen and J. F. Bomman, "The effects of exposure to enhanced UV-B radiation on the penetration of monochromatic and polychromatic UV-B in leaves of Brassia napus," *Plant Physiology*, vol. 87, no. 3, pp. 247–225, 1993.

[29] U. Kutschera and W. R. Briggs, "Seedling development in buckwheat and the discovery of the photomorphogenic shade-avoidance response," *Plant Biology*, vol. 15, no. 6, pp. 931–940, 2013.